The scaffold protein intersectin 1 facilitates various steps in the synaptic vesicle cycle

Inaugural-Dissertation

to obtain the academic degree

Doctor rerum naturalium (Dr. rer. nat.)

submitted to the Department of Biology, Chemistry and Pharmacy
of Freie Universität Berlin

by

Maria Jäpel
from Dresden, Germany

2019

Period of doctorate studies:	March 2014 to March 2019
Supervisor:	Prof. Dr. Volker Haucke
Institute:	Leibniz-Forschungsinstitut für molekulare Pharmakologie (FMP), Berlin

1st Reviewer:	Prof. Dr. Volker Haucke
2nd Reviewer:	Prof. Dr. Christian Freund

Date of defense: 11.06.2019

Affidavit

I declare that my PhD thesis at hand has been written independently and with no other sources and aids then quoted.

Berlin, March 12th, 2019

Acknowledgement

Firstly, I would like to express my sincere gratitude to my supervisor, Prof. Volker Haucke for the continuous support during my PhD study, for his guidance, motivation, inspiring discussions and immense knowledge.

I owe special thanks to Dr. Takeshi Sakaba from Doshisha University for contributing electrophysiological data to the intersectin – SNARE project. I would like to thank Prof. Christian Freund and Fabian Gerth from the Free University for the great and productive collaboration we had over the last years. I am also grateful for the financial funding by the CRC958 and the integrated research training group. Especially, I thank Simone Schlender for organizing excellent summer schools and courses.

Furthermore, I would like to thank my subgroup colleagues: Burkhard Jakob, Dennis Vollweiter, Tanja Maritzen, Gaga Kochlamazashvili, Filiz Sila Rizalar for great discussions about intersectin in all its facets and their constructive feedback. I would like to mention Tanja Maritzen again, who supported me and my projects constantly over the years and always perfectly managed the mice strains and breedings.

I also deeply acknowledge Marielle Eichhorn-Grünig who supervised me in my first half a year as a little helpless PhD student and showed me everything in the lab from western blotting to pHluorin imaging. I would also like to thank Jelena Bacetic and Arndt Pechstein who worked on intersectin before me and provided the basis for my projects.

I am grateful for the continuous support from our technicians, meaning: beautiful neurons every week, orderings, genotypings, purified proteins and the organization of the lab: Silke Zillmann, Delia Löwe, Claudia Schmidt, Maria Mühlbauer, Uwe Fink, Sophia Griese, Lena von Oertzen and Sabine Hahn. I would also like to thank the animal facilities of the FMP and MDC for taking care of the mice strains I used for my projects: Natali Wisbrun, Jeannette Unnasch, Eva Lojek, Sina Scholz, Stephanie Rode and Franziska Westphal.
Moreover, I am grateful for the support from our imaging facility: Jenny Eichhorst, Burkhard Wiesner and Dmytro Puchkov. Notably, I would like to acknowledge Martin Lehmann for the great help and motivation from my first day on and especially for his support during the intersectin – synapsin project.
Furthermore, I would like to thank (IT-)Alex Heyne and our secretaries, Alexandra Chylla and Heidi Petschik for their great organizational help.

I very much enjoyed the cheerful, collaborative and supportive atmosphere in the lab over the years and I would like to thank all present and former lab members of the department:
Jelena Bacetic, Marietta Bergmann, Svenja Bolz, Caroline Bruns, Gabrielle Capin, Gala Claßen, Katrin Diesenberg, Michael Ebner, Marielle Eichhorn-Grünig, Fabian Feutlinske, Paula Samsó Ferre, Niclas Gimber, Marine Gil, Hannes Gonschoir, Claudia Gras, Tania López Hernández, Manuel Hessenberger, Lennart Hoffmann, Burkhard Jakob, Wonyul Jang, Natalie Kaempf, Christina Kath, Katharina Ketel, Philipp Koch, Gaga Kochlamazashvili, Natalia Kononenko, Michael Krauß, Marijn Kuijpers, André Lampe, Martin Lehmann, Guan-Ting Liu, Wen-Ting Lo, Fabian Lukas, Albert Mackintosh, Marta Maglione, Charles Malek, Andrea Marat, Tanja Maritzen, Kristine Oevel, Christoph Ott, Dmytro Puchkov, Filiz Sila Rizalar, Giulia Russo, Linda Sawade, Hannah Schachtner, Christopher Schmied, Jan Schmoranzer, Kjungyuen Song, Tolga Soykan, Domenico Azarnia Tehran, Dennis Vollweiter, Alexander Wallroth, Alexander Walter, Haibin Wang, Anna Wawrzyniak and Mirjana Weimershaus.
We shared more than just lab meetings and 10x PBS, but also countless coffee breaks, seminars, BBQs, retreats, lighters, rehearsal talks, imaging buffers, failed experiments (should list that at least three times), PhD hat tinkerings, Maibowles and Christmas parties, neurons, Mensa food, headaches, hot chocolates, lab cleanings, aliquots, practical courses, discussions, lab inspections, successful experiments, birthday cakes, Gösser and Bayreuther, paper aperos, ice cream, conferences, microscopes, ideas, ...
Working with you guys made this five year journey very much enjoyable and way easier. Thank you for your endless support.

Finally, I would like to thank my friends in- and outside the lab, especially my gang ("Teil des Schiffs, Teil der Crew") and in particular Tom Dörffel. Thank you for always being there for me.
Most importantly, I want to express my deepest gratitude to my parents and my brother for supporting me throughout my studies, my thesis and my life in general. Für eure Unterstützung, Geduld und Liebe kann ich euch nicht genug danken!

Contents

Publications

This cumulative dissertation is based on the following publications:

1. Pechstein, A.; Gerth F.; Milosevic I.; **Jäpel, M.**; Eichhorn-Grünig M.; Vorontsova, O.; Bacetic, J.; Maritzen, T.; Shupliakov, O.; Freund, C.; Haucke, V.:
   Vesicle uncoating regulated by SH3-SH3 domain-based complex formation between endophilin and intersectin at synapses. *EMBO Reports*, 16(2), 2015

2. **Jäpel, M.**; Gerth, F.; Sakaba, T.; Bacetic, J.; Yao, L.; Koo, S.-J.; Maritzen, T.; Freund, C.; Haucke, V.:
   Intersectin-mediated clearance of SNARE complexes is required for fast neurotransmission. *Nature Communications*, 2019, *under review*

3. Gerth, F.*; **Jäpel, M.***; Pechstein, A.*; Kochlamazashvili, G.; Lehmann, M.; Puchkov, D.; Onofri, F.; Benfenati, F.; Nikonenko, A.G.; Maritzen, T.; Freund, C.; Haucke, V.:
   Intersectin associates with synapsin and regulates its nanoscale localization and function. *Proceedings of the National Academy of Sciences*, 114(45), 2017 (* authors contributed equally to this work)

Other publications:

- Jakob, B.; Kochlamazashvili, G.; **Jäpel, M.**; Gauhar, A.; Bock, H.; Maritzen, T.; Haucke, V.:
  Intersectin 1 is a component of the Reelin pathway to regulate neuronal migration and synaptic plasticity in the hippocampus. *Proceedings of the National Academy of Sciences*, 114(21), 2017

- Gerth, F.; **Jäpel, M.**; Sticht, J.; Kuropka, B.; Schmitt, X.J.; Driller, J.H.; Loll, B.; Wahl, M.C.; Pagel, K.; Haucke, V.; Freund, C.:
  Exon inclusion modulates conformational plasticity and autoinhibition of the intersectin 1 SH3A domain. *Structure*, 2019, *accepted*

Abstract

The multidomain scaffold protein intersectin 1 has been implicated in several cellular signaling pathways and processes. The best described function of intersectin 1 is its association with early proteins during clathrin-mediated endocytosis, a process with particular importance in the presynapse in neurons during the reformation of synaptic vesicles. However, intersectin's numerous domains interact with proteins of diverse processes conceivably involving intersectin 1's function in further pathways in the presynapse.

In the present study we identified so far unknown functions of intersectin 1 in the synaptic vesicle cycle in neurons.

Proper cycling of synaptic vesicles is essential for neurotransmission at synapses and includes several processes like clathrin-mediated reformation of synaptic vesicles. In a first project, we identified an accumulation of clathrin-coated vesicles in mice depleted of intersectin 1, a phenotype akin to loss of the endocytic protein endophilin and the phosphatase synaptojanin that is involved in uncoating of clathrin-coated vesicles. Furthermore, we found a direct interaction between intersectin 1 and endophilin in the brain which mediates the association of endophilin with the clathrin machinery. We argue that this association is involved in proper recruitment of the phosphatase synaptojanin to sites of clathrin coated vesicle formation to achieve efficient uncoating of vesicles and thereby reformation of synaptic vesicles.

In a second project, we investigated the interaction between intersectin and synapsin, a protein implicated in clustering of reserve pool synaptic vesicles. During sustained neurotransmission synapsin's dissociation from synaptic vesicles is crucial for replenishment of the recycling pool that comprises release-ready vesicles. We found that the interaction between intersectin and synapsin is regulated by a phosphorylation-dependent intramolecular lock within intersectin that enables binding to synapsin only during neuronal activity. Loss of intersectin in hippocampal neurons resulted in a mislocalization of synapsin in combination with a reduced recycling pool size. We rescued these phenotypes by reexpression of wild-type intersectin but not with a locked, synapsin-binding deficient intersectin mutant. We argue that intersectin associates with synapsin upon activity, prevents premature reclustering of synaptic vesicles and thereby enables replenishment of release-ready vesicles during sustained stimulation.

In a third project, we identified an interaction between intersectin and the assembled SNARE complex. The assembly of SNARE complexes is essential for synaptic vesicle

fusion at release sites within the active zone. Hippocampal neurons depleted of intersectin displayed exocytic depression in a frequency dependent manner, but also upon sustained stimulation. Additionally, neurons expressing an intersectin binding deficient mutant of the v-SNARE synaptobrevin 2 phenocopied this exocytic depression. We hypothesize that intersectin binds postfusion SNARE complexes and removes them from release sites to enable subsequent vesicle fusion and to prevent exocytic depression.
In summary, we showed intersectin's versatile functions within the synaptic vesicle cycle not only during clathrin-mediated endocytosis but also in synaptic vesicle clustering and exo-/endocytic coupling. Taken together, our data reveal intersectin's importance for maintaining synaptic functionality especially during sustained neurotransmission.

Zusammenfassung

Die Funktion des Multidomänen-Gerüstproteins Intersektin 1 wurde bereits in einigen zellulären Signalwegen und Prozessen beschrieben. Die am besten verstandene Funktion von Intersektin 1 ist die Assoziierung mit frühen Proteinen während der Clathrin-vermittelten Endozytose, einem Prozess, der in der Presynapse in Nervenzellen während der Erneuerung synaptischer Vesikel besonders wichtig ist. Allerdings ist bekannt, dass Intersektins zahlreiche Domänen auch mit Proteinen anderer Prozesse interagieren, weswegen Intersektin 1 möglicherweise auch an anderen Prozessen in der Presynapse beteiligt ist.

In der vorliegenden Arbeit untersuchten wir bisher unbekannte Funktionen Intersektins im Zyklus synaptischer Vesikel in der Nervenzelle.

Der korrekte Ablauf dieses Zyklus' ist essenziell für die Neurotransmission an der Synapse und umfasst verschiedene Prozesse wie die Clathrin-vermittelte Erneuerung synaptischer Vesikel. In einem ersten Projekt konnten wir die Ansammlung von Clathrin-ummantelten Vesikeln in Mäusen, in denen Intersektin 1 genetisch entfernt wurde (Intersektin 1 KO), feststellen. Dieser Phänotyp ist demjenigen ähnlich, der zuvor bei Verlust des endozytischen Proteis Endophilin oder der Phosphatase Synaptojanin, die an der Clathrin-Entmantelung beteiligt ist, gefunden wurde. Darüber hinaus fanden wir im Gehirn eine direkte Wechselwirkung zwischen Intersectin 1 und Endophilin, die die Assoziation von Endophilin mit der Clathrin-Maschinerie vermittelt. Wir argumentieren, dass diese Assoziation an der korrekten Rekrutierung der Phosphatase Synaptojanin zu Stellen Clathrin-vermittelter Vesikelbildung beteiligt ist, um ein effizientes Entmanteln der Vesikel und damit Neubildung von synaptischen Vesikeln zu erreichen.

In einem zweiten Projekt haben wir die Wechselwirkung zwischen Intersektin und Synapsin untersucht, einem Protein, das an der Clusterung synaptischer Vesikel im Reservepool beteiligt ist. Während einer langanhaltenden Neurotransmission ist die Dissoziation von Synapsin von synaptischen Vesikeln von entscheidender Bedeutung für die Wiederauffüllung des Recyclingpools, der freisetzungsfähige Vesikel beinhaltet. Wir fanden heraus, dass die Wechselwirkung zwischen Intersektin und Synapsin durch eine phosphorylierungsabhängige intramolekulare Sperre innerhalb von Intersektin reguliert wird, die die Bindung an Synapsin nur während neuronaler Aktivität ermöglicht. Der Verlust von Intersektin in Hippocampus-Neuronen führte zu einer Fehllokalisierung von Synapsin in Kombination mit einer reduzierten Größe des Recyclingpools. Wir konnten den Ausgangszustand durch Reexpression von Wildtyp-Intersektin wieder herstellen. Dies gelang jedoch nicht mit einer Intersektin-Mutante, die intramolekular gesperrt und

somit unfähig ist Synapsin zu binden. Wir behaupten, dass Intersektin bei neuronaler Aktivität mit Synapsin assoziiert, eine vorzeitige Clusterung von synaptischen Vesikeln verhindert und dadurch das Auffüllen von freisetzungsfähigen Vesikeln während einer anhaltenden Stimulation ermöglicht.
In einem dritten Projekt haben wir eine Wechselwirkung zwischen Intersektin und dem zusammengebauten SNARE-Komplex identifiziert. Die Bildung von SNARE-Komplexen ist essenziell für die synaptische Vesikelfusion an Freisetzungsstellen in der aktiven Zone. Intersektin 1 KO Hippocampus-Neurone zeigten eine frequenzabhängige exozytische Depression, die auch nach anhaltender Stimulation festgestellt wurde. Neurone, die eine Mutante des v-SNARE Proteins Synaptobrevin 2 expremieren, die nicht an Intersektin binden kann, zeigen ebenfalls diese exozytische Depression. Wir vermuten, dass Intersektin SNARE-Komplexe nach der Fusion bindet und von Freisetzungsstellen entfernt, um eine nachfolgende Vesikelfusion zu ermöglichen und eine exozytische Depression zu verhindern.
Unsere Daten zeigen Intersektins vielseitige Funktionen innerhalb des synaptischen Vesikelzyklus, nicht nur während der Clathrin-vermittelten Endozytose, sondern auch bei der Regulierung des synaptischen Vesikelclusterung und der exo- / endozytischen Kopplung. Zusammengenommen zeigen diese Daten Intersektins Bedeutung für die Aufrechterhaltung der synaptischen Funktionalität, insbesondere während einer dauerhaften Neurotransmission.

1 Introduction

1.1 Synaptic transmission at the chemical synapse

The transmission of signals from one neuron to another is the crucial step for all brain functions and essential for every activity, from breathing and muscle movement to learning and memory formation. There are around 86 billion neurons in a human brain (Azevedo et al., 2009), that each can form thousands of nerve terminals to communicate with other neurons. In this sophisticated network all neurons share the common ability to transmit electrical signals, so called action potentials (AP), along their axons to the nerve terminal by depolarizing the plasma membrane. For transmission to another neuron, the AP has to be converted from an electrical signal into a chemical signal, a process occurring at the synapse. Synapses are specialized intercellular junctions where signals are transmitted from an axonal nerve terminal to dendrites or cell bodies (soma) of other neurons, muscle cells (neuromuscular junction) or glands. These structures are separated into a presynaptic and a postsynaptic part. An incoming AP at the presynapse triggers the influx of calcium through voltage-gated calcium channels (VGCC). The increased calcium concentration induces the fusion of neurotransmitter-filled synaptic vesicles (SVs) with the plasma membrane in a process called exocytosis (Katz and Miledi, 1967). The thereby released neurotransmitters diffuse across the gap between pre- and postsynaptic membrane, bind their respective receptor and elicit a postsynaptic response that, depending on the neurotransmitter and its receptor, can be excitatory or inhibitory. On the postsynaptic site, the activation of neurotransmitter receptors converts the chemical signal again to an electrical signal. An overview of the synapse and the most important proteins and processes is shown in Figure 1.1.

1.1.1 The presynapse

The conversion of an electrical signal into a chemical one takes place at the nerve terminal, in the presynapse. This compartment stores neurotransmitter-filled SVs, but also mitochondria and harbors special membrane areas, like the active zone or the periactive endocytic zone.

Fusion of SVs in the presynapse is exclusively happening at the active zone (Gray, 1963), which comprises the cell membrane found opposite an electron dense area within

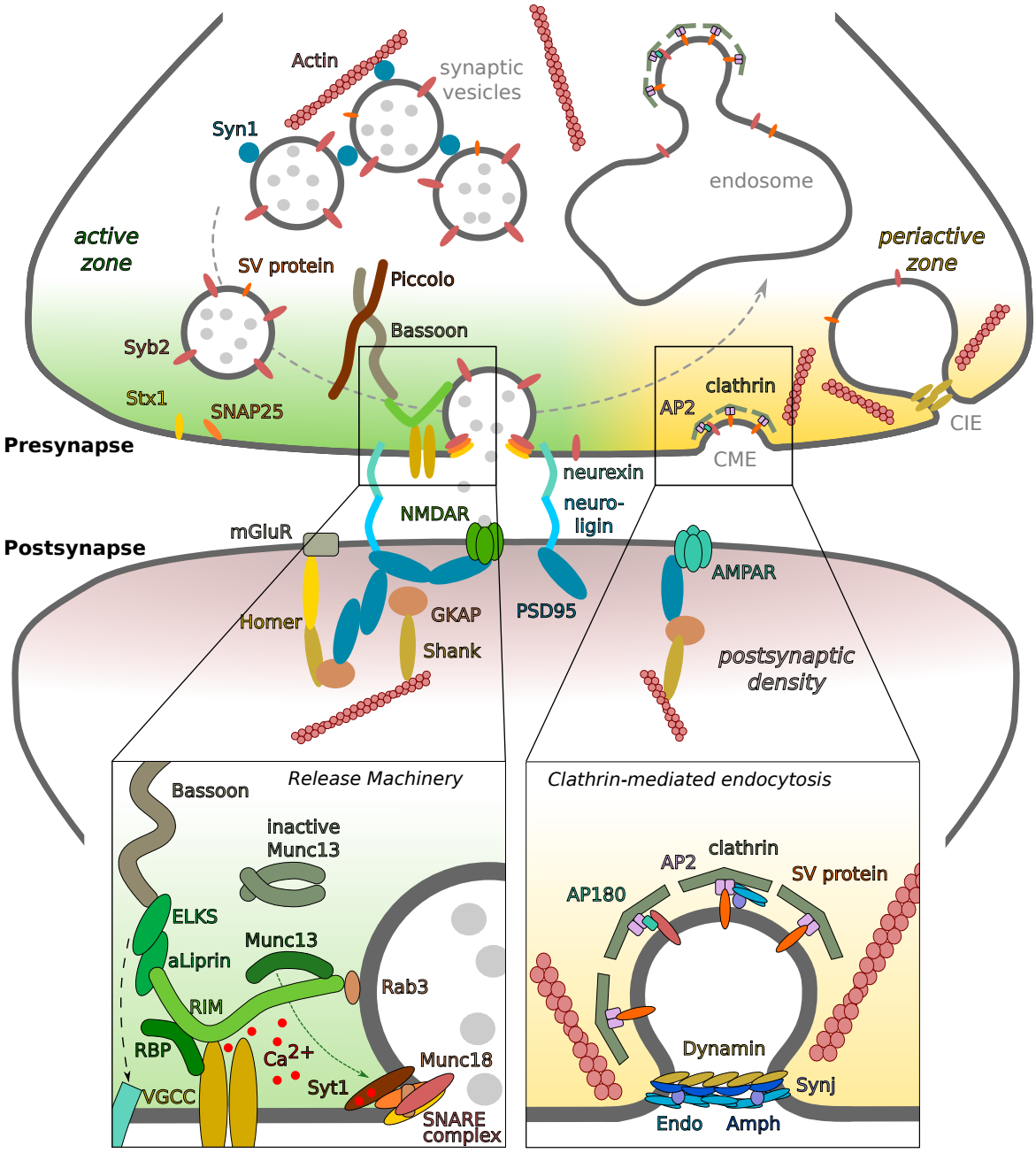

Fig. 1.1: The synapse and synaptic proteins involved in neurotransmitter release, clathrin-mediated reformation of vesicles and vesicle clustering. SVs of the reserve pool are clustered by synapsin I (SynI). Release-ready vesicles are docked and primed for fusion at the active zone (green). This process includes different proteins like RIM, RBP, Muncs and enables the coupling of SVs to VGCC. This coupling is also accompanied by the large scaffold proteins piccolo and bassoon. Upon an action potential stimulation and calcium influx SNARE complexes assemble and induce fusion with the membrane. Endocytic processes are tightly coupled to exocytosis and happen in parallel at the periactive zone (yellow). SVs are reformed from the cell membrane or from internal endosome-like vacuoles involving the function of clathrin, AP-2 and BAR-domain containing proteins like endophilin and amphiphysin. Some SV proteins, like synaptobrevin 2 (Syb2), need special adaptor proteins, (AP180). The final scission of vesicles is realized by the GTPase dynamin.

the postsynapse, called postsynaptic density (PSD) (Zhai and Bellen, 2004). Additionally, a variety of proteins locate at or close to the active zone, they are summarized as the cytomatrix of the active zone (CAZ). While the overall function of active zones is very similar in vertebrates and invertebrates, the morphology of active zones can differ strongly between synapses and species. Some synapses tether their SVs to specialized structures, which appear as electron dense projections from the cytomatrix into the cytoplasm. The neuromuscular junction (NMJ) of *drosophila melanogastor* for example harbors a so called T-bar, and ribbon synapses in vertebrates exhibit an electron dense ribbon-shaped structure (Ackermann et al., 2015).
Functionally, active zones enable SV tethering, docking, priming and eventually fusion, processes implemented by CAZ proteins. Among them are active zone scaffold proteins, like bassoon and piccolo, that orchestrate other core proteins of the active zone, like RIMs, Muncs, RIM binding protein (RBP), ELKS and α-liprin. All these proteins and their invertebrate homologs are essential for efficient vesicle fusion (Schoch et al., 2002, Augustin et al., 1999, Varoqueaux et al., 2002, Verhage et al., 2000, Wang et al., 2016, Acuna et al., 2015). They form a tightly regulated network that enables the coupling of SVs with VGCCs (Südhof, 2012). This coupling allows the rapid sensing of incoming calcium and subsequent vesicle fusion.
Another group of active zone proteins establishes alignment with the postsynaptic site. This alignment between sites of neurotransmitter release and postsynaptic neurotransmitter receptors ensures high efficiency of neurotransmitter recognition by the postsynapse (Tang et al., 2016). Well established trans-synaptic adhesion molecules are for example neurexins and their postsynaptic counterparts neuroligins (Dean and Dresbach, 2006).
While exocytosis is happening at the active zone, compensatory endocytosis takes place at the periactive zone surrounding the active zone. This compensation is necessary to retrieve the membrane area of fused SVs, to recycle SV proteins and eventually to reform SVs. In the last decade different modes of endocytosis have been described. These modes differ mainly in their speed of action but also by the use of specialized proteins and are in general dependent on the synapse type and stimulation strength (Soykan et al., 2016).

1.1.2 Synaptic vesicles

The presynapse is tightly packed with hundreds of neurotransmitter-filled SVs, which are small, spherical, membrane surrounded organelles with a size of $\sim 40\,\mathrm{nm}$ (Takamori

et al., 2006, Lehmann et al., 2015). Upon an action potential SVs fuse with the membrane and release their content to transmit a signal to a postsynaptic neuron. These vesicles carry different integral membrane proteins on their surface that are essential for proper function (Figure 1.2). Among those are neurotransmitter transporters. Dependent on the type of synapse (excitatory or inhibitory) vesicles exhibit different transporters and thereby store different neurotransmitters. One example is the vesicular glutamate transporter 1 (VGLUT1) that transports glutamate (Bellocchio et al., 2000). Neurotransmitter synthesis takes place in the cytoplasm and transport into vesicles happens in exchange for lumenal H^+. Therefore this process depends highly on the H^+ electrochemical gradient that is produced by another transporter located on SVs, the vacuolar H^+-ATPase (V-ATPase) (Edwards, 2007).

While there are only one or two copies of the V-ATPase per vesicle, other SV proteins are expressed in much higher copy numbers. The most abundant SV protein is synaptobrevin 2 (Syb2) also called vesicle-associated membrane protein 2 (VAMP2) with 70 copies per vesicle (Takamori et al., 2006). Synaptobrevin 2 is a soluble NSF (N-ethylmaleimide-sensitive factor) attachment protein receptor (SNARE) protein and is crucial for SV docking and fusion with the cell membrane by interacting with SNARE

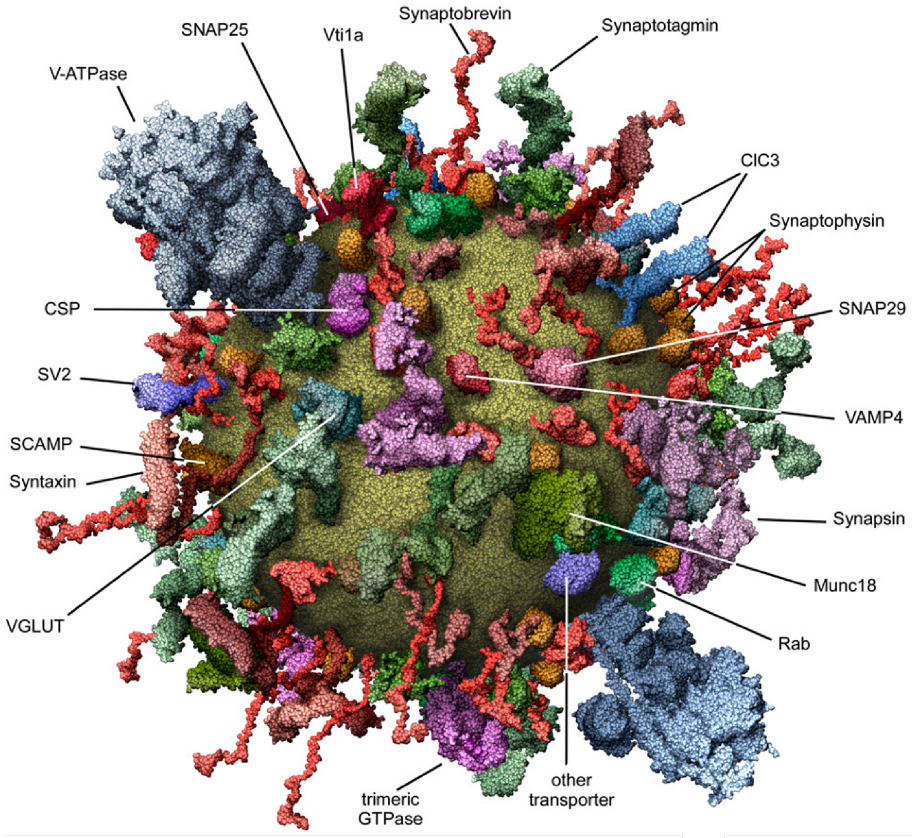

Fig. 1.2: A synaptic vesicle and its proteins. Taken from Takamori et al. (2006)

proteins at the cell membrane, syntaxin 1 (Stx1) and soluble NSF attachment protein 25 (SNAP25) (Baumert et al., 1989, Schoch et al., 2001, Imig et al., 2014). Proteins of the SNARE family share a homologous motif, called the SNARE domain, which is a 60 amino acids long stretch responsible for the formation of a four-helical bundle with SNARE motifs of other proteins (Figure 1.3). The assembly of such a SNARE complex provides the required energy to fuse two membranes with each other (Jahn and Scheller, 2006). Besides its SNARE domain, synaptobrevin 2 also contains a short NH_2-terminal domain and a COOH-terminal transmembrane domain (TMD). The complete knock-out (KO) of synaptobrevin 2 leads to a strong reduction in Ca^{2+}-evoked neurotransmitter release in forebrain synapses but also in *drosophila* NMJs (Schoch et al., 2001, Deitcher et al., 1998). Additionally, other studies described a contribution of synaptobrevin 2 to compensatory endocytosis (Deák et al., 2004).

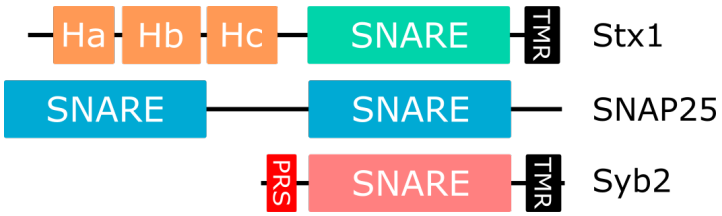

Fig. 1.3: Domain structure of the neuronal SNARE proteins. SNARE proteins are characterized by the presence of a SNARE motif. SNAP25 carries two SNARE domains and syntaxin 1 additionally encodes for an inhibitory Habc domain. Syntaxin 1 and synaptobrevin 2 contain TMDs while SNAP25 is palmitoylated to associate with the membrane (Greaves et al., 2009).

Synaptobrevin 2 was described to dimerize with the second most abundant SV protein synaptophysin (Edelmann et al., 1995). This interaction is thought to be important for synaptobrevin 2 retrieval in endocytosis (Gordon et al., 2011) but was also described to prevent synaptobrevin 2 from forming SNARE complexes at the membrane (Rajappa et al., 2016). However, the exact function of synaptophysin is still under debate.
Another SV protein essential for SV exocytosis is synaptotagmin. Synaptotagmin harbors two C2 domains (C2A and C2B) which can bind three and two calcium ions, respectively. Calcium binding to the C2 domains increase the affinity of the C2 domains to negatively charged phospholipids on the membrane. Synaptotagmin in cooperation with the SNARE complex brings the membranes together resulting in full SNARE complex assembly, membrane fusion and neurotransmitter release (Rizo and Xu, 2015).
The proteins mentioned so far carry transmembrane domains which anchor them to SV. But there are also SV associated proteins lacking a transmembrane domain. They interact with SV membrane lipids or other SV proteins. One well described protein

associated with SVs is the phosphoprotein synapsin, which is required for SV clustering but also synapse formation and maturation (Cesca et al., 2010). These and many other SV proteins are needed in different steps of the SV cycle to enable fast and reliable neurotransmission.

1.2 The synaptic vesicle cycle

Cycling of SVs in the presynapse takes approximately between 10-20 s and includes the following processes: vesicle fusion via exocytosis, vesicle reformation via endocytosis, vesicle clustering and formation of different vesicle pools (Südhof, 2004, Soykan et al., 2017). To achieve precision and high speed all these processes have to be tightly regulated and coupled (Heuser and Reese, 1973).

1.2.1 Synaptic vesicle pools and clustering

Depending on the type of synapse a single presynapse can be filled with hundreds of vesicles that can be separated into different pools (Schikorski and Stevens, 1997). Some vesicles are in close proximity or even docked to the membrane and immediately fuse in response to an action potential. These vesicles belong to the readily-releasable pool (RRP) of SVs (1-2 % of all vesicles). If the stimulus proceeds, vesicles of the recycling vesicle pool (10-20 %) will replenish the RRP and fuse. An even stronger stimulus will also recruit vesicles from the reserve pool, where usually most of the vesicles reside (80-90 %, see Rizzoli and Betz (2005), Südhof (2004)). This reserve pool is characterized by the presence of synapsins. These proteins are able to interact with SVs and actin and thereby sequester SVs within the synapse. Recent data propose additionally that synapsins together with certain interaction partners form a liquid phase in which vesicles reside and that is separated from the rest of the cytosol (Milovanovic et al., 2018). Upon a stimulus synapsin loses its high affinity for actin and SVs, and vesicles of the reserve pool are able to replenish the other pools (Bykhovskaia, 2011). Yet, the fine tuning regulation mechanisms of synapsin-mediated clustering are still under debate, especially during reclustering. However, some synapses contain additionally vesicles of a so called resting pool, that never contributes to fusion events (Fernandez-Alfonso and Ryan, 2008). Furthermore, other data also describes the existence of a superpool of SVs, which spans several terminals, is highly mobile and involved in exchange of SVs between different terminals (Staras et al., 2010).

1.2.2 Neurotransmitter release via exocytosis

The membrane SNARE proteins syntaxin 1 and SNAP25 form clusters at the plasma membrane, especially at the active zone where also phosphatidylinositol 4,5-bisphosphate ($PI(4,5)P_2$) accumulates (Martin, 2015, Aoyagi et al., 2005). At these sites vesicles of the RRP are docked by the partial assembly of trans-SNARE complexes. Proteins of the release machinery aid in the docking of vesicles. Proteins like RIM1 (Rab3-interacting molecule 1) that interact with SV associated proteins like Rab3, a small GTPase bound to SVs in its GTP loaded form, and simultaneously bind VGCC, are able to positionally prime SVs (Kiyonaka et al., 2007, Wang et al., 1997). This process enables an especially close tethering of SVs to VGCC. At these, so called release sites, calcium sensing is fast, and vesicles exhibit a maximum release probability. Notably, the number of release sites per active zone is limited and reuse of release sites is diminished upon high-frequency stimulations (Maschi and Klyachko, 2017). Besides SV priming, RIM1 additionally activates the homodimer Munc13 by forming a heterodimer with this protein (Deng et al., 2011). Munc13 is highly important for SV priming. It interacts with other active zone scaffold proteins like bassoon and piccolo and also mediates the opening of syntaxin 1 (Ma et al., 2011, Wang et al., 2009). Opening of syntaxin 1 is a necessary step during SV fusion as it allows SNARE complex formation. Under inactive conditions syntaxin 1's regulatory Habc domain folds back onto its SNARE domain and prevents the formation of SNARE complexes and premature vesicle fusion (Gerber et al., 2008). Closed syntaxin 1 molecules are bound by the protein Munc18, a protein which is also associated with the assembled SNARE complex and is essential for vesicle fusion (Verhage et al., 2000). Besides those already mentioned there are additional proteins like complexins or tomosyns in the synapse regulating the assembly of SNARE complexes and finally fusion (Trimbuch and Rosenmund, 2016, Cazares et al., 2016, Li et al., 2018).

As soon as an action potential invades the synapse, VGCCs open and the increasing local calcium concentration will lead to the full assembly of SNARE complexes and fusion. Calcium is bound by the C2 domains of synaptotagmin 1, which in its calcium bound state associates with SNARE complexes and especially with acidic membrane lipids like $PI(4,5)P_2$ that are enriched at the active zone (Park et al., 2015). This association is thought to bring vesicles even closer to the membrane and, together with the assembly of SNARE complexes, results in opening of the fusion pore. There are contrary studies in the field discussing the number of SNARE complexes needed for vesicle fusion from only one (van den Bogaart et al., 2010) complex to two (Sinha et al., 2011) or even eight

complexes (Domanska et al., 2009). Very recent data based on computational simulations and cryo-electron tomography proposes the need of six SNARE complexes (Manca et al., 2019, Li et al., 2019). Other studies suggest that the number of SNAREs influences the fusion pore formation and that especially the TMDs of synaptobrevin 2 and syntaxin 1 are needed for efficient fusion pore expansion (Chiang et al., 2018, Sharma and Lindau, 2018).
Postfusion SV proteins have to be recycled back onto vesicles via endocytosis. The still assembled postfusion SNARE complex, in its cis-conformation, has to be disassembled by the function of the ATPase N-ethylmaleimide-sensitive factor (NSF) and its cofactor soluble NSF attachment protein (SNAP) (Söllner et al., 1993). NSF in its ATP bound form can associate with SNARE complexes recognized by SNAP. Finally, the hydrolysis of around 50 ATP molecules will result in the disassembly of the SNARE complex (Ryu et al., 2016). Interestingly, the disassembly process was described to need at least 100 ms (Choi et al., 2018). This time requirement suggests that other processes precede disassembly to enable fast fusion upon higher frequency stimulations.

1.2.3 Compensatory endocytosis

Vesicle fusion leads to the expansion of the cell membrane. To compensate for this increase membrane has to be taken up again by endocytosis. Additionally, SV proteins located on the cell membrane after vesicle fusion have to be retrieved and sorted onto newly formed SVs. Different modes of endocytosis at periactive sites have been suggested in the last decades.
Clathrin-mediated endocytosis (CME) involves the coat protein clathrin that itself is unable to bind to the membrane and therefore needs adaptor proteins like AP-2 (adaptor protein 2). The first steps of clathrin-coated pit (CCP) formation though depend on proteins like the F-BAR protein FCHo that binds PI(4,5)P_2-rich sites on the membrane that show low membrane curvature (Henne et al., 2010, Di Paolo and De Camilli, 2006). Moreover, FCHo induces further membrane bending and recruits other endocytic proteins like Eps15 and intersectin, interactors of AP-2 (McMahon and Boucrot, 2011). Recognition of cargo proteins is realized by AP-2 which binds to certain motifs in their cytoplasmic tails. However, there are cargo proteins that need other adaptor proteins to be linked to AP-2 and to be internalized by CME. For example synaptotagmin 1 needs the adaptor stonin 2 (Diril et al., 2006) and the SNARE protein synaptobrevin 2 depends on association of its SNARE domain with AP180/CALM (Koo et al., 2011) to get efficiently endocytosed. After cargo recognition the clathrin coat assembles by recruitment of clathrin triskelia from the cytoplasm. Before final scission by the GTPase

dynamin the neck of the developing clathrin-coated vesicle (CCV) has to be constricted to allow dynamin binding. This constriction is accomplished by BAR proteins, like amphiphysin, endophilin or sorting nexin 9 (SNX9). Finally, the SH3 domains of these BAR proteins interact with a proline-rich peptide within dynamin to recruit the GTPase for vesicle scission. The ATPase heat shock cognate 70 (HSC70) and its cofactor auxilin are necessary for uncoating of CCVs together with the PI(4,5)P_2 phosphatase synaptojanin (Cremona et al., 1999). Uncoated vesicles are reacidified by activation of the V-ATPase and subsequently filled with neurotransmitter (Farsi et al., 2018).
CME has long time been thought to be the predominant mode for membrane retrieval at synapses (Granseth et al., 2006). But as the formation of a clathrin coat is a rather slow process (10-20 s), CME at the membrane only occurs upon low-frequency stimulations. Other endocytosis modes, like clathrin-independent endocytosis (CIE, e.g. ultrafast endocytosis) are much faster (50-500 ms) and more likely to be involved in membrane retrieval upon high-frequency stimulations. CIE does not require the assembly of a clathrin coat at the membrane, but still depends on the activity of proteins like dynamin and additionally needs actin rearrangements (Soykan et al., 2017). The resulting endocytosed structures are called endosome-like vacuoles from which synaptic vesicles are formed in a clathrin/AP-2 dependent manner that also involves cargo sorting (Kononenko et al., 2014, Watanabe et al., 2013).
There are also other endocytosis modes proposed like activity-dependent bulk endocytosis that retrieves large amounts of membrane upon prolonged high-frequency stimulations and also depends on endocytic sorting of cargo proteins like VAMP4 (Nicholson-Fish et al., 2015).

1.2.4 Coupling of exo- and endocytosis

The fusion of vesicles with the cell membrane is immediately followed by reuptake of membrane material to prevent expansion of the presynaptic terminal. Additionally, the retrieval of vesicle proteins is essential to recycle SVs. Accordingly, for most stimulation paradigms the amount of exocytosed and endocytosed membrane material is identical (Watanabe et al., 2013, Maritzen and Haucke, 2018) showing the tight coupling between exo- and endocytosis.
Experiments in which exocytosis was inhibited by genetic depletion of proteins of the release machinery or cleavage of SNARE proteins by tetanus neurotoxin resulted in a reduction of endocytic rates (Hosoi et al., 2009). This shows that exocytosis as such and the insertion of SV proteins and membranes triggers endocytosis.
The role of calcium for exocytosis during evoked neurotransmission is well established

(Katz and Miledi, 1967, Tucker and Chapman, 2002). However, the influx of calcium is also implicated in regulation of endocytosis in the synapse. Studies show that the calcium-binding protein calmodulin and its downstream effector protein the phosphatase calcineurin are involved in regulating endocytosis (Wu et al., 2009, 2014). Calcineurin targets the so called dephosphins, proteins of the endocytic machinery that are activated by dephosphorylation, among are dynamin, amphiphysin, synaptojanin, AP180 and Eps15 (Cousin and Robinson, 2001). Under resting conditions these proteins become phosphorylated by the activity of different kinases, among them cyclin-dependent kinase 5 (Cdk5) that was shown to phosphorylate dynamin (Tan et al., 2003). Interestingly, Cdk5 function was as well implicated in restraining vesicles to the resting pool, making them unavailable for exocytosis (Kim and Ryan, 2010).
The composition of membrane lipids is also important for the coupling of exo- and endocytic processes. The membrane lipid PI(4,5)P_2 is enriched at exocytic sites and was shown to be important for efficient exocytosis as it presents a binding platform for exocytic proteins like syntaxin 1, synaptotagmin 1, but also Munc13 (Martin, 2015, Walter et al., 2017). Furthermore, depletion of PI(4,5)P_2 by knock-down of its synthesizing enzyme PIPK1γ, also impairs endocytosis as it is needed to recruit endocytic proteins like dynamin, endophilin, SNX9 or AP-2 (Maritzen and Haucke, 2018).
Another mechanism of exo-/endocytic coupling was discovered when endocytic proteins were inhibited or depleted in cells and a reduction in exocytosis was reported (Shupliakov et al., 1997, Kawasaki et al., 2000, Wadel et al., 2007, Hosoi et al., 2009, Hua et al., 2013). For example, blocking dynamin or AP-2 by inhibitory peptides results in an impairment of the replenishment of release-ready vesicles in the calyx of Held synapse, an effect that was too fast to be explained by a depletion of recycled SVs (Hosoi et al., 2009, Hua et al., 2013). It was therefore hypothesized that endocytic proteins are needed to remove previously exocytosed material from release sites to provide accessible release sites for subsequent rounds of exocytosis (Neher, 2010). So far, neither the release site blocking agent nor the precise mechanism preventing this blockade has been identified.

1.3 Intersectins

Multidomain scaffold proteins, like intersectin (ITSN), are able to simultaneously interact with a plethora of other proteins via their various domains. This ability enables these proteins to link diverse proteins of the same or distinct pathways and thereby to couple and regulate diverse processes (Good et al., 2011).
The scaffold protein intersectin was first isolated from *Xenopus laevis* (Yamabhai et al.,

1998). Subsequently, intersectin orthologs were found in all metazoans (Hunter et al., 2011). There are two different genes for intersectin expressed in mammals, intersectin 1 and 2, while most lower organisms only encode one isoform. Alternative splicing gives rise to a short (ITSN-S), ubiquitously expressed and a long (ITSN-L), neuron-specific isoform of both genes. Intersectins play a key role in different cellular processes, like endocytosis, receptor trafficking and actin cytoskeleton rearrangement (Herrero-Garcia and O'Bryan, 2017). Intersectin 1 is encoded on chromosome 21 in humans and therefore implicated in Down syndrome (DS). Furthermore, intersectin is also one of the most highly expressed transcripts in Alzheimer's disease (AD) brains (Hunter et al., 2011).

1.3.1 Structure and localization

Intersectins consists of two Eps15 homology (EH) domains, a coiled coil (CC) and five Src homology 3 (SH3) domains. The long isoform contains an extended C-terminus with three additional domains, a Dbl homology (DH), a Pleckstrin homology (PH) and a protein kinase C conserved 2 (C2) domain. EH domains bind proteins with NPF (Asp-Pro-Phe) motifs and are implicated in endocytosis (Salcini et al., 1997). The EH domains of intersectin were demonstrated to interact with the endocytic proteins stonin 2, Epsin and the vesicle protein SCAMP1 (Fernández-Chacón et al., 2000, Yamabhai et al., 1998). Intersectin's CC domain was shown to interact with endocytic proteins (i.e. Eps15), but also with exocytic proteins (i.e. SNAP25) and additionally to form homo- and heterodimers (Okamoto et al., 1999, Wong et al., 2012). The five SH3 domains of intersectin represent a binding platform for various proteins of different cellular pathways. SH3 domains bind with moderate affinity to proline-rich sequences in other proteins, preferentially to a PxxP motif, following or preceding a positively charged residue (+xxPxxP or xPxxPx+) (Saksela and Permi, 2012). The SH3 domain itself is formed by five β-strands forming a sandwich, respective connecting loops (RT, nSrc and distal loop) and one short helix. Intersectin's SH3 domains are known to associate with endocytic proteins (i.e. dynamin, synaptojanin, AP-2), but also with proteins implicated in cell survival like phosphatidylinositol 3-kinase C2β or actin-remodeling, i.e. neuronal Wiskott-Aldrich syndrome protein (N-WASP) (Yamabhai et al., 1998, Roos and Kelly, 1998, Pechstein et al., 2010a, Das et al., 2007, Hussain et al., 2001) (see Figure 1.4). Furthermore, the neuron-specific intersectin 1 isoform expresses additional exons due to alternative splicing (Tsyba et al., 2008). Exon 20 for example encodes for five additional amino acids within the SH3A domain and is implicated in further regulation of interactions (Gerth et al., 2019). The DH-PH module within intersectins is a guanosine triphosphate exchange factor (GEF) for the small GTPase Cdc42 (Hussain

et al., 2001). A precise function for the C2 domain of intersectin was not described so far, but C2 domains as well as PH domains have membrane targeting properties and in case of C2 domains membrane targeting is calcium dependent (Cho, 2001).

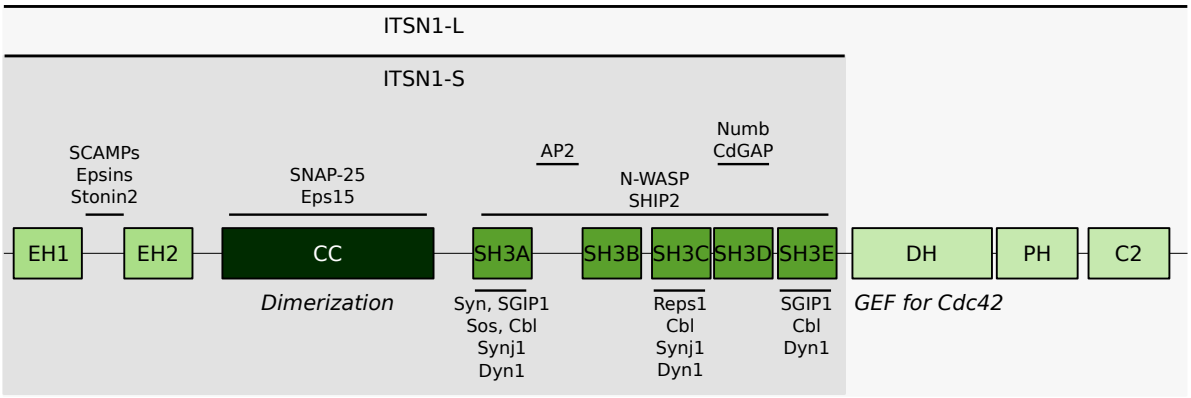

Fig. 1.4: Domain structure of intersectin 1, known interaction partners and functions.

The expression of intersectins is tissue specific, and western blot analysis showed that the short isoforms of intersectin 1 and 2 are ubiquitously expressed with the exception of neurons where the long intersectin isoform is highly enriched (Ma et al., 2003, Guipponi et al., 1998). In the brain intersectin 1 is mainly found in hippocampus, layer III of the neocortex, globus pallidus, subthalamic nucleus and the substantia nigra (Ma et al., 2003).
In mammalian epithelial cells and neurons intersectins localize throughout the cell, but also to the cell periphery. As the interactions with dynamin, AP-2 and other endocytic proteins suggest, intersectins localize to CCPs in a variety of cells (Hussain et al., 1999). Intersectin 2-L is also expressed in endothelial cells where it is important for caveolar endocytosis (Klein et al., 2009). In neurons intersectin 1-L localizes to pre- as well as postsynaptic sites. Within the presynapse, intersectin appears at the periactive zone where it is well established as an endocytic protein. Additionally, intersectin has been found in the SV cluster (Wilhelm et al., 2014, Pechstein et al., 2010b). This localization implies a role in SV clustering, although its function there has to be further determined.

1.3.2 Function in endo- and exocytosis

The best studied function of intersectin is its role in endocytosis. Intersectin interacts with many proteins of the early clathrin machinery, like FCHo, Eps15 and AP-2 (Henne et al., 2010), but also with late-stage proteins like dynamin and synaptojanin. The association with early as well as with late clathrin machinery proteins suggests a regulatory

function of intersectin in the temporal progression of endocytosis. Furthermore, it localizes to CCP necks (Sochacki et al., 2017), and overexpression of full length intersectin leads to impaired CME of the transferrin receptor in cultured fibroblasts, most likely by competition with the endogenous endocytic machinery (Sengar et al., 1999).
The function of intersectin in endocytosis was shown in many model organisms. Depletion of intersectin 1 in *C. elegans* reduced the number of SVs in NMJs, implicating intersectin 1 in recycling of vesicles. However, these worms were still viable while depletion of the *drosophila* intersectin 1 homologe dynamin-associated protein 160 kDa (Dap160) is lethal and leads to a reduction in SVs in the NMJ upon prolonged stimulation and to mislocalization of endocytic proteins, like dynamin (Koh et al., 2004, Marie et al., 2004). Interestingly, mice depleted of intersectin 1 are viable and show only mild endocytic defects in neurons (Yu et al., 2008) while other studies using the giant calyx of Held synapse did not detect any impairment in endocytosis (Sakaba et al., 2013). Still, Sakaba et al. (2013) could show that intersectin 1 is necessary for proper replenishment of release-ready vesicles. These results imply a not exclusively endocytic function of intersectin in mammalian neurons.
In particular, intersectin has been described to be important for exocytosis in neuroendocrine cells as it localizes to exocytic sites in PC12 and chromaffin cells (Momboisse et al., 2010). Depletion of intersectin additionally reduced the number of exocytic events in chromaffin cells (Yu et al., 2008). Intersectin's function in exocytosis depends on its GEF activity towards Cdc42 and actin-remodeling (Malacombe et al., 2006). Intersectin has additionally been shown to bind CdGAP and N-WASP (Jenna et al., 2002, Hussain et al., 2001). CdGAP has a GTPase-activating function towards Cdc42, which is inhibited upon intersectin binding. The interaction between intersectin and N-WASP activates Arp2/3 complexes. N-WASP and Arp2/3 complex activity lead to actin filament nucleation and branching and is together with other actin-nucleating factors necessary for endocytic processes (Kaksonen et al., 2006, Soykan et al., 2017).
This and other examples show intersectin's participation in endo- as well as exocytosis and raise the question if and how intersectins couple these processes.

1.3.3 Additional functions

Intersectins are also implicated in various cell signaling pathways. Besides their GEF activity towards Cdc42 intersectins can also bind Sos (Son of Sevenless) in mammalian synapses (Tong et al., 2000). Sos is a Ras GEF functioning downstream of receptor tyrosine kinases and is part of the ERK (extracellular signal-regulated kinase)-MAPK (mitogen-activated protein kinase) pathway. Additionally, intersectin's association with

phosphatidylinositol 3-kinase class II beta (PI3KC2β) was shown to be important for neuronal survival by activation of the PI3K-AKT pathway (Das et al., 2007). Furthermore, by binding to Cbl, a E3 ubiquitin ligase, intersectin promotes ubiquitination, endocytosis and degradation of epidermal growth factor receptor (EGFR) and thereby terminates EGF signaling (Martin et al., 2006). Moreover, intersectin interacts with the Reps1, a downstream effector of EGFR signaling (Dergai et al., 2010).
The interaction between intersectin and Numb at postsynapses, has been implicated in neurite growth and dendritic spine development. Numb has been originally described as an adaptor protein in CME. Its interaction with intersectin increases intersectins GEF activity towards Cdc42 and leads to spine growth (Nishimura et al., 2006).
Intersectin 1 has additionally been identified to have a role in neuronal migration as it associates with the very low density lipoprotein receptor (VLDLR) and its downstream signaling adaptor Dab1 to facilitate Reelin signaling (Jakob et al., 2017).

1.4 Aim of the study

The processes and signaling pathways in which intersectins are involved are diverse and numerous. Intersectins are best studied in early stages of CME. Still, it is known that intersectin also interacts with late-stage endocytic proteins like dynamin and synaptojanin. Could intersectin potentially orchestrate the temporal progression of CME by interacting with other late-stage endocytic proteins?

Furthermore, intersectin has long been implicated in the coupling of exo- and endocytic processes due to its ability to interact with proteins of both processes. The question still persists how intersectin connects these two processes mechanistically?

Intersectins localization throughout the synapse, not only to endocytic periactive sites but also to the SV cluster, suggests an additional function of intersectin besides endocytosis, conceivably in SV clustering.

This thesis aims to answer open questions about intersectin's functions in the mammalian synapse, not only in endocytosis but in the synaptic vesicle cycle as a whole. Specifically, how does intersectin enable coupling of exo- and endocytosis; is intersectin involved in SV clustering and has intersectin a specific function in late-stage endocytosis?

2 Project I: Vesicle uncoating regulated by SH3-SH3 domain-mediated complex formation between endophilin and intersectin at synapses

2.1 Overview of the project

The reformation of functional SVs after endocytosis is essential for neurotransmission and highly dependent on clathrin-mediated mechanisms. The uncoating of the clathrin cage after scission is the subsequent crucial step in reformation of SVs (Farsi et al., 2018). In this publication we show that recruitment of the N-BAR protein endophilin A1 depends on intersectin 1 and mediates vesicle uncoating (Pechstein et al., 2015).

Sensing and inducing membrane curvature is one of the early events in clathrin-mediated endocytosis and is carried out by BAR-domain containing proteins. Some of them, like the early BAR protein FCHo1/2 or amphiphysin, are able to directly interact with AP-2 and clathrin, while others like endophilin A are not. Endophilin A belongs to the N-BAR domain protein family and is encoded by three different genes in mammals (SH3GL2, SH3GL1, SH3GL3 for endophilin A1, 2, 3). Endophilin A carries an N-terminal BAR (Bin-amphiphysin-Rvs) domain and a C-terminal SH3 domain (Ringstad et al., 1997). A BAR domain is composed of α-helices forming a coiled coil dimer that binds to negatively charged membranes and forms and stabilizes membrane curvature corresponding to the convex shape of its membrane-binding surface (Peter et al., 2004). The BAR-domain of endophilin A1 associates due to its structure with the neck of late-stage CCPs where endophilin A1 also interacts with dynamin (Ringstad et al., 1999). Another function of endophilin A1 is the recruitment of the phosphatase synaptojanin to CCPs via its SH3 domain (Schuske et al., 2003). Synaptojanin is essential for postfission uncoating of CCVs probably by hydrolysis of PI(4,5)P_2 to PI(4)P (Verstreken et al., 2003, Cremona et al., 1999). Endophilin A triple KOs (TKO) were reported to die soon after birth and to show a clear delay in endocytosis and an accumulation of CCVs similar to the phenotype observed in synaptojanin KOs (Milosevic et al., 2011).
Endocytosis is a highly orchestrated process depending on the sequential recruitment of proteins (McMahon and Boucrot, 2011). Nevertheless, it is still enigmatic at which

stage and how the highly important protein endophilin A1 is recruited.
Similarly to the phenotypes observed in endophilin A TKO and synaptojanin KOs, we detected an accumulation of CCV in intersectin 1 KO lumbar spinal cord synapses, although less severe. Since the *drosophila* homologue of intersectin 1, Dap160, was already described to stabilize endocytic proteins, like endophilin, we investigated if intersectin 1 might execute a similar function in mammalian synapses.
To determine if this effect was direct or indirect we tested a possible interaction of both proteins. Indeed, endogenous immunoprecipitations from synaptosomal rat brain extract show an association between endophilin A1 and intersectin 1. We further show that only the SH3B domain of intersectin 1 interacts with endophilin A1. Interestingly, endophilin A1 associates with both intersectin isoforms. Moreover, *in vitro* binding assays confirmed the direct binding of endophilin A1's SH3 domain with the SH3B but not the SH3A domain of intersectin 1.
This interaction is evolutionary well conserved as we can additionally show the interaction in lamprey brain extract. Furthermore, an accumulation of CCVs in conjunction with a reduction of SVs was detected in the lamprey giant synapse after injection of intersectin 1 SH3B domain that conceivably competes with the endogenous interaction between intersectin 1 and endophilin A1.
The interaction could be shown to have a K_D of around 30 µM, and further NMR spectroscopy revealed the exact mode of the interaction. ^{15}N labeled endophilin A1 SH3 was supplemented with either intersectin 1 SH3B or a proline-rich peptide of VGLUT1 that is known to interact with the endophilin A1 SH3 domain (Vinatier et al., 2006, Voglmaier et al., 2006). While VGLUT1 binding was seen on the canonical proline-rich binding site, binding of intersectin 1 SH3B was detected on the opposite site on the surface of endophilin A1 SH3's β-sheet. This rather unexpected binding site mainly includes the residues E329, M331, and S336. Moreover, further NMR spectroscopy identified the RT and nSrc-loops of the intersectin 1 SH3B domain as interaction epitopes for the SH3 domain of endophilin A1.
Next, we generated mutants of endophilin A1 (E329K, S336K) to test the binding epitopes found with NMR spectroscopy. In *in vitro* binding assays and affinity chromatography experiments from rat brains we detected a strong reduction in binding of intersectin 1 SH3B to E329K, S336K mutant endophilin A1 while binding to a proline-rich peptide binding-deficient mutant of endophilin A1 was unaltered. This alteration was not due to mislocalization of endophilin A1 E329K, S336K away from the membrane as fractionation experiments showed.

To probe the functional importance of this interaction we used endophilin A TKO cortical neurons, overexpressed WT or E329K, S336K mutant endophilin A1 and EGFP-clathrin light chain and analyzed clathrin clusters. Endophilin A TKO displayed a striking increase in clathrin immunoreactivity due to a failure in clathrin uncoating and an accumulation of CCVs. Reexpression of WT endophilin A1 restored clathrin immunoreactivity while reexpression of mutant endophilin A1 only partially rescued. Additionally, we detected a decreased colocalization of endophilin and AP-2 in intersectin 1 KO hippocampal neurons demonstrating that the interaction of intersectin 1 and endophilin A1 is necessary for proper recruitment of endophilin A1 to sites of clathrin-mediated endocytosis.

In summary, this project revealed the function of intersectin 1 in recruiting endophilin A1 to sites of clathrin-mediated SV reformation via an atypical SH3-SH3 domain interaction. The described interaction links endophilin A1 to these sites and enables proper recruitment of synaptojanin and finally uncoating of CCVs.

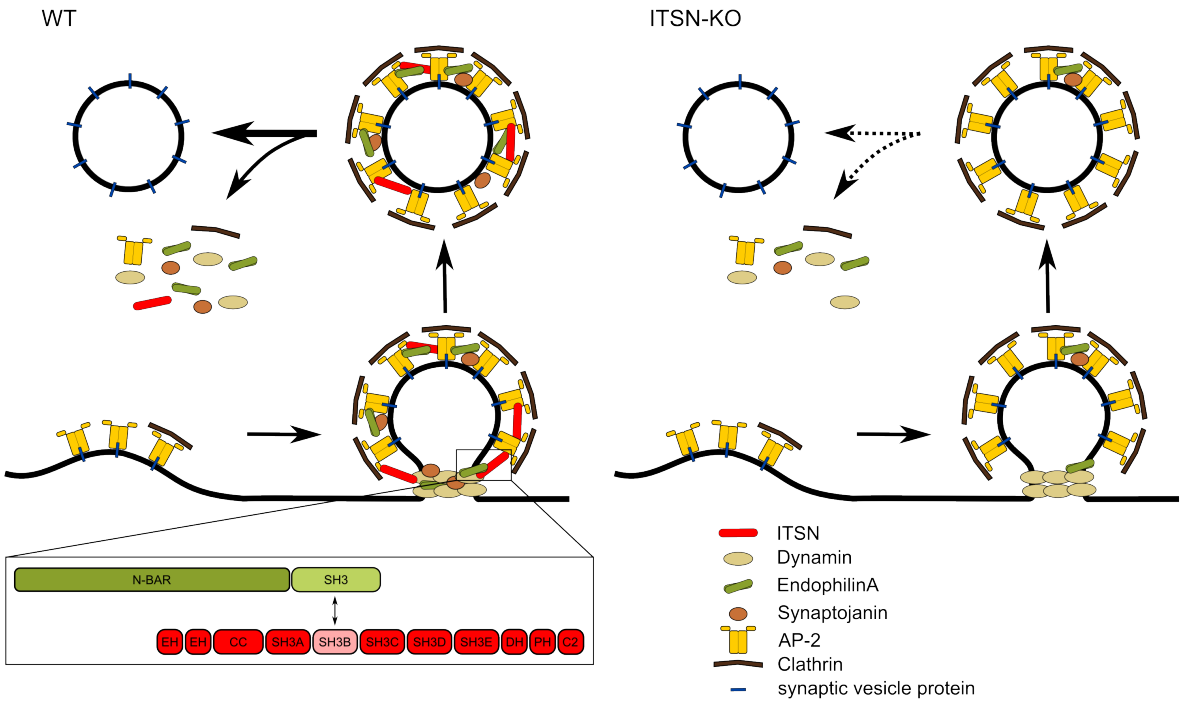

Fig. 2.1: Intersectin 1 directly associates with the BAR domain protein endophilin A1 to facilitate vesicle uncoating. Intersectin 1 recruits endophilin A1, which itself is unable to interact with the clathrin machinery, to sites of clathrin-mediated vesicle formation. Loss of intersectin 1 results in impaired endophilin and consequently synaptojanin recruitment to CCPs and defective CCV uncoating.

2.2 Original publication

Pechstein, A.; Gerth F.; Milosevic I.; **Jäpel, M.**; Eichhorn-Grünig M.; Vorontsova, O.; Bacetic, J.; Maritzen, T.; Shupliakov, O.; Freund, C.; Haucke, V.: Vesicle uncoating regulated by SH3-SH3 domain-based complex formation between endophilin and intersectin at synapses. *EMBO Reports*, 16(2), 2015.
https://doi.org/10.15252/embr.201439260

Personal contribution

The first question I wanted to answer during this project, was, if the smaller phenotypes we detected in intersectin 1 KOs compared to endophilin A TKOs and synaptojanin KOs are due to a compensation mechanism by increased expression of intersectin 2. Therefore, I carried out biochemical experiments to determine if intersectin 2 interacts as well with endophilin A1. I showed the interaction by performing GST-pull downs using GST-endophilin A1 SH3 domains and incubating them with rat brain extract or intersectin 1 or 2 transfected HEK293 cells. Furthermore, I performed immunoprecipitations from rat brain synaptosomal fractions to show the endogenous interaction between endophilin A1 and intersectin 1. Moreover, I was involved in the characterization of the endophilin A1 mutant (E329K, S336K) by showing that it interacts less efficiently with intersectin 1. Performing membrane – cytosol fractionation experiments, I detected that the endophilin mutant localizes as efficient to the membrane as wild-type endophilin A1, excluding the possibility that mislocalization of the mutant is responsible for the reduced interaction.

In a last set of experiments, I aimed to show that depletion of intersectin 1 results in a reduced recruitment of endophilin A1 to sites of clathrin-mediated endocytosis. I performed immunofluorescence stainings of endophilin A1 and AP-2 in primary hippocampal neurons from wild type and intersectin 1 KO mice (including preparation of primary hippocampal neurons from newborn mice) and detected a reduced colocalization between endophilin A1 and AP-2.

Finally, I analyzed data, was involved in writing figure legends and I designed the synopsis (Fig. 2.1).

3 Project II: Intersectin-mediated clearance of SNARE complexes is required for fast neurotransmission

3.1 Overview of the project

The regulated and precisely timed assembly of the SNARE complex is essential for fast fusion of neurotransmitter-filled SVs. Giving the fact that the number of release sites is limited, the subsequent disassembly and removal of postfusion SNARE proteins from these release sites is crucial, especially during sustained neurotransmission. In this publication we show that removal of postfusion SNARE complexes is facilitated by the scaffold protein intersectin 1 and required to sustain fast neurotransmission.

At release sites SVs are docked in close proximity to VGCCs via interactions with different proteins of the release machinery (RIM, RBP, Munc13). Calcium influx triggered by neuronal activity will reach these docked vesicles and their calcium sensor synaptotagmin 1 first, which results in full assembly of the SNARE complex and fusion of SVs. Studies have shown that the distance of a SV to the nearest release site defines its release probability, the closer a SV is the higher its release probability (Wadel et al., 2007, Eggermann et al., 2012, Böhme et al., 2016). Furthermore, the number of release sites within an active zone is limited, and the capacity of a single release site to be reused decreases under high frequency stimulation (Neher, 2010, Maschi and Klyachko, 2017). These data show that the availability and maintenance of release sites is essential to maintain fast release under sustained high frequency stimulation.
But the question remained, how can release sites become unavailable during sustained activity? One possibility is the stranding of exocytosed material within release sites. It was shown before that endocytic proteins are involved in the replenishment of release-ready vesicles and predicted that these proteins are involved in clearance of release sites from previously exocytosed material (Kawasaki et al., 2000, Wadel et al., 2007, Hosoi et al., 2009, Neher, 2010). In this project we asked what the exocytosed material is that blocks release sites during sustained neurotransmission and which mechanisms are involved in release site clearance.

Postfusion SNARE complexes remain on the membrane as cis-SNARE complexes and

could possibly block release sites before they get disassembled by NSF and αSNAP. In line with this, blocking synaptobrevin 2 by an antibody recognizing the very N-terminal proline rich sequence (PRS, see Figure 1.3) or injecting a peptide comprising this PRS (Wadel et al., 2007) impairs replenishment of release-ready vesicles in the calyx of Held synapse. This PRS may represent a binding site for endocytic proteins that are involved in release site clearance of synaptobrevin 2.

To test if synaptobrevin 2 is associated with any endocytic proteins we performed endogenous immunoprecipitations from rat brain lysate using synaptobrevin 2 specific antibodies. We identified intersectin 1 as a binding partner and verified this result with immunoprecipitations using intersectin 1 specific antibodies. Interestingly, intersectin 1 associates with all three SNARE proteins, making it plausible that intersectin 1 may interact with synaptobrevin 2 as part of the SNARE complex. Consistently, increasing the amount of assembled SNARE complexes, by either blocking SNARE complex disassembly or increasing the calcium concentration, further strengthens the binding between intersectin 1 and synaptobrevin 2.

The domains involved in this interaction could be identified as intersectin 1's SH3B domain and the PRS of synaptobrevin 2. To show this we used pull down experiments from synaptosomal rat brain extracts as well as *in vitro* binding assays using *in vitro* assembled SNARE complexes and NMR spectroscopy. We could furthermore show that intersectin 1 only associates with synaptobrevin 2 as part of the SNARE complex but not with synaptobrevin 2 alone. A mutant version of the SNARE complex lacking synaptobrevin 2's PRS (ΔPRS) showed significantly less binding to intersectin 1 SH3A-C. Still, the interaction was not completely abolished. This data corresponds well with our NMR data showing that the assembled SNARE complex binds more efficiently to intersectin 1 than a synaptobrevin 2 PRS peptide alone. Most likely, there are additional interaction platforms on the SNARE complex besides the synaptobrevin 2 PRS. A good candidate could be the linker between the two SNARE domains of SNAP25, which was described before to interact with intersectin 1 (Okamoto et al., 1999).

To prove the functional relevance of this interaction, we first tested if intersectin 1 influences SNARE assembly or disassembly. Levels of SNARE complexes were unchanged in intersectin 1 KO neurons as shown by proximity ligation assays as well as in intersectin 1 KO brains tested by immunoblotting or immunoprecipitations using syntaxin 1 specific antibodies. The *in vitro* SNARE assembly rate was unchanged after addition of intersectin 1 SH3B domain, and protein levels of the disassembly machinery were also not altered in intersectin 1 KO brains.

To verify that the intersectin 1 – SNARE complex interaction is necessary for release site

clearance, we first looked at the replenishment of release-ready vesicles after injecting intersectin 1 domain peptides (SH3A-C or SH3B) into the calyx of Held. An impairment in the replenishment rate was detected akin to the results obtained after addition of synaptobrevin 2 PRS peptide. These results clearly show that the interaction is necessary for the efficient replenishment of release-ready vesicles onto release sites, which likely involves the prior removal of SNARE complexes from these sites.
Secondly, we made use of the pHluorin approach to better understand intersectin 1's function in synaptic vesicle cycling (Sankaranarayanan and Ryan, 2000). We detected no differences in general endocytosis in intersectin 1 KO hippocampal neurons compared to WT neurons when neurons were stimulated with either high or low frequency stimulation. In a next set of experiments, we used a calibration stimulus followed by a 200 AP stimulation at high (40 Hz) or low (5 Hz) frequency. This calibration allowed us to detect robust signals independent of differences in initial release probability (Hua et al., 2013). We detected a reduction in exocytosis in intersectin 1 KO neurons when stimulated with 40 Hz that was absent when the 200 AP stimulation was applied at 5 Hz. A similar reduction was detected when neurons were stimulated with a train of six high-frequency stimulations. This short-term exocytic depression fits with the proposed function of intersectin 1 in removal of SNARE complexes. Without intersectin 1 those complexes accumulate in the active zone and disturb new exocytosis events. Following this argument the surface levels of synaptobrevin 2 should be increased in intersectin 1 KO neurons. Indeed, using an acidic-quench pHluorin protocol, we could confirm an increased surface/total ratio of synaptobrevin 2 in intersectin 1 KO neurons. Additionally, expression of the intersectin 1-binding-deficient ΔPRS mutant of synaptobrevin 2 in WT neurons exhibited an even higher surface/total ratio. Furthermore, this ΔPRS synaptobrevin 2 variant also phenocopied the intersectin 1 KO when neurons were stimulated with a train of six high-frequency stimulations. However, because the surface fraction of ΔPRS synaptobrevin 2 is drastically increased it is not clear if the exocytic depression we detected is due to acute release site clearance defects or due to a chronic lack of synaptobrevin 2 molecules on vesicles. To rule out the second possibility, we silenced neurons by incubation with tetrodotoxin (TTX) for several days. This toxin selectively blocks sodium channels in axons, inhibiting propagation of action potentials (Kiernan et al., 2005) and thereby preventing exo-/endocytic cycling in the presynapse and eventually missorting of synaptobrevin 2. Giving a train of six high-frequency stimulations to the silenced neurons, we were still able to detect the short-term exocytic depression proving the acute release site clearance defect of the synaptobrevin 2 mutant.

In summary, our results suggest a role for intersectin 1 in the removal of SNARE complexes from release sites to provide accessible sites for subsequent exocytosis events and to enable proper sorting of synaptobrevin 2 onto synaptic vesicles. The exact mechanism is still an object of ongoing research. Ideas include the direct connection of the SNARE complex to the endocytic machinery for example to dynamin or an increase in lateral diffusion of SNARE complexes away from release sites.

3.2 Original publication

Jäpel, M.; Gerth, F.; Sakaba, T.; Bacetic, J.; Yao, L.; Koo, S.-J.; Maritzen, T.; Freund, C.; Haucke, V.: Intersectin-mediated clearance of SNARE complexes is required for fast neurotransmission. *Nature Communications*, 2019, *under review*

Personal contribution

During this project I was first involved in investigating the interaction between intersectin 1 and SNARE proteins. Therefore, I performed immunoprecipitations from mice brain extract to show the endogenous interaction between intersectin 1 and synaptobrevin 2. Furthermore, I carried out immunostainings of hippocampal neurons using SNARE and intersectin 1 specific antibodies, respectively and showed the colocalization of these proteins at synapses. Therefore, I prepared primary hippocampal neuron cultures from newborn intersectin 1 KO mice and respective control WT animals. In a next step, we wanted to show the direct interaction between intersectin 1 and the assembled SNARE complex. Therefore, I overexpressed and purified GST-tagged intersectin 1 SH3 domains and the SNARE proteins, which assemble also *in vitro*. In *in vitro* binding assays I showed that intersectin 1 only binds assembled SNARE complexes but not synaptobrevin 2 alone. I demonstrated, using the ΔPRS mutant of synaptobrevin 2, that ΔPRS SNARE complexes interact less efficiently with intersectin 1 than wild-type complexes.

In a variety of control experiments I showed that the amount of SNARE complexes was unaltered in intersectin 1 KO brains. Therefore, I performed immunoblotting and immunoprecipitations of the SNARE proteins from mice brain extracts of WT and intersectin 1 KO mice. I carried out proximity ligation assays on WT and intersectin 1 KO hippocampal neurons, detecting assembled postfusion SNARE complexes. I also did not detect a change in the *in vitro* assembly rate of SNARE complexes after addition of intersectin 1 SH3B domain. Additionally, by immunoblotting I could not observe a change in the expression levels of the sorting and disassembly machinery proteins.

In another set of experiments, we wanted to prove the physiological relevance of the interaction between intersectin 1 and the SNARE complex. Therefore, I prepared primary hippocampal neuron cultures from WT and intersectin 1 KO mice and carried out pHluorin experiments after transfecting neurons with respective pHluorin constructs. Different stimulation frequencies and paradigms were used to prove that the interaction

is not involved in endocytosis but in release site clearance, a process prior to endocytosis. Additionally, I performed an acid-quench pHluorin protocol to show that synaptobrevin 2 is stranded on the cell surface of intersectin 1 KO neurons but also on the surface of WT neurons if the ΔPRS mutant of synaptobrevin 2 was expressed. I also carried out knock-downs of endogenous synaptobrevin 2 in WT hippocampal neurons and rescued with WT or ΔPRS synaptobrevin 2. I showed the knock-down and rescue efficiencies by immunostainings. I used these neurons to perform pHluorin experiments (with and without TTX treatment). I was able to mimic the intersectin 1 KO phenotype with the ΔPRS mutant proving again the physiological relevance of the interaction.
Finally, I analyzed data, designed the figures and the model, I wrote the figure legends and the manuscript together with Volker Haucke.

(3,989 words in main text)

Intersectin-mediated clearance of SNARE complexes is required for fast neurotransmission

Maria Jäpel[1], Fabian Gerth[2], Takeshi Sakaba[3], Jelena Bacetic[1,2], Lijun Yao[4], Seong-Joo Koo[1], Tanja Maritzen[1], Christian Freund[2] and Volker Haucke[1,2,5,6]

Affiliations

[1]Leibniz-Forschungsinstitut für Molekulare Pharmakologie (FMP), 13125 Berlin, Germany.

[2]Freie Universität Berlin, Faculty of Biology, Chemistry, Pharmacy, 14195 Berlin, Germany.

[3]Doshisha University, Graduate School of Brain Science, Kyoto 610‐0394, Japan.

[4]Max-Planck-Institute for Biophysical Chemistry, Membrane Biophysics, 37077 Göttingen, Germany.

[5]NeuroCure Cluster of Excellence, Charité Universitätsmedizin Berlin, 10117 Berlin, Germany.

[6]Correspondence: V.H. (haucke@fmp-berlin.de).

Abstract

The rapid replenishment of release-ready synaptic vesicles (SVs) at a limiting number of presynaptic release sites is required to sustain high frequency neurotransmission in central nervous system neurons. Failure to clear release sites from previously exocytosed material has been shown to impair vesicle replenishment and, thereby, fast neurotransmission. The identity of this material and the machinery that removes it from release sites has remained enigmatic. Here we show that the endocytic scaffold protein intersectin 1 clears release sites by direct SH3 domain-mediated association with a non-canonical proline-rich segment of synaptobrevin assembled into the SNARE complex for neuroexocytosis. Acute structure-based or sustained genetic interference with SNARE complex recognition by intersectin 1 causes a rapid stimulation-frequency-dependent depression of neurotransmission due to impaired replenishment of release-ready SVs. These findings identify a key molecular mechanism that underlies exo-endocytic coupling during fast neurotransmitter release at central synapses.

Main text

Neurotransmission at many types of synapses, e.g. to convey and process sensory signals, is based on their ability to rapidly release neurotransmitter [1, 2, 3]. The level and speed of neurotransmission during ongoing activity at such synapses is limited by the number of available release sites and, hence, by the speed of vesicle recruitment to these sites [4, 5]. Recent work from a number of systems has revealed a surprising, yet, poorly understood function of the endocytic machinery in facilitating the reuse of release sites during sustained high-frequency neurotransmission that appears to be independent of their role in endocytic membrane retrieval or synaptic vesicle (SV) recycling [6, 7, 8, 9, 10, 11]. For example, interfering with the function of the endocytic SH3 domain scaffold protein intersectin 1 or its binding partner dynamin causes a fast, stimulation-frequency-dependent depression of SV exocytosis [6, 7, 8, 9] that is independent of their putative function in endocytic SV membrane retrieval. Instead, it has been suggested that endocytic proteins are required for the clearance of release sites from previously exocytosed material to sustain high-frequency neurotransmission [4, 5, 8, 9, 12]. The physical nature of the alleged exocytosed material and the process by which it may be cleared from release sites post-exocytosis has remained largely enigmatic.

What may be the identity of the exocytosed material to be cleared from release sites? Neurotransmission by SV fusion requires the local assembly of soluble N-ethylmaleimide-sensitive factor attachment protein receptor (SNARE) complexes comprising the SV protein synaptobrevin 2 (also called VAMP2) and its cognate plasma membrane SNAREs syntaxin 1 and SNAP-25 at active zone (AZ) release sites [13, 14, 15, 16]. Accumulation of post-fusion cis-SNARE complexes during sustained high-frequency activity could conceivably constitute a kinetic bottleneck for fast neurotransmitter release as they likely would block recruitment of further release-ready SVs to AZ release sites [4, 5, 12]. SNARE complexes are disassembled by the ATPase N-ethylmaleimide-sensitive factor (NSF) and α/β–SNAPs [14, 15, 17], but exactly when and where this process occurs and how long it takes to disassemble cis-SNARE complexes *in vivo* is uncertain. Acute peptide-based perturbation experiments show that impaired NSF activity causes a rapid block in neurotransmission, suggesting that assembled post-fusion SNARE complexes may interfere with fast neurotransmission [18, 19]. Consistent with this view, it has been demonstrated that genetic loss of NSF results in the accumulation of cis-SNARE complexes on SVs [20] that may have formed on SVs *de novo* or could reflect the removal of post-fusion SNARE complexes by endocytosis within hundreds of milliseconds [21] to seconds [22]. In support of the latter scenario it has been reported that acute interference with the function of the vesicular SNARE synaptobrevin 2 at the calyx of Held produces a rapid retrograde block of vesicle recruitment [23] akin to the phenotype caused by intersectin 1 knockout (KO) in mice [8].

Here we show that intersectin 1 clears release sites by direct association with the SNARE complex via synaptobrevin 2. Our findings identify a key molecular mechanism that underlies exo-endocytic coupling that can explain why synapses in the central nervous system are able to sustain synaptic activity upon high-frequency stimulation.

Results

Replenishment of fast-releasing SVs is impaired by antibodies targeting the proline-rich segment (PRS) of synaptobrevin 2.

Previous data have suggested that replenishment of release-ready SVs requires synaptobrevin [23]. To uncover the underlying mechanism, we probed the role of synaptobrevin 2 and specifically, its proline-rich segment (PRS) that may constitute a binding site for endocytic factors, in fast neurotransmission at the calyx of Held, a large fast-firing synapse in the auditory brainstem that is amenable to electrophysiological analysis. We conducted simultaneous presynaptic and postsynaptic recordings in calyces of Held (at postnatal days 8–11) microinjected with antibody Fab fragments that specifically target the PRS of synaptobrevin 2 and applied a pulse protocol that allows for the separation of two components of transmitter release within the readily-releasable pool (RRP) of vesicles: A fast-releasing pool (FRP) that corresponds to the exocytic fusion of synchronously released SVs and a slowly releasing pool (SRP). Presynaptic terminals were depolarized from -80 mV to +70 mV for 2 ms, followed by repolarization to 0 mV for 50 ms, which triggers the fusion of all readily releasable SVs (as described earlier [6, 8, 23]). The excitatory postsynaptic current (EPSC) decayed during the pulse protocol, indicating depletion of the RRP of SVs. During the pulse two kinetic components of neurotransmitter release can be observed with time constants of a few ms for the FRP and of 20–30 ms for the SRP (Fig. 1a, left, dotted traces). When the same stimulation was repeated after a resting interval of 500 ms, the EPSC in control calyces of Held had recovered to more than 50% of its initial value (Fig. 1a, left, solid traces). In contrast, calyces injected with anti-synaptobrevin 2 PRS antibody Fab fragments displayed a slightly reduced RRP size (cumulative release: control: 4283 ± 544 vesicles; Syb Ab: 2528 ± 289 vesicles; *p = 0.035, t-test) and, more importantly, the recovery of the synaptic response during the second pulse was significantly reduced (Figure 1a, right). Variation of the interstimulus interval (ISI) between two consecutive pulses to monitor SV replenishment following depletion of the RRP revealed a pronounced slow-down of the recovery of the FRP in synaptobrevin 2-PRS antibody-injected calyces (Figure 1b). While the time course of FRP recovery in controls followed a double exponential function with time constants of a few hundreds of ms and several seconds (Figure 1b), recovery of the FRP in synaptobrevin 2 PRS antibody-injected synapses could be fitted by a single exponential function with a time constant of several seconds (Figure 1b). The kinetics of recovery of the SRP were unaffected by the injected synaptobrevin 2 PRS antibodies (Figure 1c). This phenotype is quite distinct from the observed

block of release observed upon acute interference with SNARE complex function in neuroexocytosis [24]. Instead, these data show that synaptobrevin 2 via its PRS specifically regulates the replenishment of release-ready SVs during fast neurotransmission.

Intersectin 1 directly binds to the neuronal SNARE complex via its SH3B domain and the proline-rich segment of synaptobrevin 2.

The kinetic delay in the replenishment of release-ready SVs induced by antibody Fab fragments that bind and occlude the synaptobrevin 2 PRS is highly reminiscent of the phenotype observed in calyces from knockout (KO) mice lacking the endocytic SH3 domain scaffold protein intersectin 1 [8]. We therefore reasoned that the PRS of synaptobrevin 2 might serve as a recruitment platform for the association of endocytic proteins implicated in the clearance of release sites from previously exocytosed material. Synaptobrevin 2 or complexes thereof might comprise part of this long sought-after material. We tested this hypothesis by immunoprecipitating native endogenous synaptobrevin 2 from brain lysates. Strikingly, we found that synaptobrevin 2, in addition to its well-established SNARE complex binding partner syntaxin 1, associated with the endocytic SH3 domain protein intersectin 1 (Figure 2a). Conversely, antibodies against intersectin 1 co-immunoprecipitated synaptobrevin 2 as well as SNAP-25 and syntaxin 1. These exocytic SNARE proteins were absent from immunoprecipitates of the related endocytic SH3 domain protein amphiphysin 1 (Figure 2b). Consistently, intersectin 1 colocalized with synaptobrevin 2 (Figure 2c), syntaxin 1, and SNAP-25 (Figure S1a) at presynaptic sites marked by the AZ protein bassoon in hippocampal neurons in culture. These data suggest that intersectin 1 associates with synaptobrevin 2, possibly as part of the SNARE complex.

To probe whether intersectin 1 indeed binds to synaptobrevin 2 incorporated into the exocytic SNARE complex, we analyzed whether the intersectin 1-synaptobrevin 2 association was regulated by conditions that impact on SNARE complex formation and/ or disassembly. Association of intersectin 1 with synaptobrevin 2 was potently stimulated by N-ethylmaleimide, a compound that elevates the steady-state levels of SNARE complexes by preventing their NSF-mediated disassembly (Figure 2d, e). Moreover, depletion of calcium by EGTA reduced the amount of synaptobrevin 2 and syntaxin 1 found in intersectin 1 immunoprecipitates (Figure 2f, g). These findings suggest that intersectin 1 associates with synaptobrevin 2 incorporated into the neuronal SNARE complex, a conclusion further supported by structural biochemical experiments described below.

Intersectin 1 contains five SH3 domains (termed A-E) [25] that conceivably could associate with the PRS of synaptobrevin 2 when complexed with its cognate SNAREs. We assayed the ability of GST-fused intersectin 1 SH3A-C domains to affinity-purify synaptobrevin 2, syntaxin 1, and SNAP-25 from synaptosomal lysates. We found that the SH3A-C domains but not GST alone efficiently captured synaptobrevin 2, syntaxin 1, and SNAP-25. The association of GST-intersectin 1 SH3A-C with neuronal

SNARE proteins was inhibited in a dose-dependent manner by titration of a peptide encompassing the PRS of synaptobrevin 2, but not by an unrelated control peptide (Figure 3a). Synaptobrevin 2, in addition to its incorporation into the neuronal SNARE complex, associates with synaptophysin on SVs, opening the possibility that intersectin 1-synaptobrevin 2 binding might be bridged or facilitated by synaptophysin. However, synaptophysin was absent from material affinity purified using GST-intersectin 1 SH3A-C (Figure 3a). Moreover, synaptobrevin 2 was captured with equal or higher efficiency from lysates of wild-type (WT) or synaptophysin KO mice (Figure S1b) (in agreement with a role of synaptophysin in counteracting post-fusion SNARE complex formation of synaptobrevin 2[26]). These results are most consistent with the direct association of intersectin 1 via its SH3 domains with the PRS of synaptobrevin 2 complexed with its cognate SNAREs syntaxin 1 and SNAP-25.

We tested a putative direct interaction by using purified recombinant intersectin 1 SH3 domains and the neuronal SNARE complex assembled from the complete cytoplasmic domains of synaptobrevin 2, syntaxin 1, and SNAP-25 (Figure S2a). Recombinant GST-fused intersectin 1 SH3A-C directly associated with synaptobrevin 2 contained in the assembled SNARE complex, but not with non-assembled synaptobrevin 2 presented on its own (Figure 3b, c). The SH3D-E domains of intersectin did not bind to the SNARE complex (Figure 3b). Further mapping identified the SH3B domain of intersectin 1 as the primary determinant for association with the neuronal SNARE complex (Figure 3b). Importantly, we found that SNARE complexes containing a synaptobrevin 2 mutant lacking its PRS (ΔPRS) (Figure S2b) bound less efficiently to intersectin 1 SH3A-C (Figure 3d), consistent with the acute perturbation (Figure 1) and peptide competition experiments (Fig. 3a) described above.

To further probe the mode of interaction between the neuronal SNARE complex and intersectin 1 at the atomic level, we turned to NMR spectroscopy. We used previously obtained resonance assignments for ^{15}N-isotope-labeled intersectin 1 SH3 domains [27, 28] to interpret the interaction properties by chemical shift analysis of the corresponding ^{15}N-^{1}H correlation spectra. To obtain insights into the molecular determinants of complex formation between intersectin 1 and the SNARE complex, we added ^{15}N-labelled intersectin 1 SH3B or SH3A-C domains to the unlabeled purified SNARE complex assembled from its components. Complex formation of intersectin 1 SH3B with the neuronal SNARE complex resulted in the near complete disappearance of SH3B resonances due to complex formation-dependent line broadening of residues (Figure 3e, S2c), while only the signals of the most flexible regions remained visible (Figure 3f). SH3B resonances also selectively disappeared when ^{15}N-labeled SH3A-C was incubated with the neuronal SNARE complex (Figure S2d), whereas the signals of SH3A and SH3C remained grossly unaltered. Finally, when a synaptobrevin 2-derived peptide comprising the PRS was titrated into a sample containing ^{15}N-labeled SH3B domain, line broadening could also be observed, though not to the same degree as for the full SNARE complex and only at a large excess of peptide (Figure 3e, S2c). These structural biochemical data confirm that intersectin 1

through its SH3B domain directly associates with the neuronal SNARE complex via multiple determinants that include the PRS of synaptobrevin 2 (Figure 3g).

Intersectin 1 association with the neuronal SNARE complex is required to prevent short-term depression.

To obtain insights into the physiological function of the association of intersectin 1 with the neuronal SNARE complex, we first tested whether intersectin 1, e.g. via SH3B domain association with the PRS of synaptobrevin 2, might alter SNARE complex formation. *In vitro* assembly and cellular experiments (Figure S2b, e) confirmed that the PRS of synaptobrevin 2 is dispensable for SNARE complex formation consistent with structural studies [29,30]. We were also unable to detect any effects of the purified SH3B domain of intersectin 1 on the rate or efficiency of SNARE complex formation *in vitro* (Figure S3a, b). Deletion of intersectin 1 in mice did not affect the levels of assembled neuronal SNARE complexes in mouse brain synaptosomal lysates (Figure S3c-f) or the number of cis-SNARE complexes detected by proximity ligation assays in hippocampal neurons derived from KO animals (Figure S3g, h). Moreover, we did not detect any changes in the expression levels of the SNARE disassembly factors NSF and α-SNAP in brain lysates from intersectin 1 KO mice (Figure S3i, j). These data are also consistent with the fact that loss of intersectin 1 does not impair basal neurotransmission monitored by electrophysiological or optical assays [27]. Hence, intersectin 1 does not affect SNARE complex assembly.

An important alternative function of intersectin 1 might be the clearance (e.g. by endocytic removal) of *cis*-SNARE complexes after exocytic fusion to facilitate the replenishment of release-ready SVs during fast neurotransmission. We directly probed this hypothesis by analyzing neurotransmission at the calyx of Held and in cultured hippocampal neurons following acute or sustained genetic interference with SNARE complex recognition by intersectin 1. To acutely interfere with intersectin 1-mediated recognition of the neuronal SNARE complex we microinjected its SH3B or SH3A-C domains into the calyx of Held and analyzed the effect of these perturbations on fast neurotransmission by simultaneous presynaptic and postsynaptic recordings using the paired pulse protocol described above. The recovery of the synaptic response during the second pulse was significantly reduced in calyces injected with the intersectin 1 SH3B domain (Figure 4a). Moreover, variation of the interstimulus interval (ISI) between two consecutive pulses to monitor SV replenishment following RRP depletion revealed a slow-down of the recovery of the FRP in SH3B- or SH3A-C- (consistent with [8]) injected calyces (Figure 4b), while recovery of the SRP proceeded unperturbed (Figure 4c). This phenotype strikingly resembles the phenotype elicited by injection of synaptobrevin 2 PRS antibodies (compare Figure 1) or a synaptobrevin 2-derived PRS peptide [23].

As acute protein or peptide-mediated perturbations may cause side-effects, we analyzed stimulation-induced exo-endocytosis in hippocampal neurons derived from intersectin 1 KO mice and in neurons selectively expressing mutant synaptobrevin 2 lacking its intersectin-binding PRS (ΔPRS). Primary hippocampal neurons expressing pHluorin-tagged SV proteins to monitor exocytosis/ endocytosis and subsequent reacidification were challenged with different stimulation trains and optical signals were recorded. Intersectin 1 KO neurons upon stimulation with 400 action potentials (APs) displayed normal kinetics of SV exo-endocytosis probed with synaptotagmin-pHluorin (Figure 4d). Similar results were obtained, if synaptobrevin 2-pHluorin was used as a sensor (Figure S4a) or if neurons were stimulated with 200 APs [31] or 10 APs at 20 Hz (Figure S4b). We then analyzed the effect of intersectin 1 loss on sustained neurotransmission in response to either single or multiple consecutive stimulus trains applied at different frequencies. We first applied a calibration stimulus of 50 APs followed by a 60 s recovery period and a 200 AP stimulation train applied at different frequencies. Normalization to the calibration stimulus provides a robust signal that is largely independent of initial release probability and the expression level of the pHluorin reporter [9]. High-frequency stimulation (200 APs, 40 Hz) of intersectin 1 KO neurons resulted in reduced exocytic neurotransmitter release monitored by synaptobrevin 2-pHluorin dequenching compared to neurons from WT littermates (Figure 4e, f). Importantly, no depression of neuroexocytosis was observed, if 200 APs were applied at a low frequency of 5 Hz (Figure 4g, h). A similar depression of fast neurotransmission was observed upon challenge of intersectin 1 KO neurons with six consecutive high-frequency trains of 40 APs (Figure 4i, j). These data show that intersectin 1 is required to prevent the rapid stimulation frequency-dependent depression of neurotransmission in hippocampal neurons, consistent with results from the calyx of Held [8].

What is the mechanism by which intersectin 1 prevents short-term depression of fast neurotransmission? Our biochemical data suggest that intersectin 1 may operate by binding and endocytic sorting of post-fusion SNARE complexes away from release sites. If this was the case, loss of intersectin 1 might result in the partial missorting of synaptobrevin 2 to the neuronal surface at steady-state as the pool of synaptobrevin 2 complexed with its cognate SNAREs cannot be recognized by its dedicated adaptors AP180/ CALM, which bind to the synaptobrevin 2 SNARE motif [32]. We probed the partitioning of synaptobrevin 2 between internal SV pools (i.e. quenched) and the neuronal surface using an established acid-quench protocol [32, 33]. This analysis revealed an elevated surface-stranded pool of synaptobrevin 2 in intersectin 1 KO neurons (Figure 5a), while synaptotagmin 1 was sorted normally (Figure S4c). Similar surface stranding was observed for mutant synaptobrevin 2 lacking its PRS (ΔPRS) in WT or intersectin 1 KO neurons (Figure 5a). These results are most consistent with a model, in which intersectin 1 serves to remove post-fusion SNARE complexes from the neuronal surface by

associating with the PRS of SNARE-complexed synaptobrevin 2 and this activity is required to prevent stimulation frequency-dependent depression of neurotransmission.

To test this, we analyzed the ability of intersectin 1 binding-defective synaptobrevin 2 (ΔPRS) to support high-frequency neurotransmission in hippocampal neurons depleted of endogenous synaptobrevin 2 (Figure S4d-f), a treatment that completely eliminates evoked exo-endocytic neurotransmission (Figure 5c, d). Re-expression of synaptobrevin 2 (ΔPRS) in synaptobrevin 2-knockdown neurons indeed mimicked the depression of synaptophysin-pHluorin exocytosis in response to high-frequency stimulation trains (i.e. 200 APs at 40 Hz) (Figure 5f, g) seen in intersectin 1 KO neurons (compare figure 4h,i), while the kinetics of SV endocytosis were unaltered (Figure 5e). To probe whether the exocytic depression was caused by defective clearance of surface-stranded SNARE complexes, or due to a reduced copy number of mutant synaptobrevin 2 (ΔPRS) molecules in SVs, we silenced neuronal activity by tetrodotoxin (TTX), a treatment that prevents the activity-dependent missorting of synaptobrevin 2 (ΔPRS) to the neuronal surface [33]. TTX was unable to rescue depression of fast neurotransmission in synaptobrevin 2 (ΔPRS)-expressing neurons, indicating that defective clearance of surface-stranded SNARE complexes rather than a reduced copy number of synaptobrevin 2 on SVs underlies this phenotype (Figure 5h, i).

These collective results show that intersectin 1 association with the neuronal SNARE complex via SH3-PRS interactions is required to prevent short-term depression during fast neurotransmitter release at central nervous system synapses.

Discussion

Previous data had identified a rapid retrograde action of endocytic proteins on vesicle replenishment during high-frequency neurotransmission under conditions of little or no vesicle reuse. These works have led to the proposal that endocytic factors such as dynamin and intersectin 1 [6,7,8,9,12] clear AZ release sites from previously exocytosed material. We present several lines of evidence that post-exocytic SNARE complexes represent part of this elusive material and are cleared by direct association with intersectin to allow rapid replenishment of release-ready SVs at AZs. We show that (i) intersectin 1 via association of its SH3B domain with the PRS of SNARE-complexed synaptobrevin 2 and additional, so far unidentified determinants, directly binds to assembled SNARE complexes without affecting SNARE assembly or disassembly itself. (ii) Acute interference with intersectin 1-SNARE complex association by injection of anti-synaptobrevin 2-PRS antibody Fab fragments or intersectin 1-SH3B into the calyx of Held synapse impairs replenishment of fast releasing SVs, akin to intersectin 1 KO. (iii) Finally, we demonstrate that intersectin 1 binding-defective synaptobrevin 2 (ΔPRS) is unable to support high-frequency neurotransmission in hippocampal neurons, consistent with the fact that

SNARE complex disassembly requires at least 100 ms [34,35] and, thus, would become rate-limiting at elevated firing frequencies above 20 Hz. These collective data provide strong support for the hypothesis that intersectin 1 clears release sites, at least in part, by its association with post-exocytic SNARE complexes. Non-retrieved *cis*-SNARE complexes which accumulate in the absence of intersectin 1 or upon deletion of the synaptobrevin 2-PRS could either jam release sites that may be unavailable for the recruitment of new release-ready SVs until SNARE complexes clogging the fusion zone have been removed or sequester important regulatory factors that bind to assembled SNAREs. It is possible, that the homologous intersectin 2 protein partially overlaps with intersectin 1 in clearing release sites from post-exocytic SNARE complexes. While the severe phenotype of intersectin 1/2 DKO mice [27] supports this idea, it has also prevented us from analyzing this possibility in detail. A further conclusion from our findings is that endocytic sorting of exocytosed synaptobrevin 2 is synergistically accomplished by AP180/ CALM and intersectin, which sort free [32,33] and SNARE-complexed synaptobrevin 2 molecules (this study), respectively. Consistent with this, we observe slightly elevated expression levels of intersectin 1 in brains from AP180 KO mice (Figure S3k, l).

How can the clearance process be envisioned in mechanistic terms? Intersectin 1 conceivably might target SNARE complexes for endocytosis, e.g. by associating via its SH3A and C domains[8,25] (i.e. sites that do not overlap with the binding site for the neuronal SNARE complex identified here) with dynamin, an endocytic protein known to be required for both release site clearance and presynaptic endocytosis, consistent with earlier studies [7,8,9,12,13,36]. In support of this model, we observe the partial activity-dependent missorting of synaptobrevin 2 lacking its intersectin-binding PRS to the neuronal surface, a phenotype mimicked by genetic KO of intersectin 1 (Fig. S5). At present, it is unclear whether the kinetics of presynaptic endocytosis reported to occur on timescales of hundreds of milliseconds to seconds[21,22,37,38] is compatible with the rapid clearance of release sites from SNARE complexes during fast neurotransmitter release. Hence, a second non-exclusive possibility is that intersectin 1 acts at a step directly preceding endocytosis, for example by facilitating the lateral movement of SNARE complexes away from AZ release sites prior to their endocytic removal or NSF-mediated disassembly. A model of intersectin 1-mediated endocytic removal of SNARE complexes from AZ release sites (Fig. S5) agrees well with the rapid short-term depression of neurotransmission in mutants lacking SNAP-25 [39] or the intersectin-binding partner dynamin [7], the accumulation of SNARE complexes on SVs in NSF mutants [20] (in line with the presence of both proteins on purified SVs [40], rapid depression of neurotransmitter release following peptide-mediated NSF inhibition [18,19], the previously identified (possibly indirect) association of intersectin with SNAP-25 *in vitro* [41], defects in release site clearance following injection of reagents that interfere with intersectin-dynamin complex formation [8], and reported endocytic defects in neurons acutely depleted of neuronal SNARE proteins [42]. Intersectin-mediated clearance of release sites likely acts in conjunction with other mechanisms, for example scavenging of non-SNARE-

complexed surface synaptobrevin 2 into oligomeric clusters by synaptophysin [26] and/ or the recently described complex between SCAMP5 and the endocytic adaptor AP-2 [11]. How precisely these mechanisms are coordinated with each other and with the multiple other roles of intersectin in the SV cycle [25, 27] remains an exciting area for future studies.

We predict that coupling of exocytosis and endocytosis by clearance of release sites from post-fusion SNARE complexes represents a crucial so far overlooked step that is required to sustain high-frequency neurotransmission. This process may be of particular importance for fast-firing synapses, e.g. in sensory information processing systems that fire at hundreds of Hz [4, 43, 44]. In support of this, we find that loss of intersectin-mediated release site clearance from post-fusion SNARE complexes to exhibit a much more pronounced presynaptic depression at the calyx of Held than at hippocampal synapses in cultured neurons (compare e.g. figures 1a, b or 4a, b with figures 4i, j and 5h, i). Furthermore, as excitatory and inhibitory neurons often display vastly different firing patterns, we further envision that defects in intersectin-mediated clearance of release sites from post-fusion SNARE complexes may conceivably lead to excitatory/ inhibitory imbalance often observed in neurological diseases ranging from epilepsy to autism spectrum disorders.

Methods

Antibodies

Antibodies	Source	Catalog number
Amphiphysin 1 (mouse monoclonal, used 10 µl in IP	C. David and P. DeCamilli	N/A
AP180 (mouse monoclonal, used 1:1000 in WB)	P. DeCamilli	N/A
Bassoon (guinea pig polyclonal, used at 1:100 in IF)	SySy	Cat# 141 004, RRID:AB_2290619
Bassoon (mouse monoclonal, used at 1:250 in IF)	SySy	Cat# 141 021, RRID:AB_2066979
Clathrin heavy chain (mouse monoclonal, used at 1:10 in WB)	This paper TD-1 bought hybridoma, self-purified	N/A
Dynamin 1 (rabbit polyclonal, used 1:1000 in WB)	D. Grabs and P. DeCamilli	N/A
Flag (mouse monoclonal, used at 1:200 in IF and PLA)	Sigma-Aldrich	Cat# F3165, RRID:AB_259529
GFP (chicken polyclonal, used 1:500 in IF)	Abcam	Cat# ab13970, RRID:AB_300798
Goat Anti-Chicken IgY H&L (Alexa Fluor® 488) ab150169 antibody	Abcam	Cat# ab150169, RRID:AB_2636803
Goat anti-Guinea Pig IgG (H+L) Highly Cross-Adsorbed Secondary Antibody, Alexa Fluor 568	Thermo Fisher Scientific	Cat# A-11075, RRID:AB_2534119
Goat anti-Mouse IgG (H+L) Highly Cross-Adsorbed Secondary Antibody, Alexa Fluor 568	Thermo Fisher Scientific	Cat# A-11031, RRID:AB_144696
Goat anti-Rabbit IgG (H+L) Cross-Adsorbed Secondary Antibody, Alexa Fluor 647	Thermo Fisher Scientific	Cat# A-21244, RRID:AB_2535812

HA-tag (mouse monoclonal, used 1:300 in PLA)	Covance Research Products Inc	Cat# MMS-101R-500, RRID:AB_10063630
Hsc70 (mouse monoclonal, used 1:3000 in WB)	Thermo Fisher Scientific	Cat# MA3-006, RRID:AB_325454
Intersectin 1 aa 1-440 (rabbit polyclonal, used 1:1000 in WB, 1:200 in IF, 10 µg in IP)	This paper	N/A
Intersectin 1 mAC (rabbit polyclonal, used 1:400 in IF)	This paper	N/A
NSF (rabbit polyclonal, used 1:1000 in WB)	SySy	Cat# 123 002, RRID:AB_887751
Peroxidase-AffiniPure Goat Anti-Mouse IgG (H + L) antibody	Jackson ImmunoResearch Labs	Cat# 115-035-003, RRID:AB_10015289
Peroxidase-AffiniPure Goat Anti-Rabbit IgG (H+L) antibody	Jackson ImmunoResearch Labs	Cat# 111-035-003, RRID:AB_2313567
SNAP25 (mouse monoclonal used 1:1000 in WB, 1:250 in IF)	SySy	Cat# 111 011, RRID:AB_887794
Synaptobrevin 1,2,3 (rabbit polyclonal, used 1:1000 in WB, 10 µg in IP)	SySy	Cat# 104 102, RRID:AB_887814
Synaptobrevin 2 (guinea pig polyclonal, used 1:100 in IF)	SySy	Cat# 104 204, RRID:AB_2212601
Synaptobrevin 2 (mouse monoclonal, used 1:1000 in WB)	SySy	Cat# 104 211, RRID:AB_887811
Synaptobrevin 2 (rabbit polyclonal, used 1:100 in IF)	SySy	Cat# 104 202, RRID:AB_887810
Synaptobrevin 2 N-terminal (Fab fragment)	Alexander Stein	N/A
Synaptophysin 1 (mouse monoclonal, used 1:5000 in WB)	SySy	Cat# 101 011, RRID:AB_887824
Synaptotagmin 1 (mouse monoclonal, used 1:250 in WB)	SySy	Cat# 105 011, RRID:AB_887832

Syntaxin 1 (mouse monoclonal used 10 µg in IP, 1:250 in IF)	SySy	Cat# 110 011, RRID:AB_887844
Syntaxin 1a (mouse monoclonal used 1:1000 in WB)	SySy	Cat# 110 111, RRID:AB_887848
Syntaxin 1a (rabbit polyclonal, used 1:2000 in WB)	SySy	Cat# 110 302, RRID:AB_887846
α/β-SNAP (mouse monoclonal, used 1:1000 in WB)	SySy	Cat# 112 111, RRID:AB_887783
β-Actin (mouse monoclonal, used 1:1000 in WB)	Sigma-Aldrich	Cat# A5441, RRID:AB_476744

Plasmids and siRNAs

Plasmids	**Reference**
pcDNA3 Synaptotagmin 1-pHluorin	Wienisch and Klingauf, 2006
Synaptophysin-pHluorin	L. Lagnado
pcDNA3 Synaptobrevin 2-pHluorin	Wienisch and Klingauf, 2006
pcDNA3 Synaptobrevin 2 ΔPRS-pHluorin	This paper
pcDNA3 Synaptobrevin 2-Flag	This paper
pcDNA3 Synaptobrevin 2 ΔPRS -Flag	This paper
pcDNA Syntaxin1a-HA	This paper
pCMV5-SNAP25	J. Burre and T. C. Südhof
pCMV5-Syntaxin1a	J. Burre and T. C. Südhof
pGEX-4T1 GST-Endophilin SH3	Pechstein et al., 2015
pGEX-4T1 GST-Intersectin SH3A	Pechstein et al., 2015
pGEX-4T1 GST-Intersectin SH3B	Pechstein et al., 2015
pGEX-4T1 GST-Intersectin SH3C	Pechstein et al., 2015
pGEX-4T1 GST-Intersectin SH3A-C	Pechstein et al., 2010
pGEX-4T1 GST-Intersectin SH3D-E	Pechstein et al., 2010
pET28a His-Intersectin SH3B	This paper

pET28a His-Synaptobrevin 2 aa1-96	R. Jahn
pET28a His-Synaptobevin 1 aa31-96	This paper
pET28a His-Syntaxin1a aa180-262	R. Jahn
pET28a His-SNAP25 aa1-206	R. Jahn
siRNA	**Source**
MISSION® siRNA Universal Negative Control	Sigma-Aldrich
siRNA: Synaptobrevin 2 #1: GUAAAUAGCCAGCUGUUAU	Sigma-Aldrich
siRNA: Synaptobrevin 2 #2: GCGCAUCCAGAUUGUGAAA	Sigma-Aldrich

Peptides and chemicals

Chemicals	**Source**	**Catalog number**
Tetrodotoxin	Tocris Bioscience	Cat# 1078
NEM	Sigma-Aldrich	Cat# E-1271
Peptides	**Source**	**Catalog number**
Synaptobrevin 2 PRS: MSATAATAPPAAPAGEGGPPAPPPNLT SNR	In-house peptide synthesis	N/A

Hippocampal neurons and HEK293T cells

Hippocampal neurons in culture: Neuronal cultures were prepared by surgically removing the hippocampi from postnatal mice (male or female) at p1-5, followed by trypsin digestion to dissociate individual neurons. Cultures were grown in MEM medium (Thermo Fisher) supplemented with 5% FCS and 2% B-27. 2 µM AraC were added to the culture medium at 2 days in vitro (DIV) to limit glial proliferation. Cells were transfected at DIV 7-9 using a calcium phosphate transfection kit (Promega).

HEK293T cells: HEK293T cells were obtained from ATCC (#CRL-3216™). Cells were cultured in DMEM with 4.5g/L glucose (Lonza) containing 10% heat-inactivated FBS (Gibco) and 100 U/ml penicillin, 100 µg/ml streptomycin (Gibco) during experimental procedures. HEK293T cells have a complex karyotype but due to the presence of multiple X chromosomes and the lack of any trace of Y chromosome derived sequence likely are of female origin.

Experimental procedures

Molecular cloning of constructs and siRNA experiments. The various intersectin 1 domains (human, amino acids (aa) 744-803 SH3A; 917-968 SH3B, 1006-1057 SH3C, 744-1057 SH3A-C; 1074-1211 SH3D-E) were subcloned from HA-intersectin 1L (pcDNA-3, kindly provided by Dr. Y. Groemping (MPI, Tübingen, Germany) into pGEX4T-1 (Amersham Biosciences). GFP-tagged intersectin 1 was a kind gift from P. McPherson (Montreal Neurological Institute, McGill University, Montreal, Canada).

His_6-tagged SNARE proteins [syntaxin (180-262 aa), synaptobrevin 2 (1-96), SNAP25 (1-206 aa)] were a generous gift from R. Jahn (Max Planck Institute, Göttingen, Germany). CMV-based expression plasmids encoding syntaxin1A and SNAP25 were a kind gift from J. Burre and T. C. Südhof (Stanford University, Palo Alto, CA). Flag-tagged synaptobrevin 2 (1-96) and synaptobrevin 2 ΔPRS (31-96 aa) were derived from synaptopHluorin (a kind gift from J. Klingauf, University of Münster, Münster, Germany) and were subcloned into pcDNA3. Synaptotagmin 1 fused to pHluorin was as well a kind gift from J. Klingauf (University of Münster, Münster, Germany). Synaptophysin 1 fused to pHluorin was kindly provided by L. Lagnado (MRC Laboratory of Molecular Biology, Cambridge, UK). Rat syntaxin 1a was cloned into the synaptopHluorin backbone vector and pcDNA-cHA.
A mix of siRNAs was used to knock down synaptobrevin 2 in hippocampal neurons.

Recombinant protein expression and purification. All GST-fusion proteins and His_6-tagged proteins were expressed in *Escherichia coli* and purified using GST-Bind resin (Novagen) and His-Select Nickel Affinity Gel (Sigma), respectively, according to the manufacturer's instructions. Proteins used in NMR experiments were additionally gel-filtrated on a Superdex75 16/60 or Superdex200 16/60 column (GE healthcare).

Generation of lysates for protein quantification by immunoblotting. Brains were homogenized in ice-cold homogenisation buffer (4 mM HEPES-NaOH pH 7.4, 320 mM sucrose, 1 mM PMSF, mammalian inhibitor cocktail (Sigma)) using a potter (20 strokes at 1000 rpm at 4°C). Large debris was removed by centrifugation at 900xg for 10 min at 4°C. To obtain whole brain lysate lysis buffer was added to the supernatant (final concentrations: 20 mM Hepes pH 7.4, 50 mM KCl, 2 mM MgCl2, 1 % Triton X100) and incubated for 30 min. After centrifugation at 265,000xg for 15 min at 4°C the protein concentration was measured by Bradford. For preparation of P2' lysate the supernatant after removal of large debris was centrifuged twice at 10000xg for 15 min at 4°C before addition of lysis buffer, incubation and final centrifugation at 265,000xg. For immunoblotting of the SDS-resistant SNARE complex P2' lysates of WT or ITSN1 KO mice brains were incubated at 37°C or 100 °C for 20 min.

Affinity chromatography and immunoprecipitations. For immunoprecipitation experiments antibodies were coupled to protein A/G PLUS Agarose (Santa Cruz Biotechnology) and incubated with 10-15 mg rat or mouse brain extract in buffer A (20 mM HEPES-NaOH, pH 7.4, 50 mM KCl, 2 mM $MgCl_2$, 1% Triton X-100, 1 mM PMSF, mammalian inhibitor cocktail (Sigma)) in a total volume of 1 ml for 2 h at 4°C. For experiments including calcium, lysates were incubated with 300 µM Ca^{2+} or 1 mM EGTA respectively. NEM was used in a concentration of 1 mM. Following extensive washes samples were eluted with sample buffer and analyzed by SDS/PAGE and immunoblotting.

For affinity chromatography or direct binding experiments 100 or 50 µg GST-fusion proteins were coupled to GST-Bind resin (Novagen) and incubated with 2 mg mice brain extract in a total volume of 1 ml or with 50 µg of *in vitro* assembled SNARE complex in a total volume of 300 µl for 1 h at 4°C on a rotating wheel. For the peptide competition assay GST-ITSN1-SH3A-C was incubated with different concentrations of synaptobrevin 2 PRS peptide or control peptide for 30 min before incubation with P2' lysate. Following extensive washes samples were eluted with sample buffer and analyzed by SDS/PAGE and immunoblotting.

***In vitro* SNARE complex assembly**. SNARE complexes were assembled *in vitro* by equimolar addition of purified syntaxin (180-262 aa), synaptobrevin 2 (1-96 aa) and SNAP25 (1-206 aa) and incubation for 48 h at 4°C on a rotating wheel (His-tags were cleaved before by thrombin incubation overnight.). For analysis of the kinetics of SNARE complex assembly *in vitro* a threefold excess of His_6-intersectin 1 SH3B was added to the reaction. Purified proteins and assembled SNARE complexes were analyzed by SDS-PAGE and staining with Coomassie Blue.

HEK cell transfection and immunoprecipitation. HEK cells were transfected with CMV-based expression plasmids encoding syntaxin1A, SNAP25 and Flag-synaptobrevin 2 WT or ΔPRS according to standard protocols. 12 h post-transfection cells were harvested and lysed in lysis buffer containing 0.05% saponin, 20 mM HEPES, pH 7.4, 130 mM NaCl, 10 mM NaF and 0.03% protease inhibitor cocktail. Debris was removed by centrifugation at 10,000xg for 15 min at 4°C. Same amounts of synaptobrevin WT and ΔPRS lysate were used for immunoprecipitation using specific antibodies against syntaxin1 and incubated for 2h at 4°C on a rotating wheel. Following extensive washes samples were eluted with sample buffer and analyzed by SDS-PAGE and immunoblotting.

Isolation and culture of primary hippocampal neurons and transfection. Hippocampal neurons were prepared from neonatal mouse brains (p1-p3) of the different genotypes. Hippocampi were rapidly dissected, placed into ice-cold HBSS containing 20% fetal bovine serum (FBS), and cut with a scalpel

into ca. 1 mm^3 sized pieces. The tissue pieces were washed first with HBSS containing 20% FBS and then with HBSS only and afterwards digested for 15 min in digestion buffer (137 mM NaCl, 5 mM KCl, 7 mM Na_2HPO_4, 25 mM HEPES, 5 mg/ml trypsin, 1500 units DNase) at 37°C, followed by another washing step with HBSS and gentle trituration with fire-polished Pasteur pipettes with decreasing tip diameter. 50,000 cells were plated as 25 µl drops per poly-L-lysine coated coverslip. 1 ml of plating medium (basic medium (MEM; 0.5% glucose; 0.02% $NaHCO_3$; 0.01% transferrin) containing 10% FBS, 2 mM L-glutamine, insulin and penicillin/streptomycin) was added 1 h after plating. After one day in vitro (DIV) 0.5 ml of plating medium was replaced by 0.5 ml of growth medium (basic medium containing 5% FBS; 0.5 mM L-glutamine; B27 supplement; penicillin/ streptomycin), and on DIV2 0.5 ml of growth medium containing additionally 2 µM Ara-C was added. On DIV7 0.5 ml of medium was replaced by growth medium containing 4 µM Ara-C. Neurons were maintained at 37°C in a 5% CO_2 humidified incubator until DIV14.

Neurons were transfected on DIV8-9 by calcium phosphate transfection using 6µg of DNA (6-well) and /or 3 µl of siRNA mix (100 µM), 250 mM $CaCl_2$ and water mixed with equal amounts of 2x HEPES buffered saline. The mix was incubated at room temperature for 20 min to allow precipitate formation while neurons were starved in NBA medium at 37°C, 5% CO_2 for the same time. Precipitates were added to neurons and incubated for 30 min at 37°C, 5% CO_2. After three final washing steps with HBSS medium neurons were transferred back to their conditioned medium. TTX was used in a final concentration of 1 µM for 4 days.

Immunostaining. Hippocampal neurons were fixed on DIV14 using 4% paraformaldehyde and 4% sucrose in PBS for 15 min at room temperature. After fixation neurons were blocked and permeabilized in PBS containing 10% goat serum and 0.3% Triton X-100 for 30 min. Fixed neurons were incubated with primary antibodies against proteins of interest for 1 h at room temperature. After washing with 1x PBS neurons were incubated with corresponding secondary antibodies for 1 h at room temperature. Following extensive washes coverslips were mounted using Immu-Mount (Thermo Fisher).

Electrophysiological analyses. Wister rats (postnatal days 8-11) were decapitated in accordance with the guidelines of the Physiological Society of Japan, and the animal experiments were approved by the committee of Doshisha University, Japan. Transverse brainstem slices (200 µm thickness) were obtained using a Leica VT1200S slicer (Leica Microsystems, Germany). During slicing, the brainstem was kept in ice-cold solution containing (in mM): 60 NaCl, 120 sucrose, 25 $NaHCO_3$, 1.25 NaH_2PO_4, 2.5 KCl, 25 glucose, 0.1 $CaCl_2$ and 3 $MgCl_2$. Slices were incubated at 37°C for 1-4 h in a standard extracellular solution containing (in mM): 125 NaCl, 2.5 KCl, 25 glucose, 25 $NaHCO_3$, 1.25 NaH_2PO_4, 0.4 ascorbic acid, 3 myoinositol and 2 Na-pyruvate (pH 7.4, gassed with 95% O_2 and 5% CO_2). Slices

were visualized on an upright microscope (BX-51, Olympus). Calyx of Held terminals were whole-cell voltage clamped at -80 mV using an EPC10/2 or EPS10/3 amplifier (HEKA, Germany) controlled by PatchMaster software (HEKA). The presynaptic patch pipettes (approximately 10 MΩ) were filled with intracellular solution containing (in mM): 135 Cs-gluconate, 20 TEA-Cl, 10 HEPES, 5 Na_2-phosphocreatine, 4 MgATP, 0.3 GTP, and 0.05, 0.5 EGTA (pH 7.2). During recordings, 1 µM TTX and 10 mM TEA-Cl were also included in the extracellular solution to block Na^+ and K^+ channels respectively. Various reagents (Fab fragments of antibody and SH3 domains of intersectin1) were included into the intracellular solution. The tip of the pipette was filled with reagent-free solution to improve giga-ohm sealing. Current recordings were acquired at a sampling rate of 20 kHz, after low-pass filtering at 6 kHz. Experiments were performed at room temperature. Fab fragments of the antibody raised against the N-terminus of synaptobrevin (2-17) were kindly supplied by Alexander Stein, in the Department of Neurobiology of the Max Planck Institute for Biophysical Chemistry. Intersectin1 SH3 domains were purified using His-Select Nickel Affinity Gel (Sigma). His-tags were removed by incubation with thrombin overnight.

pHluorin imaging of living hippocampal neurons. Hippocampal neurons at DIV13-15 were subjected to electrical field stimulation using an RC-47FSLP stimulation chamber (Warner Instruments) and imaged at room temperature in physiological imaging buffer [170 mM NaCl, 3.5 mM KCl, 0.4 mM KH_2PO_4, 20 mM N-Tris(hydroxy-methyl)-methyl-2-aminoethane-sulphonic acid (TES), 5 mM $NaHCO_3$, 5 mM glucose,1.2 mM Na_2SO_4, 1.2 mM $MgCl_2$, 1.3 mM $CaCl_2$, 10 µM CNQX, and 50 µM AP-5, pH 7.4] by epifluorescence microscopy [Nikon Eclipse Ti by MicroManager 4.11, eGFP filter set F36-526 and a sCMOS camera (Neo, Andor) equipped with a 40X oil-immersion objective]. Images were acquired every 2 s with 100 ms excitation at 488 nm. For evaluation of general exo- /endocytosis neurons were stimulated with 200 or 400 APs (40 Hz, 100 mA). ΔF was obtained by calculating ΔF = [F (data point fluorescence) - F0 (resting fluorescence)]. To investigate frequency dependency, neurons were stimulated with 50 APs (20 Hz, 100 mA) for normalization and after 1 min rest with 200 APs (40 Hz or 5 Hz, 100 mA). A train of six 40 APs (20 Hz, 100 mA) stimulations was used to investigate exocytic depression. Quantitative analysis of responding boutons was performed using ImageJ. Fluorescence intensities of responding boutons were corrected for background and photobleaching. To measure the steady state surface to total ratios, the surface-localized pHluorins (F_S) were first dequenched by replacing the extracellular solution TES by [2-(N-morpholino) ethanesulfonic acid] (pH 5.5). Secondly, to measure the total fluorescence of overexpressed pHluorins (F_T), 50 mM NaCl was replaced by NH_4Cl. The surface to total ratio was calculated as (baseline - F_S) / (F_T - F_S).

^{1}H-^{15}N HSQC NMR spectroscopy. Protein samples for NMR measurement were prepared in PBS with 50 mM NaCl and 0.5 mM EDTA, pH 7.4 + 10% (v/v) D_2O. ^{1}H, ^{15}N-HSQC spectra were recorded on a Bruker Ultrashield 700 Plus equipped with 5 mm triple-resonance cryoprobes. Measurements of ^{15}N-labeled intersectin 1 constructs were performed at 298 K at protein concentrations of 60 µM (SH3A-C) or 110 µM (SH3B). 1024x128 complex data points were acquired with 40 scans (SH3A-C) or 8 scans (SH3B) in each HSQC experiment. Unlabeled, preassembled SNARE complex was supplemented in an equimolar ratio. The assignment of the signals to the individual domains of the SH3A-C constructs was achieved by overlay of the spectrum with spectra of the isolated SH3 domains. The backbone assignment of the SH3B domain was published by us earlier [28].

Proximity ligation assay. Duolink® in situ kit from Sigma was used according to the standard protocol. Briefly, hippocampal neurons from WT and ITSN1 KO mice were transfected with Syb2-Flag, Stx1-HA and an empty GFP vector as transfection control. On DIV 14 neurons were fixed using 4% paraformaldehyde and 4% sucrose in PBS for 15 min at room temperature. After fixation neurons were blocked and permeabilized in PBS containing 10% goat serum and 0.3% Triton X-100 for 30 min. Fixed neurons were incubated with primary antibodies against Flag- and HA-tags for 1 h at room temperature. After washing with 1x PBS neurons were incubated with species specific PLA probes. Following a ligation and amplification reaction, coverslips were mounted using Immu-Mont (Thermo Fisher).

Statistical analyses. Quantifications for biochemical experiments were based on at least three independent experiments. Statistical data evaluation was performed using the Graph Pad Prism 5 software. If not stated otherwise in the figure legends, two-tailed student's t-tests were used to compare two groups. When several genotypes were compared, One-way ANOVA tests were followed by a Dunnett's Multiple Comparison Test to detect differences between experimental groups. When several groups were compared over time, a two-way RM ANOVA test followed by a Bonferroni multiple comparison test was used. The number of animals or cell cultures used is stated as n. Significant differences were accepted at; * < 0.05; ** < 0.01; *** < 0.005; **** < 0.0001; p>0.05 is not significant (ns).

References

1. Kopp-Scheinpflug C, Tolnai S, Malmierca MS, Rubsamen R. The medial nucleus of the trapezoid body: Comparative physiology. *Neuroscience* **154**, 160-170 (2008).

2. Lorteije JAM, Rusu SI, Kushmerick C, Borst JGG. Reliability and Precision of the Mouse Calyx of Held Synapse. *Journal of Neuroscience* **29**, 13770-13784 (2009).

3. Rancz EA, Ishikawa T, Duguid I, Chadderton P, Mahon S, Hausser M. High-fidelity transmission of sensory information by single cerebellar mossy fibre boutons. *Nature* **450**, 1245-U1212 (2007).

4. Haucke V, Neher E, Sigrist SJ. Protein scaffolds in the coupling of synaptic exocytosis and endocytosis. *Nat Rev Neurosci* **12**, 127-138 (2011).

5. Neher E. What is rate-limiting during sustained synaptic activity: vesicle supply or availability of release sites? *FNSYN* **2**, 1-6 (2010).

6. Hosoi N, Holt M, Sakaba T. Calcium dependence of exo- and endocytotic coupling at a glutamatergic synapse. *Neuron* **63**, 216-229 (2009).

7. Kawasaki F, Hazen M, Ordway RW. Fast synaptic fatigue in shibire mutants reveals a rapid requirement for dynamin in synaptic vesicle membrane trafficking. *Nature Neuroscience* **3**, 859-860 (2000).

8. Sakaba T*, et al.* Fast neurotransmitter release regulated by the endocytic scaffold intersectin. *P Natl Acad Sci USA* **110**, 8266-8271 (2013).

9. Hua YF, Woehler A, Kahms M, Haucke V, Neher E, Klingauf J. Blocking Endocytosis Enhances Short-Term Synaptic Depression under Conditions of Normal Availability of Vesicles. *Neuron* **80**, 343-349 (2013).

10. Jung SY*, et al.* Disruption of adaptor protein 2 mu (AP-2 mu) in cochlear hair cells impairs vesicle reloading of synaptic release sites and hearing. *Embo J* **34**, 2686-2702 (2015).

11. Park D*, et al.* Impairment of Release Site Clearance within the Active Zone by Reduced SCAMP5 Expression Causes Short-Term Depression of Synaptic Release. *Cell Rep* **22**, 3339-3350 (2018).

12. Wu LG, Hamid E, Shin W, Chiang HC. Exocytosis and Endocytosis: Modes, Functions, and Coupling Mechanisms. *Annu Rev Physiol* **76**, 301-331 (2014).

13. Dittman J, Ryan TA. Molecular circuitry of endocytosis at nerve terminals. *Annu Rev Cell Dev Biol* **25**, 133-160 (2009).

14. Jahn R, Fasshauer D. Molecular machines governing exocytosis of synaptic vesicles. *Nature* **490**, 201-207 (2012).

15. Jahn R, Scheller RH. SNAREs--engines for membrane fusion. *Nat Rev Mol Cell Biol* **7**, 631-643 (2006).

16. Owald D, Sigrist SJ. Assembling the presynaptic active zone. *Curr Opin Neurobiol*, (2009).

17. Weber T*, et al.* SNAREpins are functionally resistant to disruption by NSF and alpha SNAP. *J Cell Biol* **149**, 1063-1072 (2000).

18. Kuner T, Li Y, Gee KR, Bonewald LF, Augustine GJ. Photolysis of a caged peptide reveals rapid action of N-ethylmaleimide sensitive factor before neurotransmitter release. *Proc Natl Acad Sci U S A* **105**, 347-352 (2008).

19. Schweizer FE, Dresbach T, DeBello WM, O'Connor V, Augustine GJ, Betz H. Regulation of neurotransmitter release kinetics by NSF. *Science* **279**, 1203-1206 (1998).

20. Littleton JT, Chapman ER, Kreber R, Garment MB, Carlson SD, Ganetzky B. Temperature-sensitive paralytic mutations demonstrate that synaptic exocytosis requires SNARE complex assembly and disassembly. *Neuron* **21**, 401-413 (1998).

21. Watanabe S*, et al.* Ultrafast endocytosis at mouse hippocampal synapses. *Nature* **504**, 242-+ (2013).

22. Soykan T*, et al.* Synaptic Vesicle Endocytosis Occurs on Multiple Timescales and Is Mediated by Formin-Dependent Actin Assembly. *Neuron* **93**, 854-+ (2017).

23. Wadel K, Neher E, Sakaba T. The coupling between synaptic vesicles and Ca2+ channels determines fast neurotransmitter release. *Neuron* **53**, 563-575 (2007).

24. Sakaba T, Stein A, Jahn R, Neher E. Distinct kinetic changes in neurotransmitter release after SNARE protein cleavage. *Science* **309**, 491-494 (2005).

25. Pechstein A, Shupliakov O, Haucke V. Intersectin 1: a versatile actor in the synaptic vesicle cycle. *Biochem Soc Trans* **38**, 181-186 (2010).

26. Rajappa R, Gauthier-Kemper A, Boning D, Huve J, Klingauf J. Synaptophysin 1 Clears Synaptobrevin 2 from the Presynaptic Active Zone to Prevent Short-Term Depression. *Cell Rep* **14**, 1369-1381 (2016).

27. Gerth F*, et al.* Intersectin associates with synapsin and regulates its nanoscale localization and function. *Proc Natl Acad Sci U S A* **114**, 12057-12062 (2017).

28. Pechstein A*, et al.* Vesicle uncoating regulated by SH3-SH3 domain-mediated complex formation between endophilin and intersectin at synapses. *EMBO Rep* **16**, 232-239 (2015).

29. Sudhof TC, Rizo J. Synaptic Vesicle Exocytosis. *Csh Perspect Biol* **3**, (2011).

30. Sutton RB, Fasshauer D, Jahn R, Brunger AT. Crystal structure of a SNARE complex involved in synaptic exocytosis at 2.4 A resolution. *Nature* **395**, 347-353 (1998).

31. Jakob B*, et al.* Intersectin 1 is a component of the Reelin pathway to regulate neuronal migration and synaptic plasticity in the hippocampus. *Proc Natl Acad Sci U S A* **114**, 5533-5538 (2017).

32. Koo SJ*, et al.* SNARE motif-mediated sorting of synaptobrevin by the endocytic adaptors clathrin assembly lymphoid myeloid leukemia (CALM) and AP180 at synapses. *P Natl Acad Sci USA* **108**, 13540-13545 (2011).

33. Koo SJ*, et al.* Vesicular Synaptobrevin/VAMP2 Levels Guarded by AP180 Control Efficient Neurotransmission. *Neuron* **88**, 330-344 (2015).

34. Choi UB*, et al.* NSF-mediated disassembly of on- and off-pathway SNARE complexes and inhibition by complexin. *Elife* **7**, (2018).

35. Vivona S, Cipriano DJ, O'Leary S, Li YH, Fenn TD, Brunger AT. Disassembly of all SNARE complexes by N-ethylmaleimide-sensitive factor (NSF) is initiated by a conserved 1:1

interaction between alpha-soluble NSF attachment protein (SNAP) and SNARE complex. *J Biol Chem* **288**, 24984-24991 (2013).

36. Ferguson SM*, et al.* A selective activity-dependent requirement for dynamin 1 in synaptic vesicle endocytosis. *Science* **316**, 570-574 (2007).

37. Delvendahl I, Vyleta NP, von Gersdorff H, Hallermann S. Fast, Temperature-Sensitive and Clathrin-Independent Endocytosis at Central Synapses. *Neuron* **90**, 492-498 (2016).

38. Yamashita T, Hige T, Takahashi T. Vesicle endocytosis requires dynamin-dependent GTP hydrolysis at a fast CNS synapse. *Science* **307**, 124-127 (2005).

39. Kawasaki F, Ordway RW. Molecular mechanisms determining conserved properties of short-term synaptic depression revealed in NSF and SNAP-25 conditional mutants. *P Natl Acad Sci USA* **106**, 14658-14663 (2009).

40. Takamori S*, et al.* Molecular anatomy of a trafficking organelle. *Cell* **127**, 831-846 (2006).

41. Okamoto M, Schoch S, Sudhof TC. EHSH1/intersectin, a protein that contains EH and SH3 domains and binds to dynamin and SNAP-25 - A protein connection between exocytosis and endocytosis? *J Biol Chem* **274**, 18446-18454 (1999).

42. Xu JH*, et al.* SNARE Proteins Synaptobrevin, SNAP-25, and Syntaxin Are Involved in Rapid and Slow Endocytosis at Synapses. *Cell Rep* **3**, 1414-1421 (2013).

43. Matthews G, Fuchs P. The diverse roles of ribbon synapses in sensory neurotransmission. *Nat Rev Neurosci* **11**, 812-822 (2010).

44. Moser T, Starr A. Auditory neuropathy - neural and synaptic mechanisms. *Nat Rev Neurol* **12**, 135-149 (2016).

Acknowledgements

We thank Sabine Hahn, Delia Loewe and Claudia Schmidt for technical assistance, Drs. O. Shupliakov (Karolinska Institute, Stockholm, Sweden), T. C. Südhof (Stanford University, Stanford, CA, USA) and R. Jahn (Max Planck Institute for Biophysical Chemistry, Göttingen, Germany), for reagents, and Drs. G. Ahnert-Hilger (Charite Universitätsmedizin Berlin, Germany) and M. A. Pritchard (Monash University, Melbourne, Australia) for the synaptophysin and intersectin 1 knockout (KO) mice, respectively. Supported by grants from the Japan Society for Promotion of Science (JSPS) core-to-core program Advanced Research Networks (to T.S.) and the German Research Foundation (DFG) (SFB958/ A07 to C.F. and V.H. and SFB958/A01 to T.M. and V.H.).

Author contributions

M.J. performed all neuronal imaging experiments including confocal and pHluorin imaging aided by S.J.K.. T.S. planned and conducted all electrophysiological experiments together with L.Y.. M.J. and J.B. aided by T.M. carried out most biochemical experiments. F.G. and C.F. designed, carried out and analyzed the NMR experiments. T.S. C.F. and V.H. designed the study and analyzed data. M.J. and. V.H. wrote the manuscript with input from all authors.

Competing interests

The authors declare no competing interests.

Materials & Correspondence

Requests for materials and correspondence should be addressed to: V.H. (haucke@fmp-berlin.de).

Figures

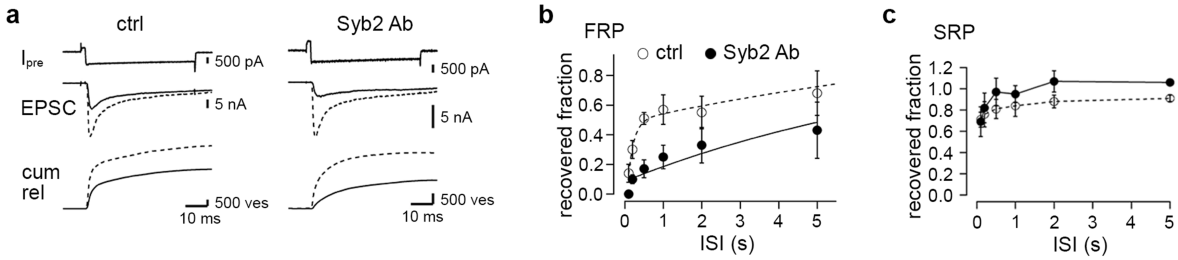

Figure 1 | Replenishment of fast-releasing SVs is impaired by antibodies targeting the proline-rich segment (PRS) of synaptobrevin 2. (a) A dual pulse protocol was used to examine SV replenishment following depletion of the RRP. The calyx of Held terminal was depolarized from -80 mV to +70 mV for 2 ms, followed by repolarization to 0 mV for 50 ms. Calcium (Ca) currents were elicited during the 0 mV period (top panel: Ipre). In response to Ca influx, EPSCs were evoked (middle panel), and cumulative release (bottom panel: cum rel) was calculated from the EPSC trace by deconvolution. Dotted line: first stimulation, solid line: second stimulation with an interval of 500 ms. Left and right panels show the data from control (ctrl) and Fab antibody (Ab) fragments targeting the PRS of synaptobrevin 2 (Syb2 Ab, 20 µg/ml in the presynaptic patch pipette), respectively. **(b, c)** The recovered fraction of the FRP **(b)** and the SRP **(c)** is plotted against the interval of the two pulses (ISI). The FRP and SRP were estimated by fitting a double exponential to the cumulative release traces (fast component and slow component). n=5 calyces from control and Syb2 Ab, respectively. Data represent mean ± SEM.

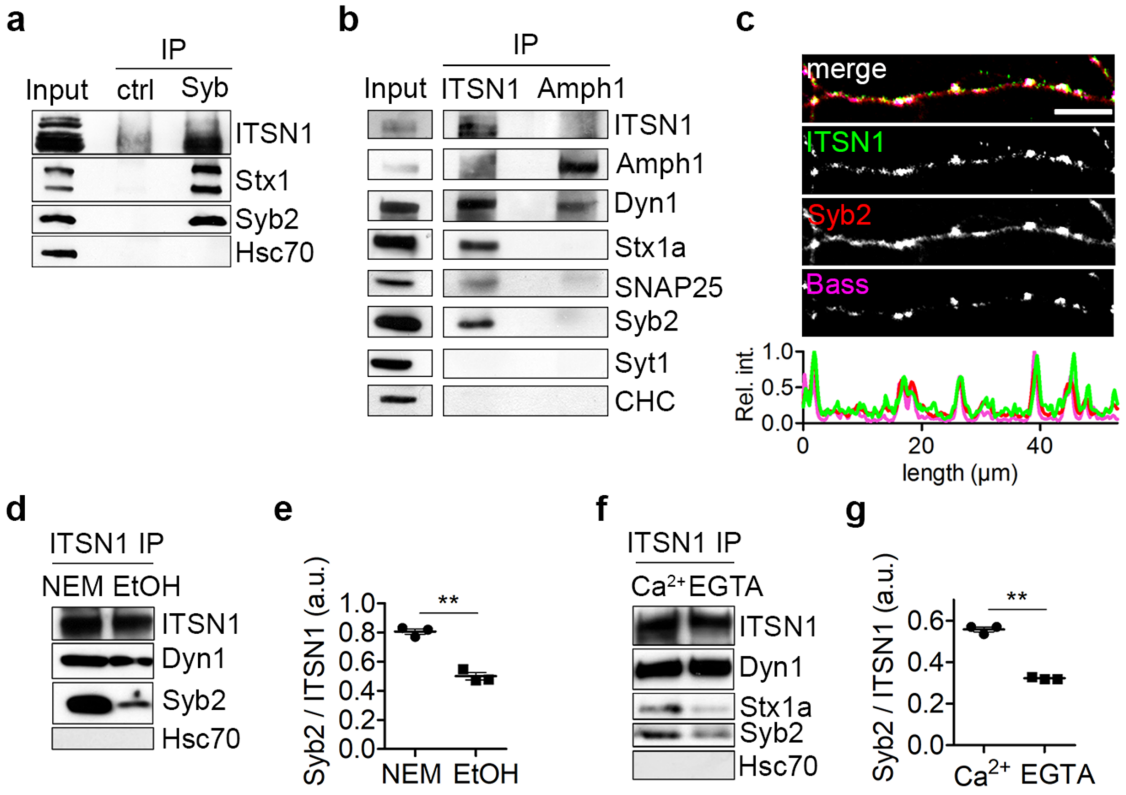

Figure 2 | Intersectin 1 associates with the neuronal SNARE complex. (a) Synaptobrevin 2 associates with intersectin 1. Immunoprecipitation from detergent-extracted rat brain lysates using either non-immune control antibodies or pan synaptobrevin 1, 2, 3 antibodies. Samples were analyzed by immunoblotting for intersectin 1 (ITSN1), syntaxin 1a (Stx1a), synaptobrevin 2 (Syb2) and heat shock cognate protein 70 (Hsc70). **(b)** Intersectin 1 co-immunoprecipitates with SNARE proteins. Immunoprecipitation from detergent-extracted synaptosomal P2' rat brain lysates using either specific antibodies against intersectin 1 (ITSN1) or amphiphysin 1 (Amph1). Samples were analyzed by immunoblotting for intersectin 1 (ITSN1), dynamin 1 (Dyn1), amphiphysin 1 (Amph1), syntaxin 1a (Stx1a), SNAP-25, synaptobrevin 2 (Syb2), synaptotagmin 1 (Syt1), or clathrin heavy chain (CHC). **(c)** Synaptobrevin 2 colocalizes with intersectin 1 at hippocampal synapses (upper). Hippocampal neurons were immunostained with antibodies against synaptobrevin 2 (Syb2), intersectin 1 (ITSN1), and the presynaptic active zone marker bassoon (Bass). Intensity line scans of representative axon segments show immunofluorescent spikes of synaptobrevin 2 (red), intersectin 1 (green), and bassoon (magenta). Scale bar, 10 µm. **(d, e)** Accumulation of assembled SNARE complexes in presence of NEM stimulates intersectin 1 complex formation with synaptobrevin 2. **(d)** Immunoprecipitation using intersectin 1-specific antibodies from detergent-extracted synaptosomal P2' rat brain lysates treated with 1 mM NEM or ethanol as control. Samples were analyzed by immunoblotting for intersectin 1 (ITSN1), dynamin 1

(Dyn1), synaptobrevin 2 (Syb2) and heat shock cognate protein 70 (Hsc70). **(e)** Data from n=3 independent experiments were quantified. Paired student's t-test, p= 0.0076; t=11.40; df=2. Data represent mean ± SEM. **(f, g)** Intersectin 1 complex formation with SNARE proteins is regulated by Ca^{2+}. **(f)** Immunoprecipitation from detergent-extracted synaptosomal P2' rat brain lysates using anti-intersectin 1 antibodies in the presence of Ca^{2+} or EGTA. Samples were analyzed by immunoblotting as in (d) and for syntaxin 1a (Stx1a). **(g)** Data from n=3 independent experiments were quantified. Paired student's t-test, p= 0.0041; t=15.51; df=2. Data represent mean ± SEM.

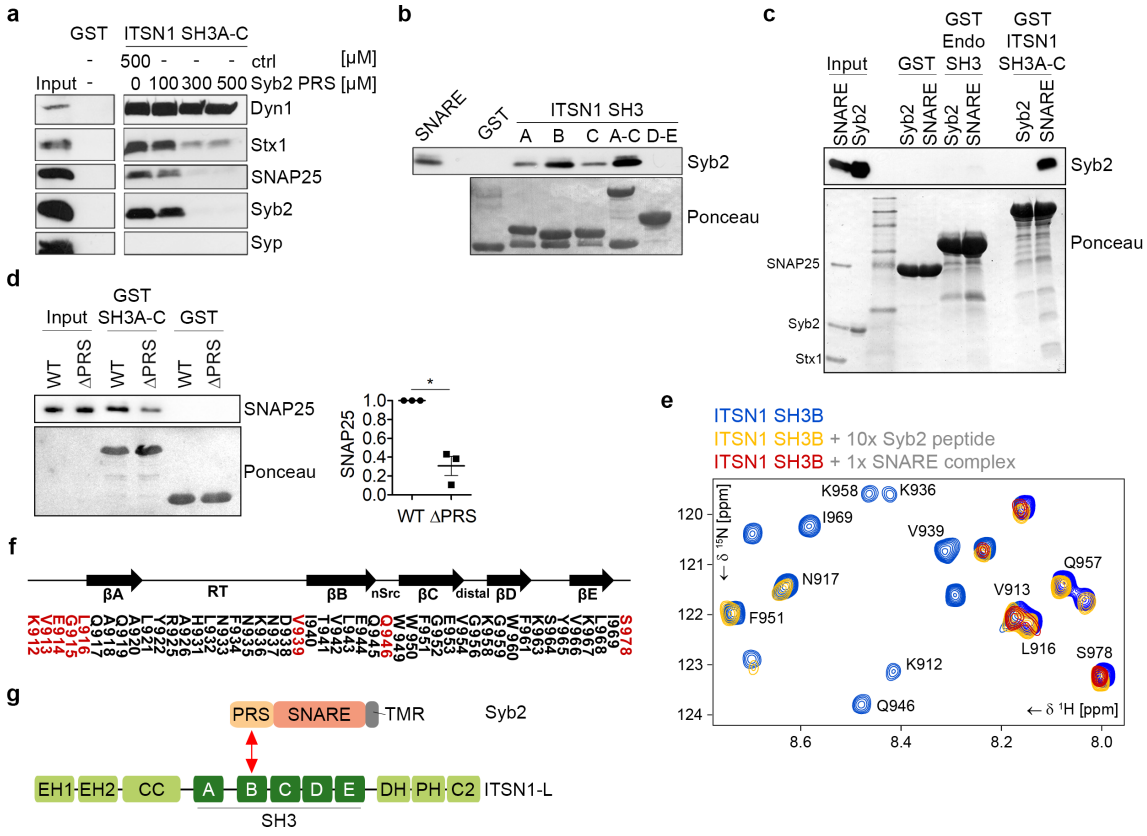

Figure 3 | Intersectin 1 directly binds to the neuronal SNARE complex via its SH3B domain and the proline-rich segment of synaptobrevin 2. (a) A peptide encompassing the N-terminal proline rich segment (PRS) of synaptobrevin 2 disrupts intersectin 1 binding to the neuronal SNARE complex. Immunoblot analysis of material affinity-purified via GST-intersectin 1 SH3A-C from detergent-extracted synaptosomal P2' rat brain lysates treated with increasing concentrations of synaptobrevin 2 PRS peptide or a control peptide. Samples were analyzed by immunoblotting for dynamin 1 (Dyn1), syntaxin 1a (Stx1a), SNAP25, synaptobrevin 2 (Syb2) and synaptophysin (Syp). **(b)** The assembled neuronal SNARE complex directly binds to the SH3B domain of intersectin 1. Immobilized GST-intersectin 1 SH3 domains were incubated with SNARE complex assembled in vitro. Samples were analyzed by immunoblotting using synaptobrevin 2-specific antibodies. **(c)** Intersectin 1 binds synaptobrevin 2 assembled into the SNARE complex but fails to associate with non-assembled synaptobrevin 2. Immobilized GST-intersectin 1 SH3A-C domains or GST-endophilin A1-SH3 (Endo-SH3) were incubated with SNARE complex assembled in vitro or with non-assembled synaptobrevin 2. Samples were analyzed by immunoblotting using synaptobrevin 2-specific antibodies. **(d)** Intersectin 1 binding to the neuronal SNARE complex is facilitated by the PRS of synaptobrevin 2. SNARE complexes assembled with synaptobrevin 2 lacking its PRS (ΔPRS) show reduced binding to the

intersectin 1 SH3A-C domain. Samples were analyzed by immunoblotting using SNAP25-specific antibodies. Quantified data from n=3 independent experiments. Paired student's t-test, p= 0.0175; t=7.464; df=2. Data represent mean ± SEM. **(e)** Selected region from assigned ^{1}H, ^{15}N-HSQC spectrum of intersectin 1 (ITSN1) SH3B (blue) overlaid with the spectrum after equimolar supplementation with the neuronal SNARE complex (red) or a 10-fold excess of synaptobrevin 2 PRS peptide (yellow, full spectrum in Figure S2C). **(f)** Schematic representation of the intersectin 1 SH3B domain structure with the amino acid sequence aligned. Residues with assigned signals that remained detectable after addition of the neuronal SNARE complex are highlighted in red. **(g)** Scheme showing the domain organization of synaptobrevin 2 and intersectin 1 and the domains involved in complex formation.

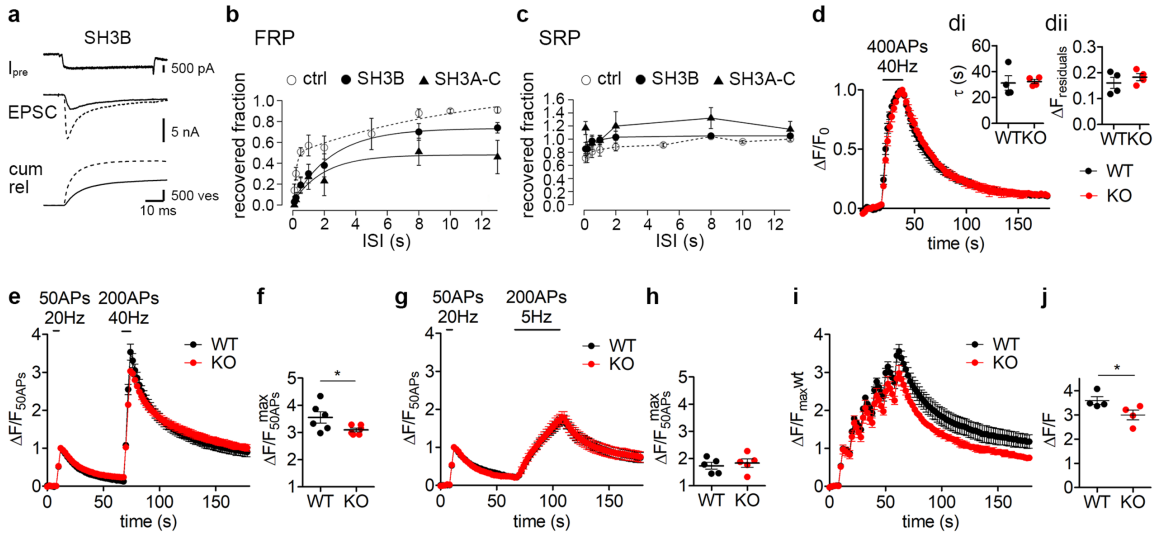

Figure 4 | Intersectin 1 association with the neuronal SNARE complex is required to prevent short-term depression. (a-c) Replenishment of fast-releasing SVs is impaired by the intersectin 1 SH3A-C or SH3B domains at the calyx of Held. (a) A dual pulse protocol was used to examine SV replenishment following depletion of the RRP in calyces injected with the SH3B domain of intersectin 1 (fig. 1a). Top, presynaptic Ca current (Ipre); middle panel: evoked postsynaptic EPSCs; bottom: cumulative release. Dotted line: first stimulation, solid line: second stimulation with an interval of 500 ms. (b,c) Kinetic analysis of FRP and SRP recovery. The recovery of the fast component of release (FRP) plotted against the stimulation interval is impaired (b), while that of the slow component is unaltered (c). Dotted, solid circles and solid triangles represent data from cells injected with control (n=8), SH3B (n=7) or SH3A-C (n=5) domain protein (5µg in the patch pipette), respectively. **(d)** Synaptotagmin 1-pHluorin endocytosis/ re-acidification is unaltered in intersectin 1 knockout (KO) hippocampal neurons. The endocytic time constant (di, p=0.8378; t=0.2231; df=3) and the residual fraction of non-retrieved synaptotagmin 1-pHluorin remaining on the neuronal surface post-stimulation (dii, p=0.1408; t=1.989; df=3) remain unchanged in absence of intersectin 1. Data are from n=4 independent experiments, Paired student's t-test. Data represent mean ± SEM. **(e-h)** Loss of intersectin 1 causes a frequency-dependent depression of exocytosis in hippocampal neurons. Average traces of synaptobrevin 2-pHluorin expressing neurons stimulated first with a 50 AP (20 Hz) train, followed by a 1 min rest and a second train of 200 APs given at high (40 Hz**, e)** or low frequency (5 Hz, **g**). Intersectin 1 KO hippocampal neurons show a significant exocytic depression compared to neurons from WT littermate controls when stimulated with high frequency **(f, h)**. Quantitative data from n=6 (40 Hz, p=0.0313) and n=5 (5 Hz, p=0.6250) independent experiments, Wilcoxon matched-pairs signed rank test. Data represent mean ± SEM. **(i, j)** Short-term exocytic depression of intersectin 1 KO hippocampal neurons in response to consecutive high-frequency trains. Average traces of synaptobrevin 2-pHluorin

expressing neurons stimulated with six consecutive 40 AP (20 Hz) trains (i). Intersectin 1 KO hippocampal neurons display significant short-term exocytic depression in response to consecutive high-frequency trains. (j) Quantitative data from n=4 independent experiments, Mann-Whitney test, p=0.0286. Data represent mean ± SEM.

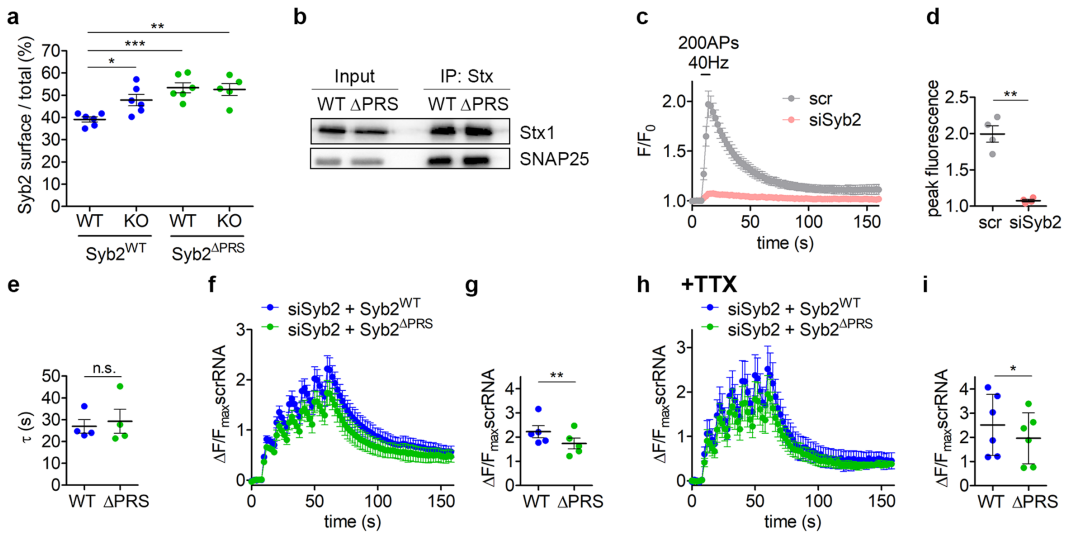

Figure 5 | Intersectin 1 association with the neuronal SNARE complex is required to prevent short-term depression and synaptobrevin 2 mislocalization. (a) Surface/ total protein ratio of pHluorin-tagged synaptobrevin 2 wild-type (WT)- or ΔPRS mutant in WT or intersectin 1 KO neurons. A significant fraction of synaptobrevin 2 is missorted to the neuronal surface in absence of intersectin 1 (KO) or upon mutational inactivation of its PRS that is required for association of synaptobrevin 2-containing SNARE complex with intersectin 1. Quantitative data (mean±SEM) from n=6 independent experiments are shown. One-way ANOVA, Dunnett's Multiple Comparison Test using ITSN1 WT, Syb2 WT data as control, F=8.991; df=3, 19. **(b)** WT and ΔPRS mutant synaptobrevin 2 form SNARE complexes with equal efficiency in living cells. Lysates of HEK293 cells co-expressing syntaxin 1A (Stx), SNAP25, and synaptobrevin 2 (Syb) WT or ΔPRS were subjected to immunoprecipitation using syntaxin 1 (Stx)-specific antibodies. Samples were analyzed by immunoblotting using syntaxin 1 and SNAP25 specific antibodies. **(c)** Depletion of synaptobrevin 2 impairs synaptophysin-pHluorin exocytosis upon stimulation with repetitive stimulation trains 200 APs at 40 Hz. Quantitative data from n=4 independent experiments are shown in **(d)**. Paired Student's t-test, p=0.0028; t=9.108; df=3. Data represent mean ± SEM. **(e)** Re-expression of WT or ΔPRS Syb2 does not alter the apparent kinetics of synaptophysin-pHluorin endocytosis following stimulation with 200 APs at 40 Hz. Quantitative data from n=4 independent experiments are shown. Paired student's t-test, p=0.4498; t=0.8669; df=3. Data represent mean ± SEM. **(f, g)** Hippocampal neurons expressing synaptobrevin 2 ΔPRS display short-term exocytic depression in response to consecutive high-frequency trains. Average fluorescence traces of synaptophysin-pHluorin expressed in hippocampal neurons depleted of endogenous synaptobrevin 2 and rescued by neuronal re-expression of FLAG-synaptobrevin 2 WT or ΔPRS mutant. Neurons were stimulated with six consecutive 40 AP (20 Hz) trains. Quantified data from n=5 independent

experiments is shown in **(g)**. Paired Student's t-test, p=0.0067; t=5.155; df=4. Data represent mean ± SEM. **(h, i)** Silencing of basal neuronal activity by TTX does not rescue exocytic depression in hippocampal neurons expressing synaptobrevin 2 ΔPRS. Average traces of synaptophysin-pHluorin-expressing neurons stimulated with 6x40 APs at 20 Hz. Neurons expressing synaptobrevin 2 ΔPRS display a reduced exocytic response. Quantified data from n=6 independent experiments is shown in **(i)**. Paired Student's t-test, p=0.0397; t=2.762; df=5. Data represent mean ± SEM.

Supplementary File for

Intersectin-mediated clearance of SNARE complexes is required for fast neurotransmission

Maria Jäpel, Fabian Gerth, Takeshi Sakaba, Jelena Bacetic, Lijun Yao, Seong-Joo Koo, Tanja Maritzen, Christian Freund and Volker Haucke

Inventory of supplementary items

Supplementary Figures

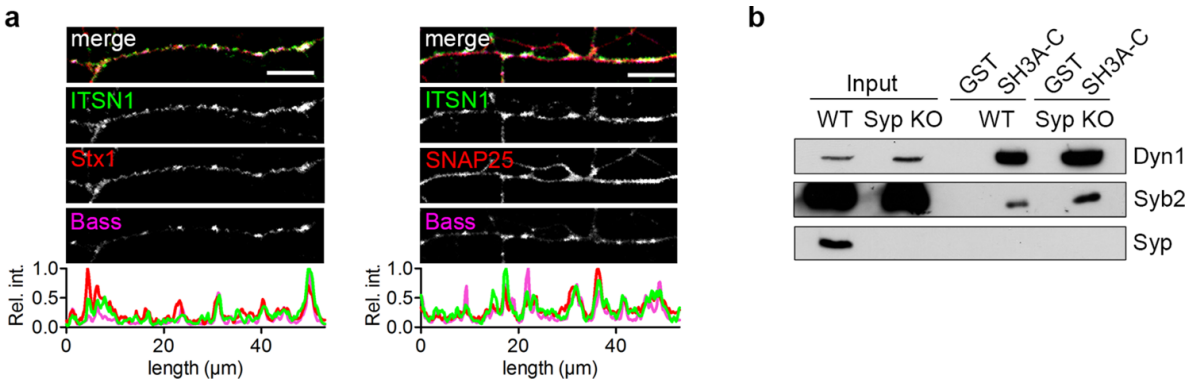

Supplementary figure S1 | Intersectin 1 colocalizes and associates with SNAREs

(a) Intersectin 1 colocalizes with SNARE proteins. Hippocampal neurons were immunostained with antibodies against intersectin 1 (ITSN1), syntaxin 1 (Stx1) or SNAP25, and the presynaptic active zone marker bassoon (Bass). Intensity line scans of representative axon segments show immunofluorescent spikes of intersectin 1 (green), syntaxin 1 or SNAP25 (red), and bassoon (magenta). Scale bar, 10 µm. **(b)** Intersectin 1 binding to the neuronal SNARE complex is independent of synaptophysin. Immobilized GST-intersectin 1 SH3A-C was incubated with detergent-extracted synaptosomal P2' rat brain lysates from wild-type (WT) or synaptophysin (Syp) KO mice. Samples were analyzed by immunoblotting.

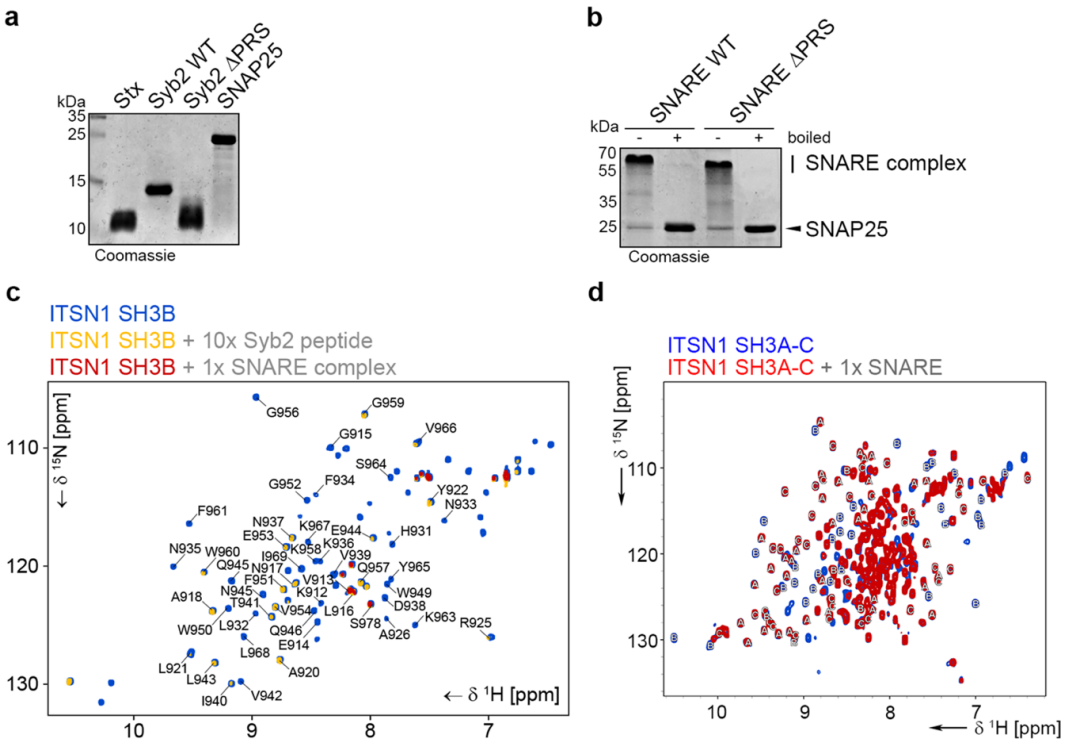

Supplementary figure S2 | Structural biochemical analysis of intersectin 1 association with the neuronal SNARE complex

(a) Coomassie blue-stained gel of purified SNARE proteins: Syntaxin 1a (Stx) amino acids (aa) 180-262, synaptobrevin 2 (Syb) WT aa1-96 or ΔPRS aa31-96, and SNAP25 aa1-206. **(b)** WT and ΔPRS mutant synaptobrevin 2 form SNARE complexes with equal efficiency. *In vitro* assembled SNARE complexes harboring WT or ΔPRS mutant synaptobrevin 2 were either boiled or non-boiled and analyzed by SDS-PAGE and staining with Coomassie Blue. Non-boiled samples reveal the formation of SDS-resistant SNARE complexes. **(c)** Assigned ^{1}H, ^{15}N-HSQC spectrum of intersectin 1 (ITSN1) SH3B (blue) overlaid with the spectrum after equimolar supplementation with the neuronal SNARE complex (red) or a 10-fold excess of synaptobrevin 2 PRS peptide (yellow, compare Figure 3E). **(d)** ^{1}H, ^{15}N-HSQC spectrum of uniformly labeled ITSN1 SH3A-C before (blue) and after (red) equimolar addition of unlabeled SNARE complex. Letters indicate the assignment of the signals to the individual SH3 domains.

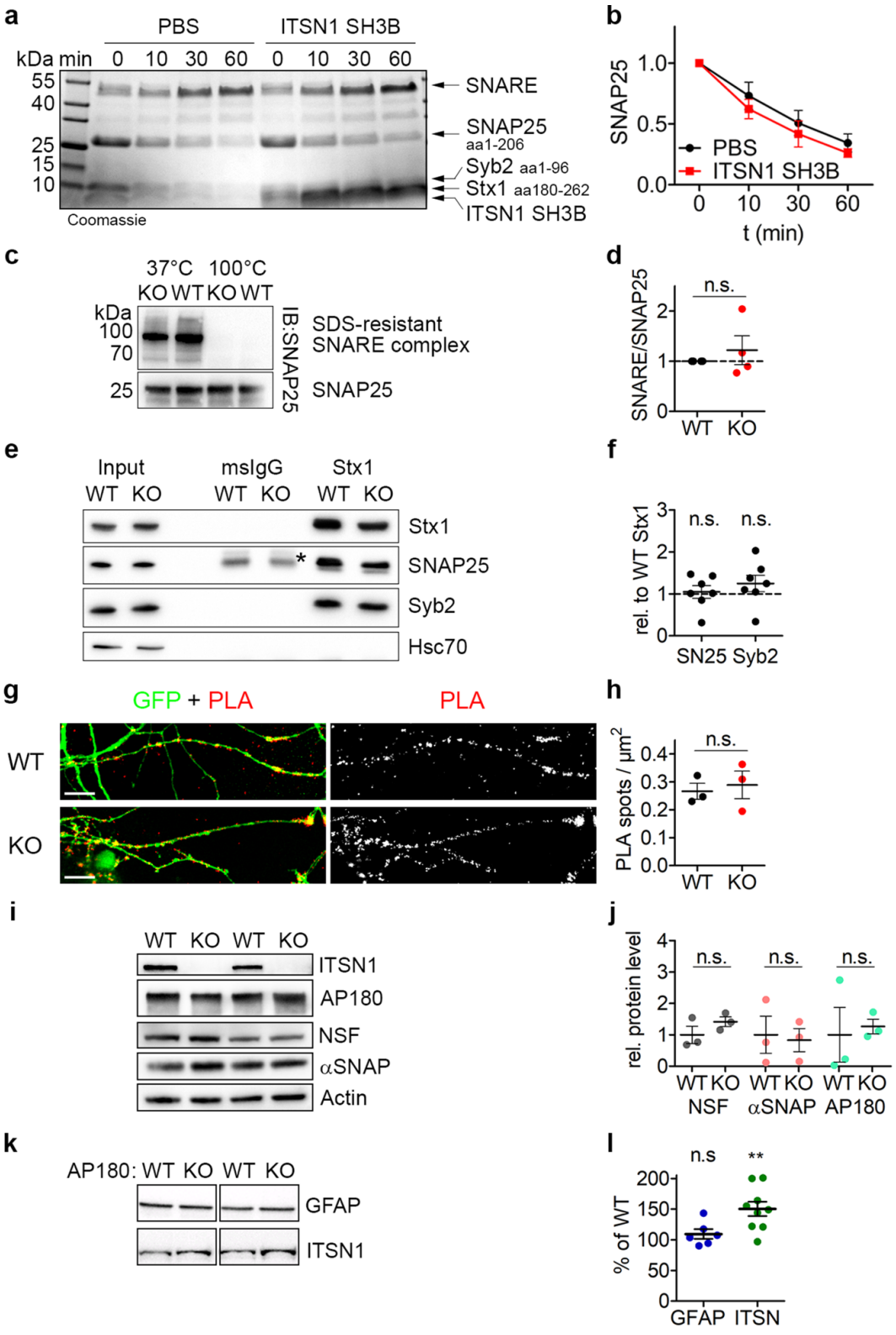
a
PBS
ITSN1 SH3B
kDa min 0 10 30 60 0 10 30 60
55
40
25
15
10
SNARE
SNAP25 aa1-206
Syb2 aa1-96
Stx1 aa180-262
ITSN1 SH3B
Coomassie
b
SNAP25
1.0
0.5
0.0
PBS
ITSN1 SH3B
0 10 30 60
t (min)
c
37°C 100°C
KO WT KO WT
kDa
100
70
25
IB:SNAP25
SDS-resistant SNARE complex
SNAP25
d
SNARE/SNAP25
n.s.
2
1
0
WT KO
e
Input msIgG Stx1
WT KO WT KO WT KO
Stx1
SNAP25
Syb2
Hsc70
*
f
rel. to WT Stx1
n.s. n.s.
3
2
1
0
SN25 Syb2
g
GFP + PLA
PLA
WT
KO
h
PLA spots / µm2
n.s.
0.4
0.3
0.2
0.1
0.0
WT KO
i
WT KO WT KO
ITSN1
AP180
NSF
αSNAP
Actin
j
rel. protein level
n.s. n.s. n.s.
4
3
2
1
0
WT KO WT KO WT KO
NSF αSNAP AP180
k
AP180: WT KO WT KO
GFAP
ITSN1
l
% of WT
n.s **
200
150
100
50
0
GFAP ITSN

Supplementary figure S3 | Intersectin 1 does not affect SNARE complex assembly or disassembly

(a, b) The SH3B domain of intersectin 1 (ITSN1) does not affect the rate of SNARE complex assembly in vitro. Representative Coomassie blue-stained SDS-PAGE gel illustrating the kinetics of SNARE complex assembly in vitro in the absence or presence of the SNARE-binding SH3B domain of intersectin 1 (a). Quantified data from n=3 independent experiments are shown in (b). Two-way ANOVA, Bonferroni post test using PBS data as control, F=0.58; df=3, 16. Data represent mean ± SEM. **(c-h)** The steady-state level of SNARE complexes is unaltered in ITSN1 KO brains. **(c, d)** Synaptosomal P2' extracts from WT and ITNS1 KO brains were incubated at 37°C (to preserve SNARE complexes) or 100°C for 20 min and analyzed by immunoblotting using SNAP25-specific antibodies. SDS-resistant SNARE complexes are detectable as a 90 kDa band that disappears upon boiling of the samples at 100°C (c). Quantified data (SNARE complex/ free SNAP25) from n=4 independent experiments are shown in (d). One-sample t-test, p=0.4985; t=0.7678; df=3. Data represent mean ± SEM. **(e, f)** SNARE complexes were isolated from detergent-extracted brain lysates from WT and ITSN1 KO mice by immunoprecipitation using syntaxin 1 (Stx1)-specific antibodies. Samples were analyzed by immunoblotting for syntaxin 1 (Stx1), SNAP25, synaptobrevin 2 (Syb2) and heat shock cognate 70 (Hsc70) (e). Quantified data from n=7 independent experiments are shown in (f). One-sample t-test for SNAP25: p=0.7662; t=0.3112; df=6. One-sample t-test for Syb2: p=0.2559; t=1.256; df=6. Data represent mean ± SEM. **(g, h)** Cis-SNARE complexes were visualized in hippocampal neurons from WT or ITSN1 KO mice by proximity ligation assays (PLA). Co-expression of synaptobrevin 2-FLAG and syntaxin 1A-HA (i.e. C-terminally tagged) allows selective detection of cis-SNARE complexes by PLA. eGFP was used as a control. Quantified PLA signals (red, g) are given as puncta per μm^2 in (h). Quantified data from n=3 independent experiments. Paired student's t-test, p=0.5267; t=0.7599; df=2. Data represent mean ± SEM. **(i, j)** Loss of intersectin 1 (ITSN1) in mice neither affects the steady-state levels of SNARE disassembly factors (NSF, αSNAP) nor those of the endocytic adaptor AP180. Brain lysates from WT and ITSN1 KO mice were analyzed by immunoblotting with antibodies specific for NSF, αSNAP, AP180, intersectin 1 (ITSN1) and actin taken as a control (i). Quantitative data from n=3 independent experiments are shown in (j). Paired Student's t-test for NSF: p= 0.4247; t=0.9947; df=2. Paired Student's t-test for αSNAP: p= 0.7616; t=0.3472; df=2. Paired Student's t-test for AP180: p= 0.8085; t=0.2759; df=2. Data represent mean ± SEM. (**k, l**) The steady state levels of intersectin 1 (ITSN1) are increased in AP180 KO brains. Brain

lysates from WT and AP180 KO mice were analyzed by immunoblotting with antibodies specific for intersectin1 (ITSN1) and Glial fibrillary acidic protein (GFAP) (k). ITSN1 levels are significantly increased compared to WT control samples (l). Data are from 6 (GFAP) and 9 (ITSN1) animals, Wilcoxon Signed Rank test for GFAP: p=0.4375 and for ITSN1: p=0.0078. Data represent mean ± SEM.

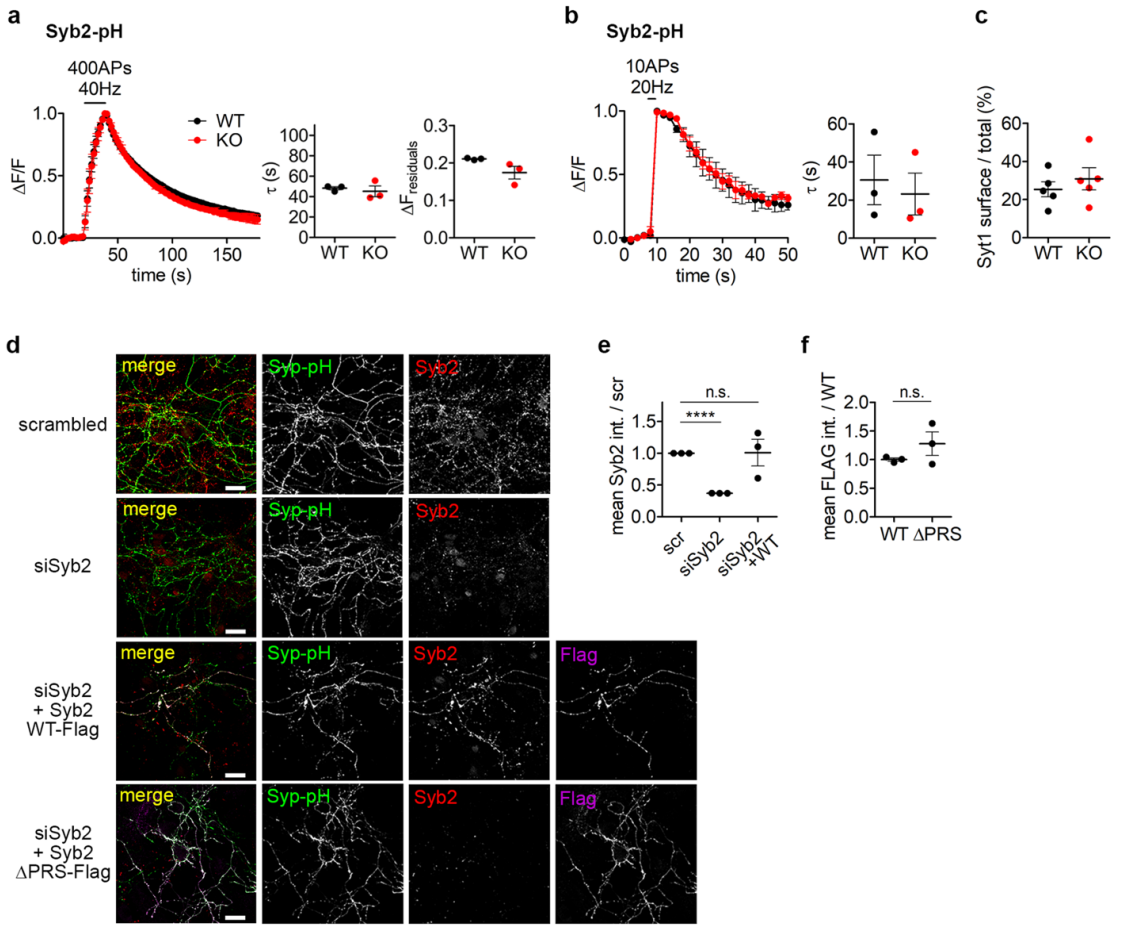

Supplementary figure S4 | Intersectin 1 loss does not cause a general impairment of SV exo- / endocytosis

(a-c) Loss of intersectin 1 does not affect the rate of SV endocytosis/ reacidification. (a, b) Time course of synaptobrevin (Syb) 2-pHluorin endocytosis/ reacidification in hippocampal neurons from WT or ITSN 1 KO mice induced by high (a) or low (b) frequency stimulation. The endocytic time constants (τ; 400 APs: p=0.5869; t=0.6416; df=2; 10 APs: p=0.1201; t=2.619; df=2) and the residual fraction of non-retrieved pHluorin molecules remaining on the surface ($\Delta F_{residuals}$; p=0.1801; t=2.025; df=2) are unchanged in ITSN1 KO neurons. Data are from n=3 independent experiments. Paired Student's t-test. Data represent mean ± SEM. (c) Loss of intersectin 1 does not affect the partitioning of synaptotagmin 1 (Syt1)-pHluorin between internal acidic compartments and the neuronal surface. The surface/ total fraction from n=3 independent experiments is plotted. Paired Student's t-test, p=0.0931; t=2.196; df=4. Data represent mean ±

SEM. **(d-f)** Efficacy of knockdown of synaptobrevin 2 (Syb2) and rescue by WT and ΔPRS synaptobrevin 2. Hippocampal neurons were co-transfected with specific siRNA targeting synaptobrevin 2 and plasmids encoding synaptophysin (Syp)-pHluorin and siRNA-resistant FLAG-synaptobrevin 2 WT or ΔPRS. Neurons were immunostained with antibodies against GFP, synaptobrevin 2 and FLAG (d). Re-expression of WT synaptobrevin 2 in hippocampal neurons depleted of endogenous synaptobrevin 2 restores normal synaptobrevin 2 levels. Data are from n=3 independent experiments. One-way ANOVA, Dunnett's Multiple Comparison Test using scrambled siRNA data as control; F=9.091; df=2; 6. Data represent mean ± SEM. (e). Synaptobrevin 2 WT and ΔPRS are expressed at similar levels. Data are from n=3 independent experiments. Paired Student's t-test, p=0.3313; t=1.272; df=2 (f). Data represent mean ± SEM.

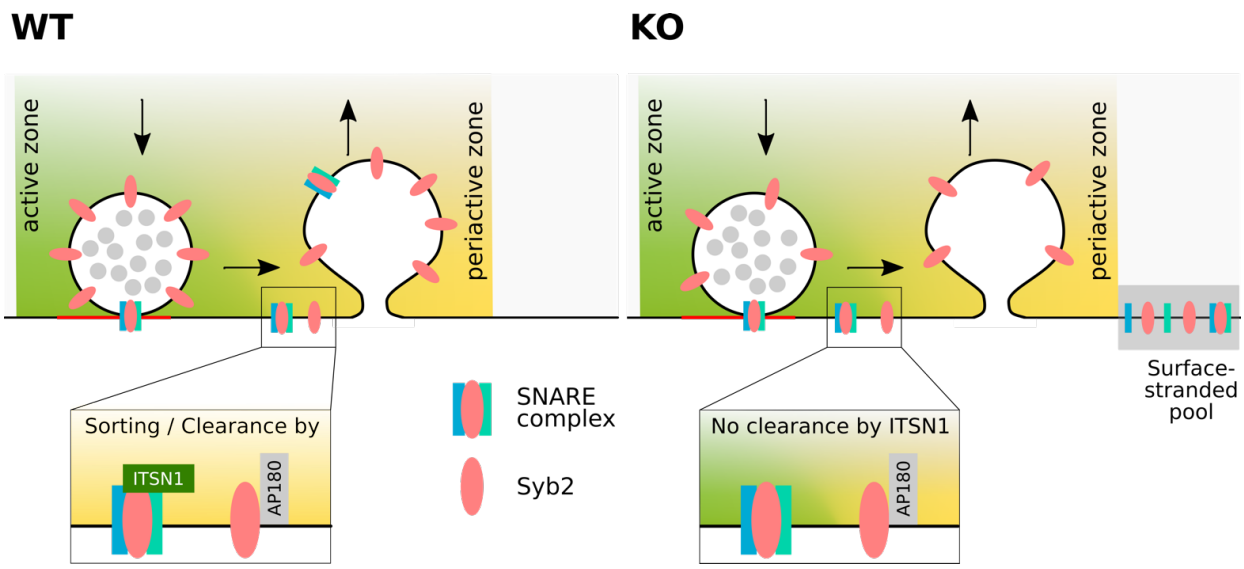

Supplementary figure S5 | Model for the intersectin-mediated clearance of neuronal SNARE complexes at active zone release sites. Left: During fast neurotransmission SNARE-complexed synaptobrevin 2 (Syb2) is endocytically sorted by intersectin 1 for rapid clearance of release sites. Right: In the absence of intersectin 1 (KO) endocytic sorting of SNARE-complexed synaptobrevin 2 (Syb2) is inpaired, resulting in a kinetic delay in release site clearance and an increased surface-stranded pool of synaptobrevin 2. Free synaptobrevin 2 not contained in SNARE complexes is sorted by dedicated endocytic adaptors such as AP180 in both genotypes.

4 Project III: Intersectin associates with synapsin and regulates its nanoscale localization and function

4.1 Overview of the project

The reserve pool of SVs is clustered in an activity dependent manner by the phosphoprotein synapsin. Also endocytic proteins, like intersectins, were shown to reside within the reserve pool, even though there function there remained enigmatic. In this publication we aimed to show the function of intersectin in regulating reserve pool clustering. We showed that the precise nanoscale localization of synapsin I is regulated by binding to intersectin under conditions of neuronal activity. This association is required for the proper replenishment of SVs from the reserve to the recycling pool of SVs and essential for sustained neurotransmission (Gerth et al., 2017).

Synapsins are phosphoproteins, which are essential for synaptic vesicle clustering and involved in synapse formation, maturation and plasticity (Cesca et al., 2010). There are three synapsin genes known in mammals, SYNI, II, III, which give rise to five different synapsin proteins via alternative splicing (Kao et al., 1999). These proteins are composed of a highly conserved N-terminus and a less conserved C-terminus. The N-terminal domain A shows the highest conservation among isoforms and species and is a target for protein kinase A (PKA) and Ca^{2+}/calmodulin-dependent protein kinase I and IV (CaMKI/IV) phosphorylation. Domain B is less conserved and is followed by the highly conserved domain C. The C-terminal part is alternatively spliced (domains D-J) and relatively different between the synapsin isoforms, yet they all carry a proline-rich domain (domain D in synapsin I) which is known to interact with several SH3 domain-containing proteins (Onofri et al., 2000). In brain mainly synapsin I and II are expressed and well characterized as SV binding proteins. The interaction of synapsins with SVs and actin is essential to build up the reserve pool of SVs. Phosphorylation by PKA at domain A negatively regulates synapsin's affinity to SV membranes and actin which leads under action potential conditions to an increase in SV mobility and refilling of the recycling vesicle pool. However, also phosphorylation at domain D by CaMKII is able to negatively regulate synapsin's ability to bind SVs (Cesca et al., 2010). In contrast,

Cdk5 phosphorylation of synapsin's domain D positively regulates synapsin's affinity for actin and thereby fine tunes the distribution of SVs between the recycling and the resting pool (Verstegen et al., 2014). Loss of synapsin causes the diffusion of synaptic vesicles into the axon away from the synapse which results in exocytic depression upon sustained stimulation (Hilfiker et al., 1999, Farisello et al., 2013).
Interestingly, the intersectin *drosophila melanogastor* homologue Dap160 has been implicated in reclustering of synapsin and SVs to the reserve pool by forming a complex with synapsin (Winther et al., 2015). In the present project we asked if intersectin also associates with synapsin in mammalian synapses and if so, which function this interaction has in hippocampal synapses.

We first investigated the possible interaction between synapsin I and intersectin 1 in the mammalian brain. Using specific antibodies against synapsin I and intersectin 1, respectively, we confirmed the interaction by endogenous immunoprecipitations. Additionally, we observed colocalization of both intersectin isoforms with synapsin at synapses of hippocampal neurons. As synapsin was shown before to interact with SH3 domain-containing proteins, we tested which of the five SH3 domains of intersectin 1 is involved in the binding. Synapsin I bound strongly to the SH3A domain of both intersectin isoforms. Furthermore, we probed which of the synapsin I domains is required for the association with intersectin 1 SH3A. Numerous synapsin I truncation mutants were tested. Only mutants lacking domain D were unable to associate with the SH3A domain. Domain D of synapsin I harbors three proline-rich peptide motifs (PRP) of which PRP2 is highly necessary for the interaction.
Following the characterization of the interaction we were interested in its physiological role in the synapse. Therefore, we generated a mouse line lacking both intersectin isoforms (using intersectin 2 KO as control). The expression of presynaptic proteins including synapsin I, the number and density of SVs as well as synapsin's ability to disperse and recluster upon stimulation were unaltered in intersectin 1/2 double KO (DKO) hippocampal neurons. Next, we made use of super-resolution stimulated emission depletion (STED) microscopy to investigate the nanoscale localization of synapsin I within the synapse of hippocampal neurons. As a control we labeled the active zone protein bassoon and the postsynaptic protein homer 1 which show a distance of around 120 nm in control and intersectin 1/2 DKO neurons. In contrast, the synapsin I localization in intersectin 1/2 DKO neurons showed a significant shift further away from the active zone marker bassoon while other intersectin 1 interaction partners did not show such a change. A similar shift was detected when an intersectin-binding-deficient mutant of synapsin I was expressed in WT neurons. This data reveals the importance of

the intersectin – synapsin I interaction for the proper positioning of synapsin within the synapse.
As synapsin was shown to be essential for the replenishment of the recycling SV pool, we investigated if the mislocalization of synapsin impairs synaptic transmission in acute slices of intersectin 1/2 DKO brains. While basal synaptic transmission was not impaired in intersectin 1/2 DKO slices, sustained stimulation resulted in a reduced cumulative amplitude of excitatory postsynaptic potentials (EPSP) after 500 pulses at 20 Hz. This data show, that intersectin, via its interaction with synapsin I, is needed for SV replenishment of the recycling pool from the reserve pool.

Intersectin was initially described to function in endocytosis; this so far unknown role of intersectin requires a mechanism regulating its different interactions. As most interactions in the synapse are regulated by activity-dependent phosphorylation/dephosphorylation, we investigated if changing phosphorylation conditions change intersectin's ability to associate with synapsin I. Indeed, intersectin 1 showed an increased binding to synapsin I under phosphorylation conditions in endogenous immunoprecipitations. Since we observed that phosphorylation of synapsin I by PKA or CaMKII is unlikely to be the reason for this increased binding, we hypothesized that phosphorylation of intersectin might cause a conformational change and enable binding. In line with the idea of a conformational change in intersectin, we detected a drastic decrease in the association between synapsin I and GST-SH3A-E compared to a GST-SH3A fusion protein. To elucidate if an intramolecular interaction within intersectin is responsible for this differences we applied NMR spectroscopy. We used intersectin 1 SH3A-E constructs in which SH3A was selectively labeled with ^{15}N and compared them to ^{15}N-SH3A alone. We detected shift changes that were larger than the changes we detected after addition of a fourfold excess of SH3B-E, which clearly speaks for an intra- instead of an intermolecular binding. Furthermore, we could map the binding epitope to the linker region between SH3A and SH3B. Specifically, we identified the first 20 amino acids of the linker to fold back onto the SH3A domain by a non-classical SH3 binding motif (PKLALR). We hypothesized that synapsin I only binds to intersectin 1 if the linker does not bind to the SH3A domain (open). As soon as the linker folds back, the SH3A domain is locked and an association with synapsin I is blocked. We confirmed this idea and could furthermore show that phosphorylation of two threonine residues in close proximity to the binding motif is responsible for the opening of SH3A. As expected, phosphomimetic mutants show increased binding to synapsin I. Interestingly, intersectin's association with the endocytic protein dynamin is not influenced by this phosphoregulated autoinhibition.

To prove the physiological importance of the phosphoregulated interaction between intersectin and synapsin I we generated different intersectin 1 mutants (open, locked), expressed them in intersectin 1/2 DKO hippocampal neurons and investigated the nanoscale distribution of synapsin I. While the WT intersectin 1 and the phosphomimetic 'open' intersectin 1 mutant could rescue the synapsin I localization, the non phosphorylatable 'locked' intersectin 1 mutant failed to rescue. To test this concept even further we used synaptophysin-pHluorin assays (Sankaranarayanan and Ryan, 2000) and analyzed the different SV pool sizes. Confirming our model, the recycling SV pool size was decreased in intersectin 1/2 DKO neurons. This phenotype was rescued by reexpression of WT intersectin 1 but not by reexpression of the synapsin-binding-deficient 'locked' mutant.

In summary, we show here the function and regulation of the so far unknown interaction between the scaffold protein intersectin and the SV-associated protein synapsin I in mammalian synapses. This interaction is tightly regulated by an intramolecular switch within intersectin enabling association of the two proteins only under conditions of neuronal activity. We suggest a model in which intersectin binds free synapsin I molecules, prevents them from premature reclustering of SVs and thereby facilitates replenishment of the recycling SV pool.

4.2 Original publication

Gerth, F.*; **Jäpel, M.***; Pechstein, A.*; Kochlamazashvili, G.; Lehmann, M.; Puchkov, D.; Onofri, F.; Benfenati, F.; Nikonenko, A.G.; Maritzen, T.; Freund, C.; Haucke, V.: Intersectin associates with synapsin and regulates its nanoscale localization and function. *Proceedings of the National Academy of Sciences*, 114(45), 2017 (* authors contributed equally to this work)
`https://doi.org/10.1073/pnas.1715341114`

Personal contribution

During this project I was mainly involved in the functional assays proving the importance of the interaction between intersectin 1 and synapsin I. I prepared primary hippocampal neuron cultures from newborn intersectin 1/2 DKO mice and respective control animals (intersectin 2 KO). These cultures I used for immunostainings showing that both intersectin isoforms colocalize with synapsin at synapses and to prove that the protein levels of synapsin I are unaltered in DKO neurons. The association with intersectin 2, I additionally showed by using GST-tagged SH3A domains of intersectin 1 and 2, respectively, and performing pulldown experiments from mice brain extracts. I also used primary hippocampal neuron cultures to demonstrate that dispersion and reclustering of synapsin I upon stimulation is not impaired in intersectin 1/2 DKO neurons. Furthermore, I performed immunostainings for super-resolution STED imaging to visualize synapsin and other intersectin interaction partners within the synapse. I rescued the observed synapsin specific phenotype by overexpressing WT intersectin 1. To prove the specificity of the interaction I also conducted rescue experiments with intersectin 1 mutants that were unable to rescue. Following transfection of hippocampal neurons, I also performed pHluorin experiments to show the altered size of the SV recycling pool as a consequence of synapsin mislocalization. Furthermore, I was able to restore this phenotype after coexpression with WT intersectin 1, but not with mutant intersectin 1.
Finally, I analyzed the data and was involved in designing figures, writing figure legends and the manuscript.

Intersectin associates with synapsin and regulates its nanoscale localization and function

Fabian Gerth[a,1], Maria Jäpel[b,1], Arndt Pechstein[a,b,1], Gaga Kochlamazashvili[b], Martin Lehmann[b], Dmytro Puchkov[b], Franco Onofri[c], Fabio Benfenati[c,d], Alexander G. Nikonenko[e], Kristin Fredrich[f], Oleg Shupliakov[f,g], Tanja Maritzen[b], Christian Freund[a,2], and Volker Haucke[a,b,2]

[a]Faculty of Biology, Chemistry, and Pharmacy, Freie Universität Berlin, 14195 Berlin, Germany; [b]Department of Molecular Pharmacology and Cell Biology, Leibniz-Forschungsinstitut für Molekulare Pharmakologie, 13125 Berlin, Germany; [c]Department of Experimental Medicine, University of Genoa, 16132 Genoa, Italy; [d]Center for Synaptic Neuroscience and Technology, Istituto Italiano di Tecnologia, 16163 Genoa, Italy; [e]Department of Cytology, Bogomoletz Institute of Physiology, 01024 Kiev, Ukraine; [f]Department of Neuroscience, Karolinska Institutet, 171 77 Stockholm, Sweden; and [g]Institute of Translational Biomedicine, St. Petersburg State University, 199034 St. Petersburg, Russia

Edited by Pietro De Camilli, Howard Hughes Medical Institute, Yale University, New Haven, CT, and approved September 28, 2017 (received for review September 1, 2017)

Neurotransmission is mediated by the exocytic release of neurotransmitters from readily releasable synaptic vesicles (SVs) at the active zone. To sustain neurotransmission during periods of elevated activity, release-ready vesicles need to be replenished from the reserve pool of SVs. The SV-associated synapsins are crucial for maintaining this reserve pool and regulate the mobilization of reserve pool SVs. How replenishment of release-ready SVs from the reserve pool is regulated and which other factors cooperate with synapsins in this process is unknown. Here we identify the endocytic multidomain scaffold protein intersectin as an important regulator of SV replenishment at hippocampal synapses. We found that intersectin directly associates with synapsin I through its Src-homology 3 A domain, and this association is regulated by an intramolecular switch within intersectin 1. Deletion of intersectin 1/2 in mice alters the presynaptic nanoscale distribution of synapsin I and causes defects in sustained neurotransmission due to defective SV replenishment. These phenotypes were rescued by wild-type intersectin 1 but not by a locked mutant of intersectin 1. Our data reveal intersectin as an autoinhibited scaffold that serves as a molecular linker between the synapsin-dependent reserve pool and the presynaptic endocytosis machinery.

neurotransmission | synaptic vesicles | multidomain scaffold | intramolecular regulation | NMR spectroscopy

Neurotransmission is based on the fusion of readily releasable synaptic vesicles (SVs) at the presynaptic active zone (1, 2). Fusing SVs are concomitantly replenished by compensatory endocytosis of SV membranes and clathrin-mediated reformation of SVs (3, 4). During sustained periods of activity the recycling vesicle pool is refilled by mobilization of SVs from the reserve pool (5). The synapsins (synapsin I, II, and III), are major SV-associated phosphoproteins encoded by three distinct genes that are required for the formation and maintenance of the reserve/recycling pools of SVs via association with the actin cytoskeleton (6–8). Activity-dependent phosphorylation of synapsin I by several kinases at distinct sites regulates its association with SV membranes and F-actin to control SV mobilization from the reserve pool (6). Consistently, loss of synapsin I causes depletion of reserve pool SVs and a marked impairment in inhibitory transmission (9, 10), resulting in an epileptic and autistic phenotype in mice (8, 11) and humans (12).

Endocytic proteins are enriched within the presynaptic compartment at steady state (13). Upon synaptic activity they are recruited to the so-called "periactive zone" that surrounds active zone (AZ) release sites to facilitate endocytic membrane internalization and SV reformation. Among the endocytic proteins shown to undergo activity-dependent movement to the periactive zone are intersectin 1 and 2, large scaffolds containing five Src homology domain 3 (SH3) domains (Fig. S1*A*), which bind to a plethora of exo/endocytic and actin regulatory proteins. Intersectins have been suggested to regulate actin dynamics and to couple the exo/endocytic limbs of the SV cycle (14). Intersectin 1 deletion in mice causes a comparably mild presynaptic phenotype (15, 16), while its overexpression is associated with Down syndrome in humans (17). Loss of Dap160, the *Drosophila melanogaster* homolog of mammalian intersectins, has been linked to defects in neurotransmission, SV cycling, and SV pool organization (18, 19), suggesting that intersectins serve as multifunctional scaffolds that coordinate different steps in the SV cycle (14). How these diverse functions of intersectin are controlled in molecular terms is unknown.

Here we combine mouse genetics, superresolution imaging, electrophysiology, and NMR-based structural studies to identify a key role for intersectin in SV replenishment at hippocampal synapses by regulated complex formation with synapsin I.

Results

Intersectin Associates with Synapsin I in Central Synapses. The molecular basis for the enrichment of endocytic proteins in nerve terminals (13) is unknown. Hence, we screened for possible interactions between known presynaptic components and the endocytic

Significance

Mutations in genes regulating neurotransmission in the brain are implicated in neurological disorders and neurodegeneration. Synapsin is a crucial regulator of neurotransmission and allows synapses to maintain a large reserve pool of synaptic vesicles. Human mutations in synapsin genes are linked to epilepsy and autism. How synapsin function is regulated to allow replenishment of synaptic vesicles and sustain neurotransmission is largely unknown. Here we identify a function for the endocytic scaffold protein intersectin, a protein overexpressed in patients with Down syndrome, as a regulator of synapsin nanoscale distribution and function that is controlled by a phosphorylation-dependent autoinhibitory switch. Our results unravel a hitherto unknown molecular connection between the machineries for synaptic vesicle reserve pool organization and endocytosis.

Author contributions: A.P., G.K., M.L., D.P., F.B., O.S., C.F., and V.H. designed research; F.G., M.J., A.P., G.K., D.P., and F.O. performed research; F.G., M.J., A.P., M.L., F.O., F.B., A.G.N., K.F., T.M., and C.F. contributed new reagents/analytic tools; F.G., M.J., A.P., G.K., M.L., D.P., C.F., and V.H. analyzed data; and C.F. and V.H. wrote the paper.

The authors declare no conflict of interest.

This article is a PNAS Direct Submission.

[1]F.G., M.J., and A.P. contributed equally to this work.

[2]To whom correspondence may be addressed. Email: christian.freund@fu-berlin.de or haucke@fmp-berlin.de.

This article contains supporting information online at www.pnas.org/lookup/suppl/doi:10.1073/pnas.1715341114/-/DCSupplemental.

NEUROSCIENCE

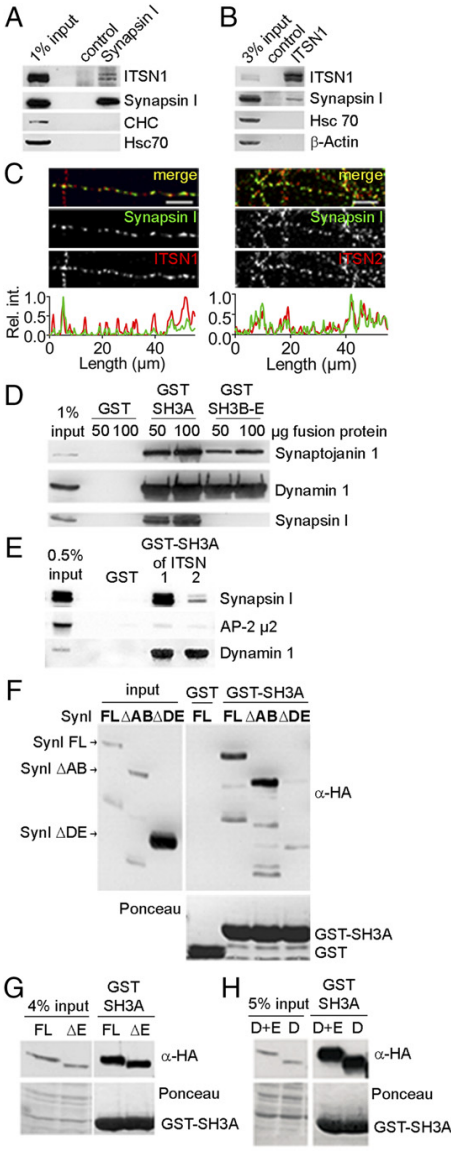

Fig. 1. Intersectin 1/2 associate with synapsin I. (*A* and *B*) Synapsin I and intersectin 1 form a complex. Immunoprecipitation from detergent-extracted rat brain lysates using specific antibodies. Samples were analyzed by immunoblotting. CHC, clathrin heavy chain; Hsc70, heat shock cognate protein 70; ITSN1, intersectin 1. (*C*) Intersectin 1 and 2 colocalize with synapsin I at hippocampal synapses. (*Upper*) Hippocampal neurons were immunostained with antibodies against synapsin I and intersectin 1 (*Left*) or 2 (*Right*). (*Lower*) Intensity line scans of representative axon segments show immunofluorescent spikes of synapsin 1 (green trace) and intersectin 1 or 2 (red trace). (Scale bars: 10 μm.) (*D*) Synapsin binds intersectin 1-SH3A. Immunoblots of pulldowns from rat brain extracts with immobilized GST fusion proteins. (*E*) As in *D* using GST-SH3A domains of intersectin 1 or 2 or GST as a control. (*F–H*) The intersectin 1-SH3A domain binds to the synapsin D domain. Shown are anti-HA immunoblots of pulldowns from detergent-extracted Cos7 cell lysates expressing the indicated synapsin Ia mutants. See Fig. S1*B*.

machinery. Mass spectrometry analysis and immunoblotting of native immunoprecipitates from brain lysates captured by antibodies (Tables S1 and S2) against the abundant presynaptic protein synapsin I identified the SH3 domain scaffold protein intersectin 1 as a synapsin-binding partner (Fig. 1*A*). Conversely, synapsin I was found in intersectin 1 immunoprecipitates (Fig. 1*B*). Moreover, synapsin I and intersectin 1 colocalized at synapses of cultured hippocampal neurons (Fig. 1*C*), consistent with the enrichment of both proteins within the presynaptic compartment at the ultrastructural level (20). Hence, intersectin and synapsin I are present in a complex at mammalian synapses in vivo, in agreement with the ability of synapsins to bind to SH3 domain-containing proteins (21).

Mammalian intersectin 1 contains five sequential SH3 domains (SH3A–E) (14) that enable interactions with proline-rich regions of exo/endocytic proteins. To assess if these SH3 domains mediate the formation of a complex with synapsin I, affinity purification experiments employing GST fusion proteins were performed. Synapsin I avidly bound to the isolated SH3A domain of intersectin 1, but not to an SH3B–E domain array (Fig. 1*D*). By contrast, the SH3 domain-binding endocytic proteins dynamin 1 and synaptojanin 1 interacted with either fusion protein (Fig. 1*D*). The SH3A domain of the closely related intersectin 2 also bound to synapsin I, albeit with reduced efficiency compared with intersectin 1 (Fig. 1*E*), in agreement with the partial colocalization of synapsin I with intersectin 1 and 2 at hippocampal synapses (Fig. 1*C*).

To identify the intersectin-binding determinants within synapsin I, we analyzed various truncation mutants of synapsin Ia for their ability to associate with intersectin 1-SH3A. Synapsin Ia is composed of five sequential domains, A–E (Fig. S1*B*) (6). Initial analysis of truncation mutants mapped the intersectin 1 binding to the distal D and E domains of synapsin Ia (Fig. 1*F* and Fig. S1*B*). Further truncation analysis revealed that domain E was dispensable (Fig. 1*G* and Fig. S1*B*), whereas the D domain was necessary and sufficient for the association of synapsin I with intersectin 1 (Fig. 1*H* and Fig. S1*B*).

SH3 domains are known to associate with proline-rich sequences, often flanked by basic residues. To elucidate the minimal sequence required for the interaction with intersectin 1, we searched the D domain for basic PxxP peptide (proline-rich peptide, PRP) motifs. We identified three such motifs in the D domain of synapsin Ia (Fig. S1*B*). Deletion of PRP2 in synapsin Ia significantly reduced intersectin 1 association, while simultaneous deletion of both PRP2 and PRP3 [full-length (FL) Δ*r*PRP2+3] abolished the interaction completely (Fig. S1*B*). Conversely, NMR spectroscopy confirmed the ability of PRS2 to directly bind to intersectin 1-SH3A (Fig. S1*C*).

We conclude that intersectin and synapsin associate via the recognition of proline-rich motifs within synapsin Ia that bind to the SH3A domain of intersectin 1.

Intersectin Regulates the Nanoscale Localization of Synapsin to Promote SV Replenishment. Based on the physical association of intersectin with synapsin I, we hypothesized that intersectin regulates synapsin function in vivo. To test this hypothesis, we generated intersectin 2-KO (hereafter "2KO") mice (Fig. S2*A*) and crossed them with intersectin 1-KO (hereafter, "1KO") mice (16) to obtain double-KO (DKO) mice lacking intersectins 1 and 2 (Fig. S2*B*). While 1KO or 2KO mice showed a Mendelian distribution and were viable and fertile, DKO mice were born well below Mendelian ratios (Fig. 2*A*), and the surviving animals suffered from decreased postnatal viability (Fig. 2*B*) and displayed reduced weight (Fig. 2*C*), in contrast to an earlier study using a Gene Trap-based intersectin 1 line (22). A significant weight reduction was already observed in compound KO mice lacking the two intersectin 1 alleles and one intersectin 2 allele (Fig. 2*C*). Furthermore, DKO mice displayed behavioral abnormalities such as strongly reduced digging (Fig. S2*C*), a phenotype related to autism spectrum disorders and also observed in synapsin-KO mice (11).

Loss of intersectins 1/2 did not affect the expression or presynaptic levels of SV proteins, including synapsin I, or any other exo/endocytic protein analyzed (Figs. S2*D* and S3*A*). Consistent with the normal SV protein levels, analysis by electron microscopy did not reveal overt differences in the total SV density or in the number of docked SVs at steady state (Fig. S3*B*). Although not

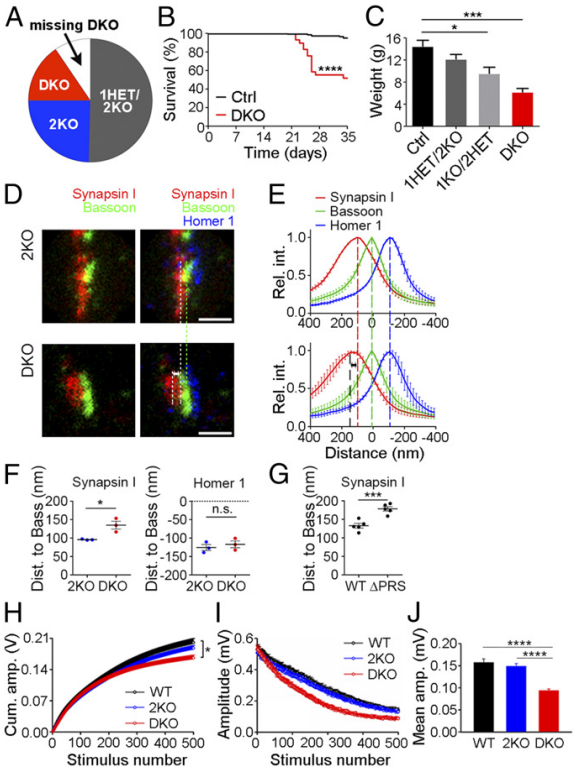

Fig. 2. Intersectin 1/2 regulates synapsin I nanoscale distribution and presynaptic function. (*A*) Genotype distribution in 249 litters of intersectin 1HET/2KO mice. Thirty-eight percent fewer DKO mice were born than would be expected from a Mendelian distribution. (*B*) Kaplan–Meier survival analysis of DKO (n = 29) and control animals (all other allelic combinations; n = 144). Statistical analysis by log-rank (Mantel–Cox) test and Gehan–Breslow–Wilcoxon test. (*C*) Weight of male DKO mice and controls (postnatal day 21–36). DKO mice show a dramatically reduced weight with the lightest mice being the most prone to die ($n_{(\text{controls = other genotypes})}$ = 33; $n_{(\text{intersectin 1HET/2KO})}$ = 18; $n_{(\text{intersectin 1KO/2HET})}$ = 9; $n_{(\text{DKO})}$ = 8); one-way ANOVA followed by Tukey's posttest. (*D–F*) Altered nanoscale localization of synapsin I in DKO hippocampal neurons. Neurons were immunolabeled with antibodies against synapsin I, bassoon, and homer 1 and were imaged by three-channel time-gated STED (gSTED). (*D*) Representative sum intensity projected gSTED images displayed as two- or three-channel overlays show an increased distance between synapsin I and bassoon in DKO synapses. (Scale bars: 500 nm.) (*E*) Averaged aligned line profiles from 314–343 synapses show an increased distance between synapsin I and bassoon (set to 0 nm) in DKO synapses. Colored dashed lines indicate maximum values of intersectin 2KO used as control. The black dashed line indicates the maximum value for synapsin in DKO synapses. Data are expressed as mean ± SEM. (*F*) Average distances between synapsin I and homer 1 and bassoon. Data are from three independent experiments with 40–171 synapses each; unpaired Student's t test, *P < 0.05; n.s., not significant. (*G*) Average distance of WT or ΔPRS mutant synapsin IA–E–GFP from bassoon. Data are from five independent experiments; paired Student's t test; ***P = 0.0008. (*H–J*) Reduced cumulative response amplitudes in acute slices from DKO mice stimulated with 500 stimuli at 20 Hz. (*H*) Cumulative amplitudes were significantly different between genotypes by one-way RM ANOVA (P = 0.01), and the HS test showed a significant difference between WT and DKO mice (P = 0.02) at the 500th pulse. (*I*) Accelerated synaptic rundown during stimulation with 500 pulses in DKO slices. (*J*) Results extracted from *I* show reduced mean amplitudes of responses between stimulus pulses 400 and 500. One-way RM ANOVA (P < 0.0001), followed by the HS test indicates significant differences between WT and DKO (P < 0.0001) as well as between 2KO and DKO (P < 0.0001; WT, n = 12, N = 4; 2KO, n = 14, N = 6; DKO, n = 11, N = 5). All column diagrams display mean ± SEM.

required for synapsin I expression, it is conceivable that intersectin may regulate the localization of synapsin within the presynaptic compartment. To address this question we first studied the effect of intersectin 1/2 loss on the activity-induced axonal dispersion and reclustering of synapsin I (23). We observed similar activity-induced dispersion of synapsin I into the axon, followed by its reclustering into presynaptic puncta reflecting reassociation with reserve pool SVs (6, 23) in hippocampal neurons from intersectin 1/2 DKO mice and from phenotypically normal 2KO littermates used as control (Fig. S3*C*). Thus, intersectin is not required for synapsin association with or dissociation from SVs.

Next we analyzed the effect of intersectin 1/2 loss on the nanoscale distribution of synapsin I by isotropic multicolor time-gated stimulated emission depletion microscopy (time-gated STED) (Fig. S4 *A* and *B*). To this aim, hippocampal neurons were triply stained for synapsin I, the AZ marker bassoon, and the postsynaptic scaffold homer 1. Acquired z-stacks were summed, and the distribution of each marker along line profiles perpendicular to bassoon and homer 1 labeling were quantitatively analyzed (Fig. S4*B*). The AZ marker bassoon was located at a mean distance of about 120 nm from postsynaptic homer 1^+ sites, consistent with recent stochastic optical reconstruction microscopy (STORM) microscopy data (24), and this distribution was unaffected by the absence of intersectin 1/2 (2KO: 125 nm ± 8.2 nm; DKO: 117 ± 9.1 nm) (Fig. 2 *D–F*). In contrast, we found a marked shift of the synapsin I peak away from the AZ center in intersectin 1/2-DKO neurons (2KO: 95 nm ± 0.9 nm; DKO: 135 nm ± 10 nm) (Fig. 2 *D–F*). A similar shift was seen when the distribution of intersectin-binding–defective mutant synapsin I (FLΔPRP2+3) (Fig. S1*B*) expressed in WT neurons was analyzed (synapsin$I^{\Delta PRS}$) (Fig. 2*G* and Fig. S4 *I* and *J*). Loss of intersectin 1/2 did not affect the nanoscale distribution of endophilin A1 or the clathrin adaptor AP2, endocytic proteins associated with intersectin (Fig. S4 *C–H*). These data show that intersectin regulates the nanoscale distribution of synapsin I at central mammalian synapses, in agreement with the physical association of the two proteins.

Previous data had shown that the synapsin-dependent reserve SV pool mediates the replenishment of the recycling vesicle pool (5) during periods of sustained activity (7, 25). We therefore analyzed synaptic transmission in acute slice preparations from intersectin single-KO or DKO mice. Single or combined loss of intersectins 1 and 2 had no effect on baseline synaptic transmission measured as fiber volley (FV) and field excitatory postsynaptic potential (fEPSP) amplitude ratios over a range of stimulation intensities (Fig. S5 *A* and *B*). However, when challenged by sustained stimulation with 500 pulses at 20 Hz [an established protocol to probe vesicle replenishment (26)], intersectin 1/2-deficient synapses showed a significant reduction in their cumulative amplitudes compared with WT controls (Fig. 2*H*), while the initial AMPA receptor (AMPAR)-mediated responses were similar (Fig. S5*C*). This deficit was caused by enhanced synaptic rundown following 150 or more stimulation pulses (Fig. 2*H*) due to a reduced rate of SV replenishment in the absence of intersectin 1/2 (Fig. 2 *I* and *J*). A similar activity-dependent depression of neurotransmission has been reported for synapsin I-KO mice (25, 26). The presence of one intersectin isoform was sufficient for functionality, as deletion of intersectin 1 alone did not result in defective SV replenishment (Fig. S5 *D–F*). Our data suggest that intersectin controls SV replenishment from the reserve pool at mammalian synapses, likely by regulating synapsin localization.

Formation of the Synapsin I–Intersectin 1 Complex Is Controlled by an Intramolecular Switch in Intersectin 1. Our data unravel an unexpected function of intersectin 1 in synapsin-dependent SV replenishment, in addition to its established role in endocytosis. This poses the question: Which mechanisms differentially regulate the formation of the intersectin 1–synapsin I complex at synapses? Many synaptic proteins undergo activity-regulated cycles of phosphorylation/dephosphorylation (6, 27), which often affect their formation of complexes with other proteins. We therefore analyzed

the potential role of protein phosphorylation in regulating intersectin 1–synapsin I association. Immunoprecipitations from rat brain extracts under either phosphorylation- or dephosphorylation-promoting conditions showed that the complex between intersectin 1 and synapsin I remained at the detection limit under dephosphorylating conditions but was strongly increased under phosphorylation-promoting conditions, while binding of the endocytic protein dynamin 1 was concomitantly reduced (Fig. 3 *A* and *B*). As synapsin I is one of the major brain phosphoproteins (6), we explored a potential role of synapsin I phosphorylation in regulating its association with intersectin 1. However, neither phosphorylation by protein kinase A (PKA) nor by Ca^{2+}-calmodulin–dependent protein kinase II (CaMKII) had any effect on its ability to bind intersectin (Fig. 3*C*). Alternatively, formation of the intersectin 1–synapsin complex might be regulated by phosphorylation-induced conformational changes within intersectin 1, which is heavily phosphorylated at multiple sites (https://www.phosphosite.org/homeAction.action). To further explore this possibility and delineate the intersectin 1 site responsible for such regulation, we analyzed the ability of intersectin 1-SH3 domain fragments of various lengths to bind synapsin Ia. We found that, while the isolated SH3A domain efficiently captured synapsin Ia from brain lysates, a larger protein fragment encompassing the entire SH3 domain module (SH3A–E) bound synapsin I with strikingly reduced efficiency (Fig. 3*D*), suggesting that intersectin 1 may be autoinhibited.

To gain mechanistic insights into such potential intramolecular regulation of intersectin 1, we utilized NMR spectroscopy. We used sortase-mediated ligation (Fig. S6*A*) to generate an SH3A–E construct in which the SH3A domain was selectively labeled with ^{15}N. A comparison of the spectra of the isolated ^{15}N-SH3A domain and the ligated ^{15}N-SH3A–E module revealed large chemical shift changes (Fig. 3*E* and Fig. S6*B*). These changes were similar to but larger than those observed when a fourfold excess of SH3B-E was added *in trans*, indicative of an intramolecular interaction (Fig. 3*E*). Mapping the intramolecular binding epitope onto a homology-modeled structure of the intersectin 1-SH3A domain identified a large interaction surface that includes the canonical binding site for proline-rich ligands (Fig. 3*F*). Further truncation experiments paired with affinity chromatography from brain lysates and NMR spectroscopy of ^{15}N-SH3A variants showed that an extension of the SH3A domain by about 20 amino acids into the linker between the SH3A and SH3B domains is sufficient to prevent synapsin I binding (Fig. S6*C*) and elicits spectral shifts similar to those seen for the ligated SH3A–E module (Fig. S6*D*). However, this 20-residue peptide does not harbor any classical class I/II SH3-binding motif (RxxPxxP or PxxPxR) (Fig. S7*A*). Subsequent peptide SPOT analysis using single alanine substitutions identified the motif PKLALR as a central determinant for SH3A binding (Fig. 3*G*). This sequence deviates from the preferred proline-rich recognition sequence of the intersectin 1-SH3A domain (PxϕPXR) determined by phage display technology (Fig. S7*B*). A suboptimal ligand may, in fact, be a prerequisite for the conformational transition that allows the intramolecular binding to be replaced by intermolecular interactions.

A prediction of this conformational switch model for intersectin function in SV cycling vs. synapsin-mediated SV replenishment is that synapsin binding should be particularly sensitive to the conformational state of the SH3A domain of intersectin 1. In contrast to dynamin, synapsin I is therefore predicted to selectively associate with the open, but not the locked, form of the domain. To test this, we used quantitative mass spectrometric analysis of labeled native protein samples to identify proteins associated with the conformationally "open" SH3A or an extended intramolecularly locked version of SH3A ("locked SH3A") when immobilized on beads (Fig. 4*A*). We identified peptides from 11 proteins as potentially specific binding partners of SH3A, which included known intersectin 1 interactors such as dynamins 1–3, synaptojanins 1/2 (14), and synapsins as well as other interactors, most notably the AZ protein piccolo (Fig. S7*C* and Table S3). Strikingly, synapsin I/II were the only proteins from these 11 candidates that associated predominantly with

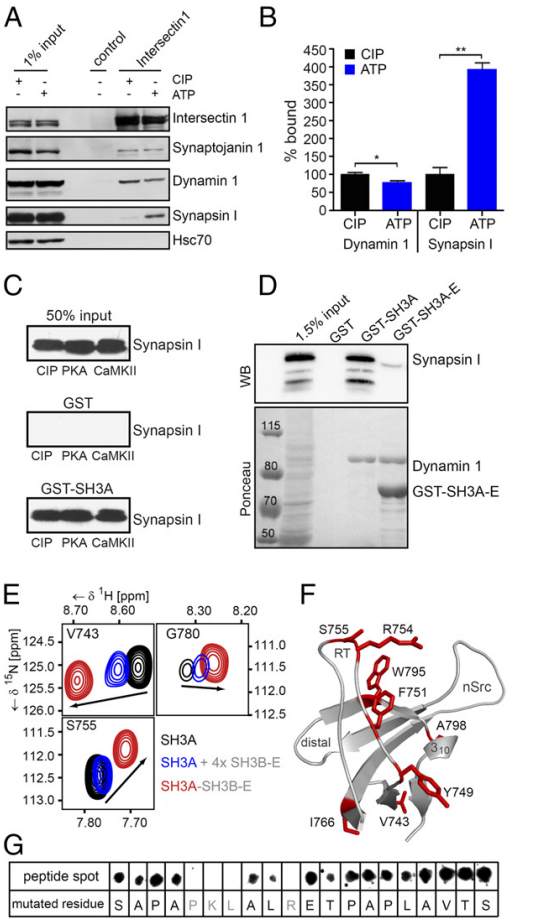

Fig. 3. Regulation of intersectin 1-SH3A domain function by an intramolecular switch. (*A* and *B*) Synapsin I preferentially binds phosphorylated intersectin 1. (*A*) Immunoprecipitations under phosphorylation-promoting (ATP) or dephosphorylation-promoting (calf intestinal phosphatase, CIP) conditions from detergent-extracted rat brain lysates. Samples were analyzed by immunoblotting. (*B*) Quantification of data shown in *A*. Data are shown as mean ± SEM; $n = 3$; $^*P < 0.05$; $^{**}P < 0.01$; Student's t test. (*C*) Phosphorylation of synapsin I at S9 (site 1; PKA) or at S566/S603 (sites 2/3; CaMKII) does not affect its binding to GST–intersectin 1-SH3A. Immobilized GST–intersectin 1-SH3A was incubated with in vitro dephosphorylated or phosphorylated synapsin I. Samples were analyzed by immunoblotting. Data are shown as mean ± SEM; all nonsignificant; one-way ANOVA. (*D*) Synapsin I does not interact with intersectin 1-SH3A in the context of the other SH3 domains. Immunoblot analysis of immobilized intersectin 1 GST–SH3A and GST–SH3A–E fusion proteins incubated with rat brain extract. (*E*) Intramolecular clamping of SH3A. Selected regions from overlays of ^{15}N-HSQC spectra of intersectin 1-SH3A recorded before (black) and after (red) ligation to SH3B-E or of SH3A after *in trans* addition of a 4× excess of SH3B-E (blue). (*F*) Epitope mapping of the SH3A intramolecular interaction. Red, residues that show chemical shift changes greater than mean ± SEM (0.11 ppm) or disappearing due to line broadening upon ligation to SH3B-E. The domain structure was predicted using the phyre2 web server (34). (*G*) Immobilized peptide spots of an 821- to 840-aa SH3A-B interdomain linker peptide with residues successively mutated to A (alanine scanning). Peptides were probed for interaction with GST-SH3A by immunoblotting. Gray, residues that lead to signal loss upon mutation.

the conformationally open but not the locked version of SH3A (Fig. 4*A* and Table S3). This confirms that the formation of the synapsin–intersectin 1 complex is regulated by the intramolecular interaction of its SH3A domain with the adjacent

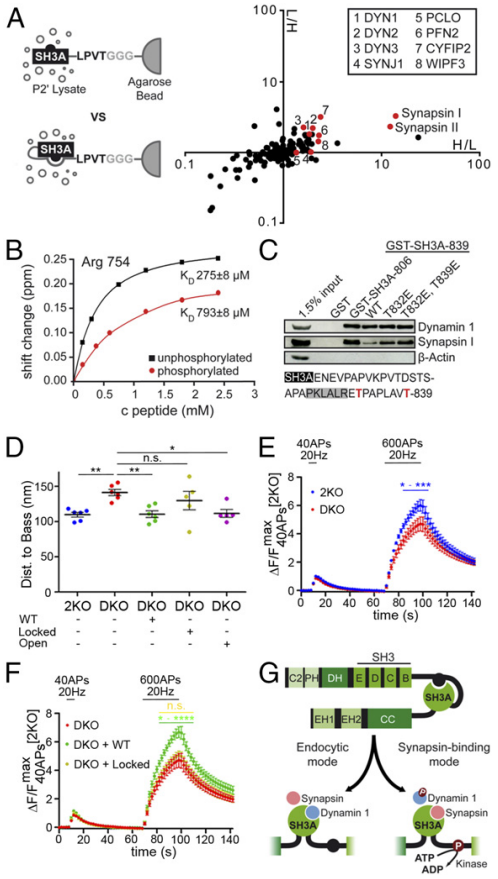

Fig. 4. The intersectin switch regulates complex formation with synapsin I. (*A–C*) Synapsin binds preferentially to open intersectin 1-SH3A. (*A*, *Left*) Scheme of the pull-down MS experiment. (*Right*) Scatter plot of $^{16}O/^{18}O$ isotope ratios of identified proteins (red, see Fig. S7*B* and Table S3) from two independent experiments (forward and reverse labeling). Only synapsins I/II associate preferentially with SH3A vs. locked SH3A. (*B*) NMR titration experiment (exemplary curve from signal of SH3A-R754), with an SH3A–B interdomain linker-derived peptide. Black: dephosphorylated; red: T832 and T839 phosphorylated. K_d (dephosphorylated) = 275 ± 8 µM; K_d (phosphorylated) = 793 ± 52 µM. (*C*, *Upper*) Immunoblots of pulldowns using intersectin 1 GST–SH3A with various linker lengths and mutations within the intramolecular binding site. (*Lower*) Scheme of mutated T residues (red) relative to the intramolecular binding site (gray). (*D*) WT or constitutively active open (T832E, T839E) but not locked (A828P, T832A, T839A) mutant intersectin 1 rescue-defective synapsin 1 nanoscale distribution (average distances of synapsin I to bassoon) in DKO neurons. Data are from six independent experiments; one-way ANOVA with Dunnett's posttest, $*P < 0.05$. (*E* and *F*) Average traces of synaptophysin–pHluorin–expressing neurons stimulated (20 Hz) with 40 APs (RRP; see Fig. S8 *G* and *H*) or 600 APs to measure the size of the recycling SV pool. Data were normalized to the maximum of the 40-AP peak of 2KO controls. Data are the mean ± SEM of 4–10 independent experiments; two-way RM ANOVA using Bonferroni's multiple comparisons test (control: DKO), $*P < 0.05$, $**P < 0.01$. (*E*) DKO neurons show a decreased recycling SV pool size; $*P < 0.05$, $***P < 0.001$. (*F*) WT but not locked mutant (A828P, T832A, T839A) intersectin 1 rescues the reduced recycling SV pool size in DKO neurons; $*P < 0.05$, $****P < 0.0001$. (*G*) Model for phosphoregulated conformational switching of intersectin 1 function in SV endocytosis and SV mobilization via synapsin binding.

PKLALR-containing linker sequence. Consistent with this model, NMR experiments using the selectively labeled SH3A–E construct showed that a 10-fold molar excess of a dynamin-based PRP was able to compete and thus open the intramolecular lock on SH3A, while the synapsin-derived PRP2 peptide did not (Fig. S7*D*).

These results further suggest that phosphorylation could be necessary to release the clamped conformation of intersectin 1-SH3A and enable its association with synapsin to regulate SV mobilization. In line with this, two of the phosphorylation sites within intersectin 1, T832 (28) and T839 (https://www.phosphosite.org/homeAction.action), are in close proximity to the PKLALR-containing linker sequence (Fig. S7*A*). To analyze the role of these phosphosites in regulating the formation of the intersectin 1–synapsin I complex, we synthesized phosphopeptides corresponding to the PKLALR-containing linker sequence of intersectin 1 and analyzed their ability to bind to SH3A. Phosphorylation of T832/T839 caused a threefold drop in the affinity for SH3A (Fig. 4*B*), suggesting that phosphorylation of these residues substantially shifts the equilibrium toward conformational opening of intersectin 1, thereby enabling the association of synapsin I with the intersectin-SH3A domain. We tested this directly by generating phosphomimetic mutants of the extended SH3A construct. While the T832E mutation alone led to only slightly increased synapsin I binding of the corresponding GST–SH3A-linker fusion proteins, the simultaneous introduction of two phosphomimetic mutations, T832E and/or T839E, restored synapsin I binding almost to the level of constitutively open SH3A lacking the linker sequence (Fig. 4*C*).

To probe the physiological relevance of the formation of the phosphoregulated intersectin 1–synapsin I complex, we generated a nonphosphorylatable and reinforced locked mutant of intersectin 1 (A828P, T832A, T839A) unable to associate with synapsin (Fig. S7*E*) and analyzed its ability to restore the defective nanoscale distribution of synapsin I in intersectin 1/2-DKO neurons. Reexpression of WT or constitutively open intersectin 1 (T832E, T839E) in intersectin 1/2-DKO neurons shifted the nanoscale localization of synapsin I to that observed in WT neurons, while reexpression of locked mutant intersectin 1 did not (Fig. S8 *A–F*). To test whether complex formation with synapsin underlies the observed regulation of SV replenishment by intersectin 1/2, we measured the effects of manipulating intersectin function in hippocampal neurons using synaptophysin-pHluorin assays to probe SV pool sizes (5, 29). As expected from our electrophysiological analysis (Fig. 2), we observed that the recycling SV pool size probed by 600 action potentials (APs) applied at 20 Hz was reduced in intersectin 1/2-DKO neurons (Fig. 4 *E* and *F*). The size of the readily releasable vesicle pool (RRP) and the kinetics of exocytic release were unaltered (Fig. S8 *G* and *H*). The reduced size of the recycling SV pool was fully restored by reexpression of WT intersectin 1 in DKO neurons, whereas synapsin-binding–defective locked mutant intersectin 1 was without effect (Fig. 4 *E* and *F*).

These collective data suggest that phosphorylation triggers a conformational opening of intersectin 1 to allow its SH3A domain to form a complex with synapsin I (Fig. 4*G*) and thereby regulate mobilization of reserve pool SVs.

Discussion

We show here by superresolution microscopy and by complementary genetic, electrophysiological, and biochemical approaches that intersectin 1 regulates SV replenishment through interactions with synapsin I. The defective nanoscale localization of synapsin I in synapses from intersectin 1/2-DKO mice correlates with and likely underlies impaired replenishment of SVs from the synapsin-dependent reserve pool under conditions of sustained stimulation, while the RRP and the overall number of SVs are unaltered. Impaired sustained neurotransmission is a hallmark of synapsin-KO mice (6, 25), which suffer from a greatly reduced recycling SV pool due to SV dispersion into the axon. We propose a model based on these data in which intersectin 1/2, in addition to its proposed role in SV endocytosis and/or recycling (14), fulfills a second presynaptic function in regulating SV replenishment from the reserve pool (5) via its association with synapsin I.

During sustained stimulation the activity-dependent phosphorylation of synapsin reduces its affinity for SV membranes to

allow SV mobilization for the replenishment of the recycling SV pool (6). Although the precise mechanism of intersectin action in SV replenishment remains to be determined, one possibility supported by our superresolution imaging data is that intersectin, a protein absent from SVs (30), acts as a molecular sink within the periactive zone that locally sequesters free synapsin I under conditions of sustained activity. This prevents premature rebinding of synapsin I to SVs and thereby resequestering SVs into the reserve pool, and thus facilitates the refilling of the RRP that drives exocytosis.

An important finding from our study is that the affinity of the intramolecular interaction in intersectin is finely tuned for its low-affinity interaction partner synapsin I and that phosphorylation at multiple sites, including T832 and T839, controls access to its SH3A domain. The precise signaling pathways that control intersectin phosphorylation remain to be determined. Presynaptic neurotransmission is regulated by several protein kinases, most notably cyclin-dependent kinase 5 (Cdk5) (31) but also others such as CaMK or PKA (6) that may conceivably phosphorylate intersectin 1 to enable SV replenishment under conditions of sustained activity. In addition to these phosphoregulatory mechanisms, the synapsin I–intersectin 1 complex may be regulated by other intersectin-binding partners. Irrespective of these mechanistic considerations, our data unravel a molecular link between the synapsin-dependent reserve SV pool and the presynaptic endocytosis machinery. Furthermore, the physical and functional association of intersectins (22) and synapsins may underlie the role of these proteins in learning and memory and in the pathogenesis of neurological disorders (32, 33).

Materials and Methods

All experiments in the present study were conducted in accordance with the guidelines of the Landesamt für Gesundheit und Soziales Berlin (LAGeSo) and with their permission. Intersectin 1/2-DKO mice were bred under the license G0357/13 by the LAGeSo.

Acquisition of ^{1}H-^{15}N Heteronuclear Single-Quantum Correlation Spectra. 2D heteronuclear single-quantum correlation (HSQC) spectra were recorded on a Bruker UltraShield 700 Plus equipped with a 5-mm triple-resonance cryoprobe. Measurement of the ^{15}N-labeled intersectin 1 domain, as well as selectively labeled five-domain constructs, was accomplished at 298 K and protein concentrations of 100–200 μM (isolated domains) or 40–60 μM (ligated five-domain constructs). Samples with a volume of 550–660 μL were buffered in a modified PBS (50 mM NaCl, 2.7 mM KCl, 10 mM Na_2HPO_4, 2 mM KH_2PO_4, 0.5 mM EDTA, pH 7.5) + 10% (vol/vol) D_2O. Complex data points (1,024 × 128) were acquired with eight (isolated domains) or 40 (ligated five-domain constructs) scans in each HSQC experiment. Resulting spectra were processed using TopSpin 3.2 (Bruker), and figures were prepared using Sparky 3.1.1.1 (T. D. Goddard and D. G. Kneller, University of California, San Francisco).

Statistical Analysis. Quantifications for biochemical experiments were always based on at least three independent experiments. Statistical data evaluation was performed using GraphPad Prism 4 software. Student's *t* tests and one-way ANOVA tests with Tukey's posttest were used to compare means if not stated otherwise in the figure legends. Electrophysiological data were statistically evaluated with SigmaStat using Student's *t* tests or repeated-measures (RM) ANOVA with the factor genotype. Significant differences were accepted at $^{****}P < 0.0001$; $^{*}P < 0.05$. When several genotypes were compared, ANOVA tests were followed by a Holm–Sidak (HS) posttest to detect differences between experimental groups. *N* indicates the number of animals or cell cultures used; *n* indicates the numbers of slices measured or the number of synapses analyzed in the data shown in Figs. 2 and 4 and Figs. S5 and S8.

For further information, see *SI Materials and Methods* available online.

ACKNOWLEDGMENTS. We thank Claudia Schmidt, Maria Mühlbauer, Delia Löwe, and Silke Zillmann for expert technical assistance. This work was supported by German Research Foundation Grants SFB958/A07 and -/Z03 (to C.F. and V.H.) and SFB958/A01 (to T.M. and V.H.), NeuroCure Cluster of Excellence Grant Exc-257 (to V.H.), and Telethon-Italy Grant GGP13033, CARIPLO Grant 2013-0879, and Italian Ministry of Health Grant RF 2013 (to F.B.).

1. Haucke V, Neher E, Sigrist SJ (2011) Protein scaffolds in the coupling of synaptic exocytosis and endocytosis. *Nat Rev Neurosci* 12:127–138.
2. Sudhof TC (2004) The synaptic vesicle cycle. *Annu Rev Neurosci* 27:509–547.
3. Kononenko NL, Haucke V (2015) Molecular mechanisms of presynaptic membrane retrieval and synaptic vesicle reformation. *Neuron* 85:484–496.
4. Saheki Y, De Camilli P (2012) Synaptic vesicle endocytosis. *Cold Spring Harb Perspect Biol* 4:a005645.
5. Rizzoli SO, Betz WJ (2005) Synaptic vesicle pools. *Nat Rev Neurosci* 6:57–69.
6. Cesca F, Baldelli P, Valtorta F, Benfenati F (2010) The synapsins: Key actors of synapse function and plasticity. *Prog Neurobiol* 91:313–348.
7. Fornasiero EF, et al. (2012) Synapsins contribute to the dynamic spatial organization of synaptic vesicles in an activity-dependent manner. *J Neurosci* 32:12214–12227.
8. Rosahl TW, et al. (1995) Essential functions of synapsins I and II in synaptic vesicle regulation. *Nature* 375:488–493.
9. Baldelli P, Fassio A, Valtorta F, Benfenati F (2007) Lack of synapsin I reduces the readily releasable pool of synaptic vesicles at central inhibitory synapses. *J Neurosci* 27:13520–13531.
10. Farisello P, et al. (2013) Synaptic and extrasynaptic origin of the excitation/inhibition imbalance in the hippocampus of synapsin I/II/III knockout mice. *Cereb Cortex* 23:581–593.
11. Greco B, et al. (2013) Autism-related behavioral abnormalities in synapsin knockout mice. *Behav Brain Res* 251:65–74.
12. Fassio A, et al. (2011) SYN1 loss-of-function mutations in autism and partial epilepsy cause impaired synaptic function. *Hum Mol Genet* 20:2297–2307.
13. Denker A, Kröhnert K, Bückers J, Neher E, Rizzoli SO (2011) The reserve pool of synaptic vesicles acts as a buffer for proteins involved in synaptic vesicle recycling. *Proc Natl Acad Sci USA* 108:17183–17188.
14. Pechstein A, Shupliakov O, Haucke V (2010) Intersectin 1: A versatile actor in the synaptic vesicle cycle. *Biochem Soc Trans* 38:181–186.
15. Sakaba T, et al. (2013) Fast neurotransmitter release regulated by the endocytic scaffold intersectin. *Proc Natl Acad Sci USA* 110:8266–8271.
16. Yu Y, et al. (2008) Mice deficient for the chromosome 21 ortholog Itsn1 exhibit vesicle-trafficking abnormalities. *Hum Mol Genet* 17:3281–3290.
17. Dierssen M, et al. (2001) Functional genomics of Down syndrome: A multidisciplinary approach. *J Neural Transm Suppl* 131–148.
18. Koh TW, Verstreken P, Bellen HJ (2004) Dap160/intersectin acts as a stabilizing scaffold required for synaptic development and vesicle endocytosis. *Neuron* 43:193–205.
19. Winther AM, et al. (2015) An endocytic scaffolding protein together with synapsin regulates synaptic vesicle clustering in the Drosophila neuromuscular junction. *J Neurosci* 35:14756–14770.
20. Pechstein A, et al. (2010) Regulation of synaptic vesicle recycling by complex formation between intersectin 1 and the clathrin adaptor complex AP2. *Proc Natl Acad Sci USA* 107:4206–4211.
21. Onofri F, et al. (2000) Specificity of the binding of synapsin I to Src homology 3 domains. *J Biol Chem* 275:29857–29867.
22. Sengar AS, et al. (2013) Vertebrate intersectin1 is repurposed to facilitate cortical midline connectivity and higher order cognition. *J Neurosci* 33:4055–4065.
23. Chi P, Greengard P, Ryan TA (2001) Synapsin dispersion and reclustering during synaptic activity. *Nat Neurosci* 4:1187–1193.
24. Dani A, Huang B, Bergan J, Dulac C, Zhuang X (2010) Superresolution imaging of chemical synapses in the brain. *Neuron* 68:843–856.
25. Vasileva M, Horstmann H, Geumann C, Gitler D, Kuner T (2012) Synapsin-dependent reserve pool of synaptic vesicles supports replenishment of the readily releasable pool under intense synaptic transmission. *Eur J Neurosci* 36:3005–3020.
26. Gitler D, et al. (2004) Different presynaptic roles of synapsins at excitatory and inhibitory synapses. *J Neurosci* 24:11368–11380.
27. Cousin MA, Robinson PJ (2001) The dephosphins: Dephosphorylation by calcineurin triggers synaptic vesicle endocytosis. *Trends Neurosci* 24:659–665.
28. Giansanti P, et al. (2015) An augmented multiple-protease-based human phosphopeptide atlas. *Cell Rep* 11:1834–1843.
29. Ryan TA, Li L, Chin LS, Greengard P, Smith SJ (1996) Synaptic vesicle recycling in synapsin I knock-out mice. *J Cell Biol* 134:1219–1227.
30. Takamori S, et al. (2006) Molecular anatomy of a trafficking organelle. *Cell* 127:831–846.
31. Kim SH, Ryan TA (2010) CDK5 serves as a major control point in neurotransmitter release. *Neuron* 67:797–809.
32. Garcia CC, et al. (2004) Identification of a mutation in synapsin I, a synaptic vesicle protein, in a family with epilepsy. *J Med Genet* 41:183–186.
33. Lakhan R, Kalita J, Misra UK, Kumari R, Mittal B (2010) Association of intronic polymorphism rs3773364 A>G in synapsin-2 gene with idiopathic epilepsy. *Synapse* 64:403–408.
34. Kelley LA, Sternberg MJ (2009) Protein structure prediction on the web: A case study using the Phyre server. *Nat Protoc* 4:363–371.
35. Kuropka B, Royla N, Freund C, Krause E (2015) Sortase A mediated site-specific immobilization for identification of protein interactions in affinity purification-mass spectrometry experiments. *Proteomics* 15:1230–1234.
36. Kofler M, et al. (2009) Proline-rich sequence recognition: I. Marking GYF and WW domain assembly sites in early spliceosomal complexes. *Mol Cell Proteomics* 8:2461–2473.

Supporting Information

Gerth et al. 10.1073/pnas.1715341114

SI Materials and Methods

Maintenance and Breeding of Mouse Strains. The 1KO mice were a kind gift of Melanie A. Pritchard, Department of Biochemistry & Molecular Biology, Monash University, Clayton, VIC, Australia (16). To generate 2KO mice (line name: ITSN2$^{tm1.1Tmar}$), a neomycin resistance (Neo) cassette flanked by loxP and FRT sites was placed between exon 2 and 3 of the ITSN2 gene, and an additional loxP site was introduced behind exon 4 using homologous recombination in hybrid C57BL/6N × 129/SvEv ES cells. The targeted ES cells were microinjected into C57BL/6 blastocysts. Resulting chimeras with a high percentage of agouti coat color were mated to C57BL/6 FLP mice to remove the Neo cassette from the recombinant allele. Animals with the deleted Neo cassette were crossed with CMV-Cre deleter mice to generate the KO allele in which exons 3 and 4 are deleted, which results in a frameshift. The 1KO and 2KO single-KO mouse lines were crossed to obtain intersectin 1/2-DKO mice. In the beginning intersectin1 HET/intersectin2 HET mice were crossed with each other to obtain DKO mice. After establishing that 2KO mice do not show any impairment of viability, DKO mice were generated by crossing intersectin1 HET/2KO mice with each other to adhere to the three Rs (replacement, reduction, refinement). In these breedings 2KO mice were used as controls. All experiments in the present study were conducted in accordance with the guidelines of the LAGeSo Berlin and with their permission. Intersectin 1/2-DKO mice were bred under the license G0357/13.

Behavioral Experiments. Intersectin DKO mice and controls were singly kept in a home cage containing only bedding material, a paper towel, and two food pellets for 10 min. The interval was recorded and the number of digging events was scored by an observer in a genotype-blind manner.

Antibodies. See Tables S1 and S2.

Plasmids. Human HA-intersectin 1L (L = long isoform) in pcDNA-3 was provided by Y. Groemping, Max Planck Institute for Intelligent Systems, Tübingen, Germany. The sequences encoding the various intersectin 1 domains (human amino acids 738–803 SH3A; 738–1,220 SH3A–E; 806–1,220 SH3B–E) were amplified from this vector and subcloned into pGEX4T-1 (Amersham Biosciences). Intersectin 1 SH3A-linker point mutants (T832E, T839E) were generated by overlap extension PCR and were confirmed by DNA sequencing. For sortase-mediated ligation the SH3A domain (residues 721–818) was cloned into pET21a with the C-terminal 814-**K**PVTD-818 motif mutated to the sortase ligation motif LPVTG. Intersectin 1 SH3B–E (amino acids 820–1,220) was cloned into pET21a extended by an N-terminal GG motif for sortase A (SrtA)-mediated ligation. SrtA d59 WT from *Staphylococcus aureus* (residues 60–206) for the catalysis of intersectin 1 construct ligation was expressed with a C-terminal His-tag from pET23a. All GST-fusion proteins and His_6-tagged proteins were expressed in *Escherichia coli* and purified using GST-Bind resin (Novagen) and His-Select Nickel Affinity Gel (Sigma), respectively, according to the manufacturer's instructions. Proteins used in NMR experiments were additionally gel-filtrated on a Superdex75 16/60 or Superdex200 16/60 column (GE Healthcare). Rat HA-synapsin 1 and truncation and deletion mutants thereof were subcloned into pcHA-MK or peGFP-MK for mammalian expression. The HA-fusion proteins were expressed in Cos7 cells, while the eGFP-tagged variant was used for expression in hippocampal neurons.

Protein Sequences. Amino acid labeling for human (hu) and rat (r) intersectin protein variants and peptides correspond to the following National Center for Biotechnology Information (NCBI) protein entries: huITSN1, NP_003015; rITSN1, NP_062100.

Peptides. The following synthetic peptides were used in this study: *Homo sapiens* synapsin 1-derived peptide ^{467}PPQPGPGPQR-QGPPLQQRPPP^{487} (termed "PRP2") and *H. sapiens* dynamin 1-derived peptide ^{811}GAPPVPSRPGASPDPFGPPPQVPSRPNRA^{839}.

Generation of Lysates for Protein Quantification by Immunoblotting. Brains were homogenized in ice-cold lysis buffer [20 mM Hepes-NaOH (pH 7.4), 100 mM KCl, 2 mM $MgCl_2$, 1% Triton X-100, 1 mM PMSF, mammalian inhibitor mixture (Sigma)] using a potter (20 strokes at 900 × *g* at 4 °C). After a 30-min incubation homogenates were centrifuged for 10 min at 4 °C to pellet debris. The protein concentration in the supernatant was measured by the Bradford assay before equal protein amounts were diluted in Laemmli sample buffer. Proteins were detected by Western blotting using either HRP-labeled or fluorescent secondary antibodies in combination with a camera-based detection system. Protein intensities were normalized to a loading control (actin or Hsc70).

Affinity Chromatography and Immunoprecipitations. Detergent extracts were prepared from homogenized brain or synaptosomal P2 lysates from rats or mice using established procedures (20). For immunoprecipitation experiments, antibodies were coupled to protein A/G PLUS Agarose (Santa Cruz Biotechnology) and were incubated with 10–15 mg rat or mouse brain extract in buffer A [20 mM Hepes-NaOH (pH 7.4), 50 mM KCl, 2 mM $MgCl_2$, 1% Triton X-100, 1 mM PMSF, mammalian inhibitor mixture (Sigma)] in a total volume of 1 mL for 2 h at 4 °C. Following extensive washes, samples were eluted with sample buffer and analyzed by SDS/PAGE and immunoblotting. For affinity chromatography or direct binding experiments, 100 or 50 μg GST-fusion proteins were coupled to GST-Bind resin (Novagen) and incubated with 2 mg mouse brain extract in a total volume of 1 mL for 1 h at 4 °C on a rotating wheel. Following extensive washes, samples were eluted with sample buffer and analyzed by SDS/PAGE and immunoblotting.

Electrophysiological Analyses. Six- to eight-week-old 1KO, 2KO, or intersectin-DKO mice and the corresponding control mice were used for acute hippocampal electrophysiology. Mice were decapitated quickly after cervical dislocation, and the brains extracted into ice-cold dissection artificial cerebrospinal fluid (ACSF) containing (in mM): 2.5 KCl, 1.25 NaH_2PO_4, 24 $NaHCO_3$, 1.5 $MgS0_4$, 2 $CaCl_2$, 25 glucose, and 250 sucrose (pH 7.4). The brains were dissected into equal hemispheres and were glued with their cut surface onto the object-mounting platform and sectioned into 350-μm-thick sagittal slices using a vibroslicer (VT 1200S; Leica). Slices were collected in a resting chamber to recover for at least 1.5 h at room temperature (22–24 °C) before recordings. The resting chamber was filled with ACSF in which 250 mM sucrose was replaced with 120 mM NaCl (pH = 7.35–7.4) and was continuously oxygenated with carbogen (95% O_2/5% CO_2). Slices were transferred into a submerged recording chamber (RC-27L; Warner Instruments) supplied with continuously bubbled ACSF with a solution exchange of 3–5 mL/min at room temperature. An upright microscope (BX61WI; Olympus) was used to position the slices to provide access to the CA1 region of the hippocampus for electrode placement and recordings. Glass stimulating (1–1.5 MΩ) and recording (1.5–2.5 MΩ) electrodes filled with ACSF were placed in a

visually preselected area of the CA1 stratum radiatum and were slowly advanced until the maximal fEPSPs were obtained. Schaffer collateral projections were stimulated with 0.2-ms electrical pulses at 0.05 Hz at the stimulation intensity, which induced ∼30–50% of the maximal responses to monitor baseline responses. After 10 min of stable baseline recordings, input–output stimulus response curves were made as a measure of basal excitatory synaptic transmission. Stimulation intensity was increased by 10-μA steps until the maximal fEPSPs were obtained, and presynaptic input and FV amplitudes vs. postsynaptic output fEPSP amplitudes were plotted. Recordings were performed in the presence of the GABA and NMDA receptor antagonists picrotoxin (100 μM) and DL-2-amino-5-phosphonovaleric acid (APV) (50 μM), respectively, to avoid inhibitory modulation of fEPSPs and NMDA receptor-induced plasticity. To prevent spontaneous epileptiform activity, which is otherwise readily induced in the CA3 region in the presence of the GABAergic antagonist picrotoxin, we introduced a cut with a sharp blade between the CA3 and CA1 region. To measure the size of the releasable SV pool (i.e., the RRP of SVs and the SV replenishment rate during prolonged stimulation of CA1 synapses in intersectin-KO mice), we applied repeated stimuli of 500 pulses at 20 Hz with a stimulation intensity that induced half-maximal amplitudes. Such sustained stimulation initially facilitated synaptic responses, which later depressed reaching the so-called "slow decay" steady-state responses, which could be interpreted as the SV replenishment rate from the reserve pool to the RRP. The measurements were performed blindly, i.e., without knowing the genotypes of recorded mice. The stimulus artifacts were blanked to facilitate perception of fEPSPs. For data presentation, 2KO mice from two mouse lines (intersectin 2KO mice generated within the intersectin 2KO line and intersectin 2KO mice generated within the independently bred intersectin 1/2-DKO line) were pooled together as controls for intersectin DKO mice, as no differences for any electrophysiological parameters were observed. The data were recorded at a sampling rate of 10 kHz, low-pass filtered at 3 kHz, and analyzed using PATCHMASTER software and EPC9 amplifier (Heka Elektronics). SigmaPlot (Systat) and IGOR Pro (WaveMetrics) software were used for data analyses and presentation. Values are depicted as mean ± SEM; "*n*" and "*N*" indicate the number of tested slices and mice, respectively.

Isolation, Culture, and Transfection of Primary Hippocampal Neurons. Hippocampal neurons were prepared from neonatal (postnatal day 1–3) mouse brains of the different genotypes. Briefly, hippocampi were rapidly dissected, placed into ice-cold HBSS containing 20% FBS, and cut with a scalpel into *ca*. 1-mm^3 pieces. The tissue pieces were washed first with HBSS containing 20% FBS and then with HBSS only and afterwards were digested for 15 min in digestion buffer (137 mM NaCl, 5 mM KCl, 7 mM Na_2HPO_4, 25 mM Hepes, 5 mg/mL trypsin, 1,500 units DNase) at 37 °C, followed by another washing step with HBSS and gentle trituration with fire-polished Pasteur pipettes with decreasing tip diameters. Fifty thousand cells were plated as 25-μL drops on poly-L-lysine–coated coverslips. One milliliter of plating medium (minimum essential media [MEM (Thermo Fisher 51200-020), 0.5% glucose; 0.02% $NaHCO_3$; 0.01% transferrin] containing 10% FBS, 2 mM L-glutamine, insulin, and penicillin/streptomycin) was added 1 h after plating. After 1 d in vitro (DIV) 0.5 mL of plating medium was replaced by 0.5 mL of growth medium (basic medium containing 5% FBS, 0.5 mM L-glutamine, B27 supplement, penicillin/streptomycin), and on DIV2 0.5 mL of growth medium containing additionally 2 μM Ara-C was added. On DIV7 0.5 mL of the medium was replaced by growth medium containing 4 μM Ara-C. Neurons were maintained at 37 °C in a 5% CO_2 humidified incubator until DIV14.

Neurons were transfected on DIV8–9 by calcium phosphate transfection using 6 or 4 μg of DNA (for six-well or 12-well plates, respectively), 250 mM $CaCl_2$, and water mixed with equal amounts of 2× Hepes-buffered saline. The mix was incubated at room temperature for 20 min to allow precipitate formation while neurons were starved in neurobasal medium (Thermo Fisher Scientific) at 37 °C, 5% CO_2 for the same amount of time. Precipitates were added to neurons and incubated for 30 min at 37 °C, 5% CO_2. After three final washing steps with HBSS medium, neurons were transferred back to their conditioned medium.

Electron Microscopy Analyses. Hippocampal neuronal cultures were fixed with 2% glutaraldehyde for 1 h, osmificated, dehydrated, and embedded in epoxy resin. Ultrathin sections were contrasted and imaged on a Zeiss 900 transmission electron microscope. Three independent experiments (i.e., three independently generated neuronal cultures) were analyzed. Morphometry was performed on 20 synapses per experiment per genotype (60 synapses per genotype in total).

Immunostaining. Hippocampal neurons were fixed on DIV14 using 4% paraformaldehyde and 4% sucrose in PBS for 15 min at room temperature. For dispersion and reclustering experiments neurons were stimulated before fixation with 900 APs at 10 Hz in physiological buffer [170 mM NaCl, 3.5 mM KCl, 0.4 mM KH_2PO_4, 20 mM *N*-Tris(hydroxy-methyl)-methyl-2-aminoethane-sulphonic acid (TES), 5 mM $NaHCO_3$, 5 mM glucose, 1.2 mM Na_2SO_4, 1.2 mM $MgCl_2$, 1.3 mM $CaCl_2$] using an RC-47FSLP stimulation chamber (Warner Instruments). For the dispersion condition, neurons were fixed immediately after stimulation. For the reclustering condition, stimulated neurons were given 2 min of rest before fixation. After fixation neurons were blocked and permeabilized in PBS containing 10% goat serum and 0.3% Triton X-100 for 30 min. Fixed neurons were incubated with primary antibodies against proteins of interest for 1 h at room temperature. After washing with 1× PBS, neurons were incubated with corresponding secondary antibodies for 1 h at room temperature. Following extensive washes coverslips were mounted using Immu-Mount (Thermo Fisher) for normal confocal microscopy or Prolong Gold Antifade (Invitrogen) for STED microscopy.

3D Time-Gated STED Imaging of Neurons. STED imaging with time-gated detection was performed on a Leica SP8 TCS STED microscope (Leica Microsystems) equipped with a pulsed white-light excitation laser (WLL; ∼80 ps pulse width, 80 MHz repetition rate; NKT Photonics) and two STED lasers for depletion at 592 nm and 775 nm. The pulsed 775-nm STED laser was triggered by the WLL. Within each independent experiment samples from intersectin 2KO and DKO neurons were acquired with equal settings. Three-channel STED imaging was performed by sequentially exciting Alexa 488, Alexa 594, and ATTO647N at 488 nm, 598 nm, and 646 nm, respectively. Emission from Alexa 488 was depleted with the 92-nm laser, whereas the 775-nm STED laser was used to deplete both Alexa 594 and ATTO647N. Time-gated detection was set from 0.3–6 ns for all dyes. Fluorescence signals were detected sequentially by hybrid detectors at appropriate spectral regions separated from the STED laser. Five optical slices of 130 nm were acquired with an HC PL APO CS2 100×/1.40 N.A. oil objective (Leica Microsystems), a scanning format of 1,024 × 1,024 pixels, eight-bit sampling, and sixfold zoom, yielding a voxel dimension of 18.9 × 18.9 × 130 nm. To minimize thermal drift, the microscope was housed in a heatable incubation chamber (LIS Life Imaging Services). The effective lateral resolution of the TCS SP8 STED microscope was previously determined using 40-nm fluorescent beads (Life Technologies; excitation/emission maxima at 505/515 nm or 660/680 nm) to be 54 nm for the 488-nm channel and 45 nm for the 647-nm channel.

Raw data obtained from three-channel time-gated STED (gSTED) imaging were analyzed with ImageJ (NIH). Synapses

from sum intensity projected z-stacks were selected based on clearly separated bassoon and homer 1 clusters. Multicolor line profiles were generated perpendicular to the bassoon/homer 1 cocluster with a length of 1 μm and a width of 0.4 μm using the ImageJ Macro (Macro_plot_lineprofile_multicolor from Kees Straatman, University of Leicester, Leicester, UK). Intensity values from individual synapses were exported to Excel, and all profiles were aligned to the maximum of the bassoon peak. The position of the bassoon maximum was set to zero.

pHluorin Imaging of Living Neurons. Neurons at DIV13–15 were subjected to electrical field stimulation using an RC-47FSLP stimulation chamber (Warner Instruments) and imaged at 37 °C in physiological imaging buffer [170 mM NaCl, 3.5 mM KCl, 0.4 mM KH_2PO_4, 20 mM TES, 5 mM NaHCO3, 5 mM glucose, 1.2 mM Na2SO4, 1.2 mM MgCl2, 1.3 mM CaCl2, 10 μM CNQX, and 50 μM AP-5, pH 7.4] by epifluorescence microscopy [Nikon Eclipse Ti by MicroManager 4.11, sCMOS camera (Neo; Andor) equipped with a 40× oil-immersion objective]. Images were acquired every 2 s with 100-ms excitation at 488 nm. Neurons were stimulated with 40 APs (20 Hz, 100 mA) and after 1 min rest at 600 APs (20 Hz, 100 mA). Quantitative analysis of responding boutons was performed using ImageJ. Fluorescence intensities of responding boutons were corrected for background and photobleaching. To compare peak fluorescence values, RRP curves were normalized to baseline. To get a measure for the size of the recycling SV pool, curves were normalized to the maximum peak fluorescence of the first stimulation of the control (2KO).

Synapsin–Intersectin 1-SH3 Domain-Binding Assays. Synapsin 1 was purified from bovine brain and phosphorylated in vitro on specific sites by PKA (site 1) or CaMKII (sites 2 and 3). The binding of dephosphorylated or phosphorylated synapsin 1 to the intersectin 1-SH3A domain was tested as previously described (21). One hundred micrograms of fusion protein-coupled beads were incubated with 25, 50, and 100 nM of purified synapsin 1 in 500 μL of binding buffer for 3–5 h at 4 °C. Synapsin 1 recovery was determined by densitometric scanning of the fluorograms and interpolation in a synapsin 1 standard curve.

SrtA-Mediated Ligation. SrtA-mediated ligation was used for the selective ^{15}N-labeling of individual SH3 domains within SH3A–E domain intersectin 1 constructs. The ligation was carried out between an intersectin 1 SH3A construct harboring an LPVTG motif downstream of the His-tag and individual intersectin 1 SH3B–E four-domain constructs harboring an N-terminal GG motif. Introduction of the sequential motifs required for SrtA-mediated ligation resulted in a mutation of **K**PVT**DS** to **L**PVT**GG** within the SH3A–SH3B interdomain linker of the resulting five-domain construct. A total of 4–8 mg of SH3A LPVTG was added in sevenfold molar excess to the respective GG SH3B–E construct. Ligation was then carried out applying 5 mg of SrtA in TBS supplemented with 5 mM $CaCl_2$, pH 8.2 for 2 h at room temperature. To further increase the yield of the ligation product, additional amounts of GG SH3B–E were added after the equilibrium of the reaction was reached, followed by another 2 h of incubation at room temperature. This procedure was repeated two to three times with the last incubation step carried out overnight at 4 °C. Subsequent to the ligation reaction the resulting five-domain construct was purified by applying the mixture to a StrepTrap HP column (GE Healthcare). The eluate was then incubated for 2 h at 34 °C with TEV protease to remove the strep-tag. Finally, the solution was gel-filtrated on a Superdex75 16/60 column (GE Healthcare) equilibrated with a modified PBS buffer (50 mM NaCl, 2.7 mM KCl, 10 mM Na_2HPO_4, 2 mM KH_2PO_4, 0.5 mM EDTA, pH 7.5).

Domain Assignment of Human Intersectin 1-SH3A. Triple-resonance spectra for the backbone assignment of the intersectin 1 SH3 ^{1}H-^{15}N HSQC spectrum were recorded on Bruker UltraShield 700 Plus equipped with a 5-mm triple-resonance cryoprobe. The ^{15}N,^{13}C-labeled SH3A was applied in concentration of 960 μM in 1× PBS + 10% (vol/vol) D_2O + 0.01% NaN_3, pH 7.4. In total, 1,024 × 92 × 92 complex data points were acquired with eight (HNCA), 12 [HN(CA)CO, HN(CO)CA], or 18 (HNCACB) scans. Assignment of the HSQC signals was accomplished using CcpNmr Analysis 2.2.2 software.

Interactome Analysis. Human intersectin 1-SH3A constructs were covalently immobilized to agarose beads via SrtA-mediated ligation (35). P2′ lysates were prepared from six WT mouse brains, and 400 μL of lysate (3.6 mg/mL) were added to each 30-μL aliquot of beads. After 2 h of incubation at 4 °C, the beads were washed five times with lysis buffer [20 mM Hepes (pH 7.4), 50 mM KCl, 2 mM $MgCl_2$, 1% Triton X-100] and three times with lysis buffer without Triton X-100. After 3× equilibration with 50 μL ABC buffer (50 mM ammonium bicarbonate in ^{16}O or ^{18}O water), bound proteins were eluted for 10 min at 60 °C with 1% RapiGest SF Surfactant (Waters) in ^{16}O or ^{18}O ABC buffer. Eluted proteins were then digested with trypsin overnight at 37 °C in solution using either ^{16}O- or ^{18}O-water to allow quantitative MS/MS analysis of the resulting peptides. Pulldowns were performed in two independent experiments, allowing isotope labeling in a crossover manner (forward and reverse labeling). After inactivation of trypsin with 1% TFA, ^{16}O- and ^{18}O-labeled samples were combined, and the complex peptide mixture was separated applying a 2D liquid chromatography approach on C18 material. Quantitative MS analysis was carried out on a Thermo Scientific LTQ Orbitrap, and resulting data were processed on Mascot Distiller.

Peptide SPOT Array. Peptide SPOT membranes were synthesized as described (36) and washed for 10 min with 100% ethanol before use. The membranes were blocked with 5% BSA in PBS, 1 mM DTT for 3 h and after three washings with PBS, 1 mM DTT they were incubated with purified GST–SH3A (10 μg/mL) in PBS supplemented with 5% BSA and 1 mM DTT overnight at 4 °C. Subsequently, the membranes were developed applying a GST-specific primary and an HRP-coupled anti-rabbit secondary antibody (Santa Cruz Biotechnology) (1 h incubation each) with washing with PBS, 0.05% Tween between the incubation steps.

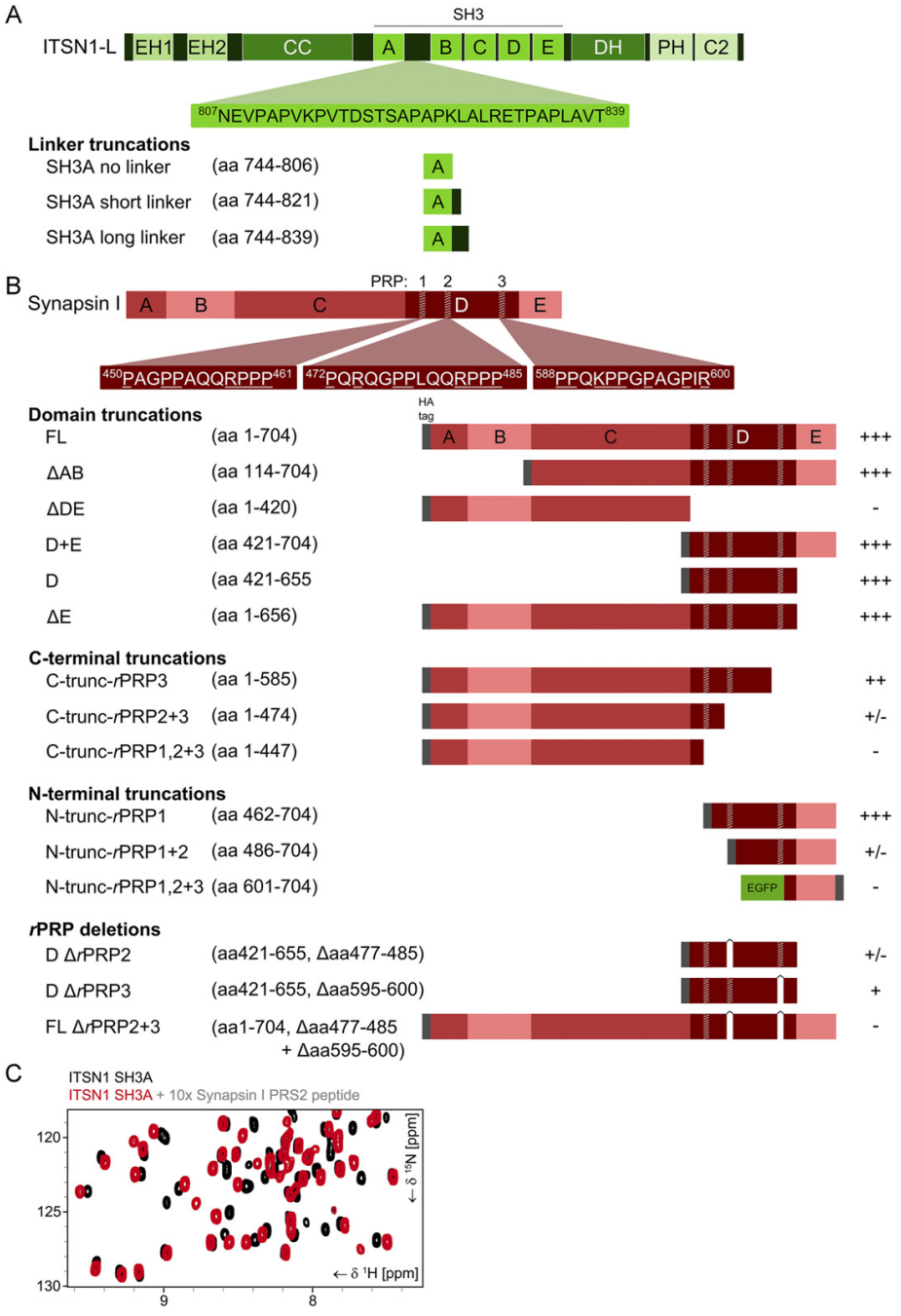

Fig. S1. Molecular analysis of intersectin 1–synapsin I complex formation. (*A*) Schematic representation of the intersectin 1 domain organization. In addition to its five SH3 domains the protein contains two N-terminal epsin homology (EH) domains, a coiled-coil (CC) domain, a pleckstrin homology (PH)-Dbl homology (DH) domain unit, and a C-terminal C2 domain of unknown binding specificity. The amino acid sequence represents the linker region C-terminal of the intersectin 1-SH3A domain that underlies the intramolecular lock mechanism. Shown below are three different truncation mutants that were used to identify the sequence important for the lock mechanism. (*B*) Schematic representation of the synapsin I domain organization. The three putative SH3 domain-binding PRPs within the synapsin I-D domain are indicated, and their amino acid sequences are shown. Prolines and basic residues are underlined. Shown below are the truncation mutants that were used for binding studies. The + and − on the right indicate binding efficiency in affinity chromatography assays. (*C*) Overlay of sections from ^{1}H-^{15}N-HSQC spectra of intersectin 1-SH3A recorded before (black) and after (red) supplementation with a 10-fold molar excess of a synthetic peptide derived from the synapsin I PRS2 sequence.

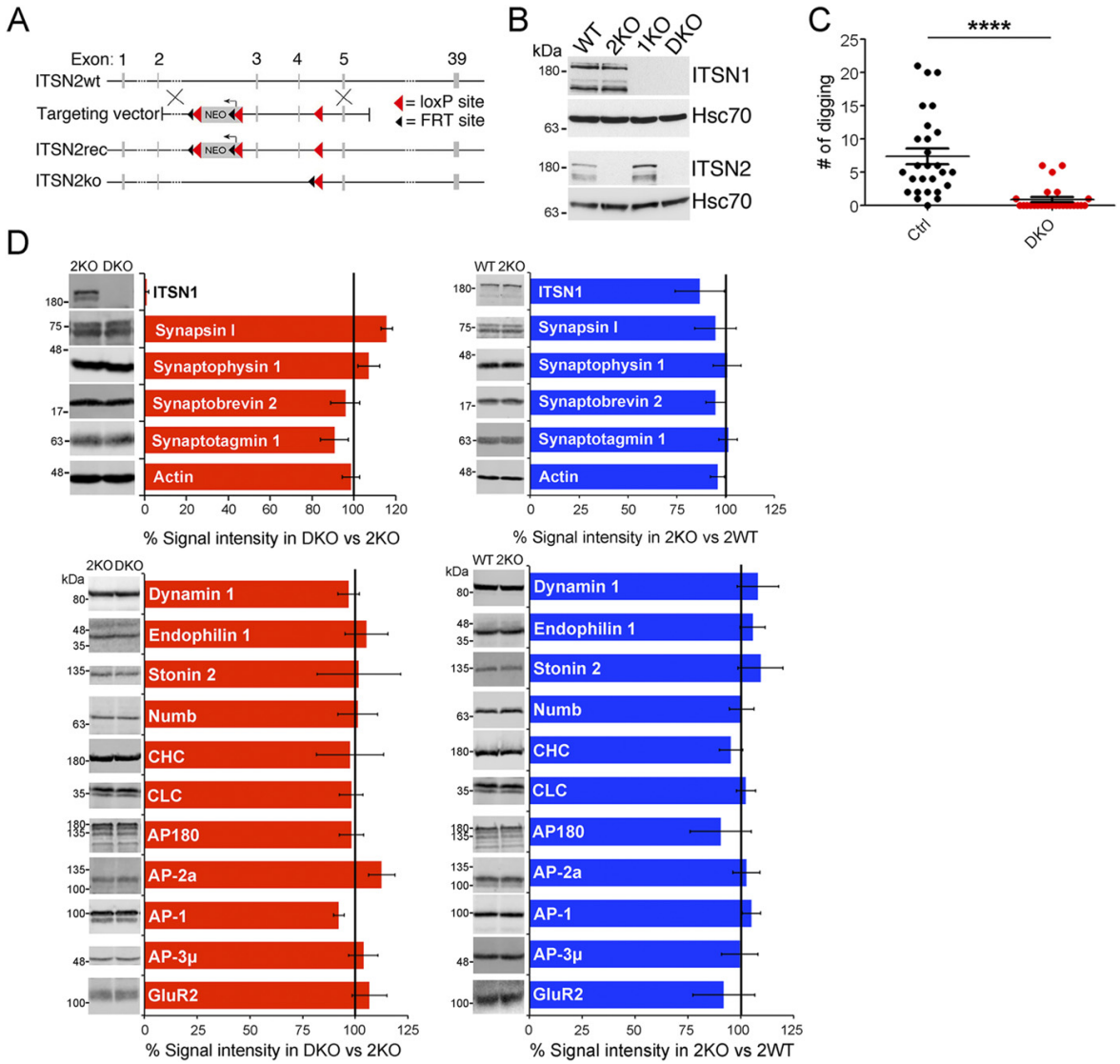

Fig. S2. Generation of intersectin 1/2-DKO mice. (*A*) Scheme of the targeting strategy for the generation of 2KO mice. (*B*) Brain lysates from mice of the indicated genotypes were analyzed by immunoblotting with antibodies specific for the indicated proteins. The Western blot shows the absence of intersectin 1 and/or intersectin 2 protein in the respective KO mice and confirms the specificity of the intersectin antibodies used. (*C*) When mice were monitored for 10 min in their home-cage environment, DKO mice showed increased digging behavior (control $n = 27$, DKO $n = 26$; significance was evaluated with the Mann–Whitney test). ****$P < 0.0001$. (*D*) Brain lysates from mice of the indicated genotypes were analyzed by immunoblotting with antibodies specific for the indicated proteins. None of the proteins showed a significant difference compared with the control samples.

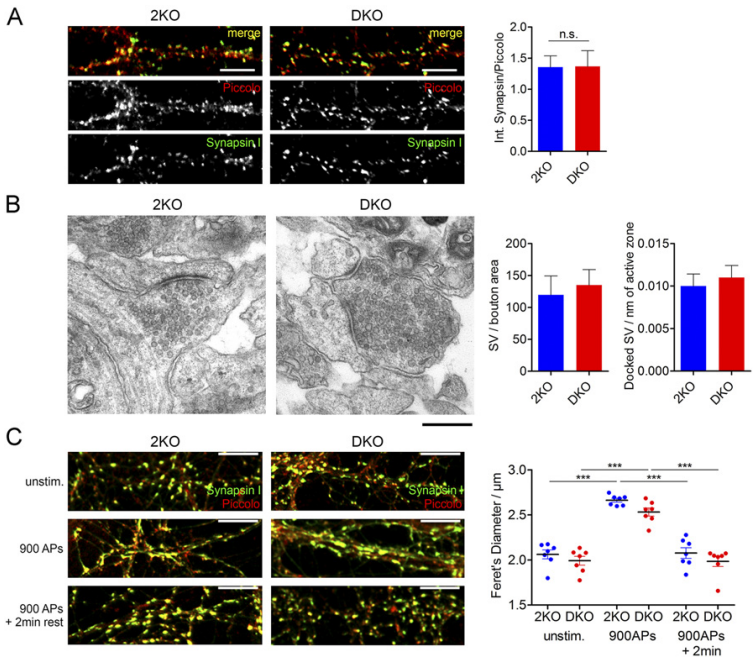

Fig. S3. Presynaptic ultrastructure and synapsin I expression and dispersion in hippocampal neurons from intersectin 1/2-DKO mice. (*A*) Synaptic synapsin I levels are unaltered in intersectin DKO neurons. Cultured hippocampal neurons from intersectin 2KO and DKO mice were fixed and immunostained with antibodies against synapsin I and piccolo. (*Left*) Representative merged and single-channel images of synapsin I and piccolo staining. (Scale bars: 10 μm.) (*Right*) Quantification of relative synapsin I fluorescence intensity normalized to piccolo levels (mean ± SEM, $n = 7$). (*B*) Electron micrographs of intersectin 2KO and DKO synapses (*Left*) show no difference in mean SV density per bouton area or in the number of docked SVs per AZ length (*Right*); data are shown as mean ± SEM, $n = 3$, 60 synapses per genotype. (Scale bar: 400 nm.) (*C*) Synapsin I dispersion and reclustering is unaltered in intersectin-DKO synapses. Cultured hippocampal neurons from intersectin 2KO and DKO mice were stimulated with 900 APs and were fixed either immediately or after 2 min of rest. Fixed cells were immunolabeled with synapsin I- and piccolo-specific antibodies. (*Left*) Representative images showing the dispersion of synapsin I into the axons upon stimulation and its reclustering after 2 min of rest. (Scale bars: 10 μm.) (*Right*) Quantification of dispersion and recovery by measuring the Feret's diameter (measure for the size of synapsin I clusters) indicating a significant increase upon stimulation followed by a significant decrease after 2 min rest; data are shown as mean ± SEM, $n = 7$. Dots represent seven independent experiments. Statistical significance was evaluated using one-way ANOVA and a Tukey's multiple comparison test; $^{***}P < 0.001$.

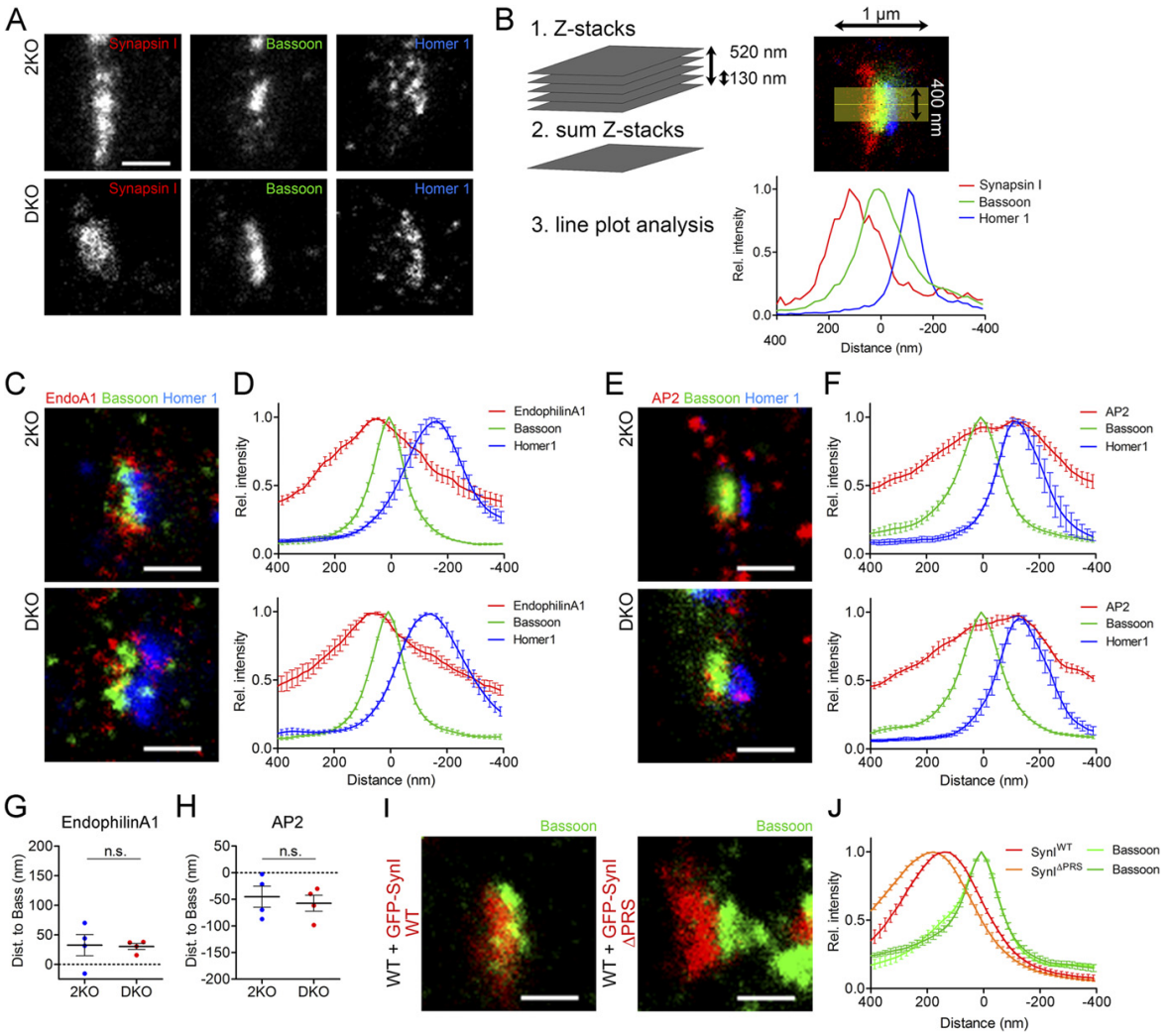

Fig. S4. Superresolution imaging of synaptic protein localization in hippocampal neurons from intersectin 1/2-DKO mice. (*A*) Single channels of the representative sum intensity projected gSTED images shown in Fig. 2. (Scale bar: 500 nm.) (*B*) For analysis of the nanoscale localization of synapsin 1, gSTED images were sum intensity projected, and synapses were selected based on clearly separated bassoon and homer 1 clusters. Multicolor line profiles were generated perpendicular to the bassoon/homer 1 cocluster with a length of 1 µm and a width of 0.4 µm. (*C–H*) Nanoscale localizations of two other interaction partners of intersectin 1/2 are unaltered in DKO synapses. DIV14 cultured hippocampal neurons were immunolabeled with antibodies against endophilin A1 (*C* and *D*) or AP2α (*E* and *F*), AZ marker bassoon, and postsynaptic scaffold protein homer 1 and were imaged by three-channel gSTED. Representative sum intensity projected gSTED images are displayed as three-channel overlays. (Scale bars: 500 nm.) (*D* and *F*) Line plot profiles from side views were aligned to bassoon and averaged. Data show mean intensity values ± SEM. (*G* and *H*) Average distances of endophilin A1 (*G*) and AP2 α (*H*) to the AZ marker bassoon. The dashed line represents bassoon. Dots represent four independent experiments. Statistical significance was evaluated using a paired Student's *t* test; n.s., not significant. (*I*) Representative sum intensity projected gSTED images displayed as three-channel overlays show an increased distance between overexpressed synapsin $1^{\Delta PRS}$ and the AZ marker bassoon in comparison with WT synapsin 1. (Scale bar: 500 nm.) (*J*) Line plot profiles from side views were aligned to bassoon and averaged. Data are mean intensity values ± SEM.

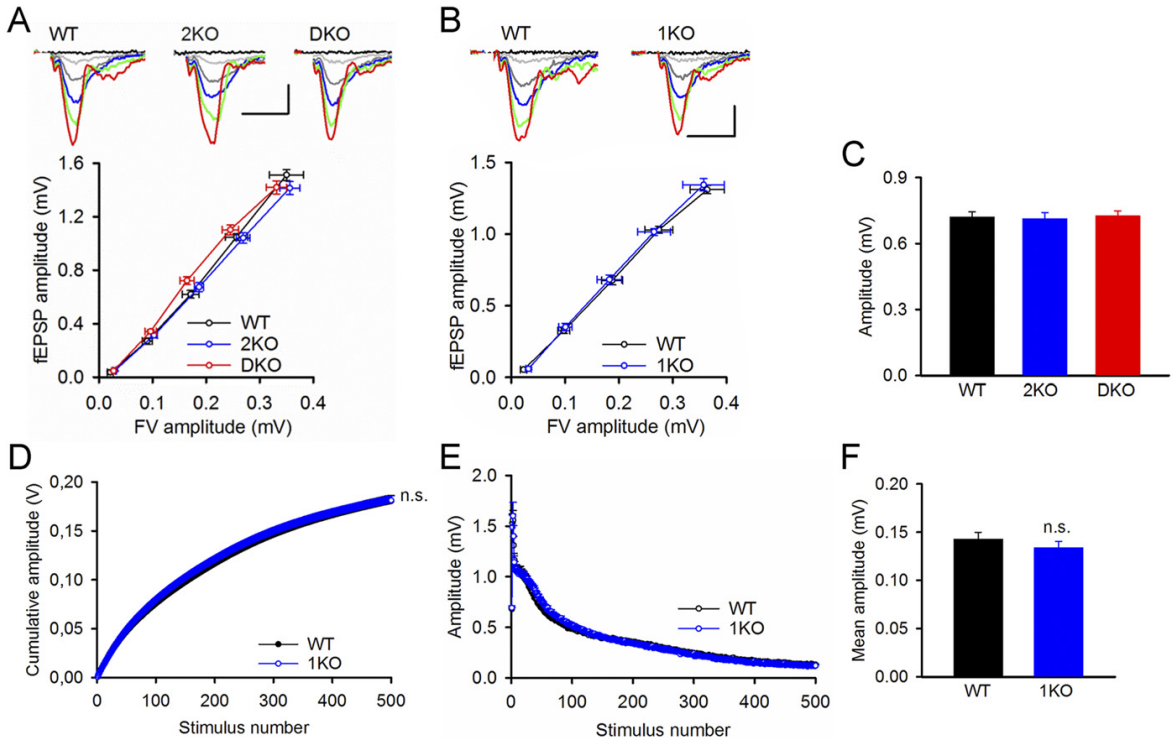

Fig. S5. Electrophysiological analysis of synaptic transmission in intersectin-KO mice. (*A*, *Upper*) Normal basal synaptic transmission in intersectin 2KO and DKO mice measured as FV and fEPSP amplitude ratios over a range of stimulation intensities. Two-way RM ANOVA did not detect differences between WT and 2KO mice in amplitude ($P = 0.11$) or FV ($P = 0.93$) or between WT and DKO mice in amplitude ($P = 0.49$) or FV ($P = 0.24$). (Scale bars: 0.5 mV and 10 ms.) (*Lower*) Representative fEPSP examples color coded for each genotype show recordings with increasing stimulation intensities (10–60 μA). (*B*, *Upper*) Normal basal synaptic transmission in 1KO mice measured as FV and fEPSP amplitude ratios over a range of stimulation intensities. Two-way RM ANOVA did not detect any difference between WT and 1KO mice in amplitude ($P = 0.73$) or FV ($P = 0.71$). (Scale bars: 0.5 mV and 10 ms.) (*Lower*) Representative fEPSP examples show recordings with increasing stimulation intensities (10–60 μA) in WT and 1KO mice. (*C*) Normal initial AMPAR-mediated responses measured as first amplitude during 500 pulse stimuli. Note that 50% of maximal response was used for repeated stimulation. One-way RM ANOVA detected no significant effect of genotype ($P = 0.942$). (*D*) Normal cumulative amplitudes were detected during sustained stimulation in 1KO mice. No difference between genotypes was detected at the 500th pulse (*t* test; $P = 0.92$). (*E*) Normal fEPSP amplitudes during 500-pulse stimulation in 1KO mice. (*F*) Normal SV replenishment rate in 1KO mice. Results were obtained from *C* showing the replenishment rate of releasable SVs between stimulus pulses 400 and 500. No difference was detected between genotypes (*t* test; $P = 0.36$). Recordings were performed in the presence of the GABA antagonist picrotoxin (100 μM) and the NMDA receptor antagonist APV (50 μM). CA3 and CA1 connections were dissected using a sharp blade (WT $n = 12$, $N = 5$; 1KO $n = 13$, $N = 5$).

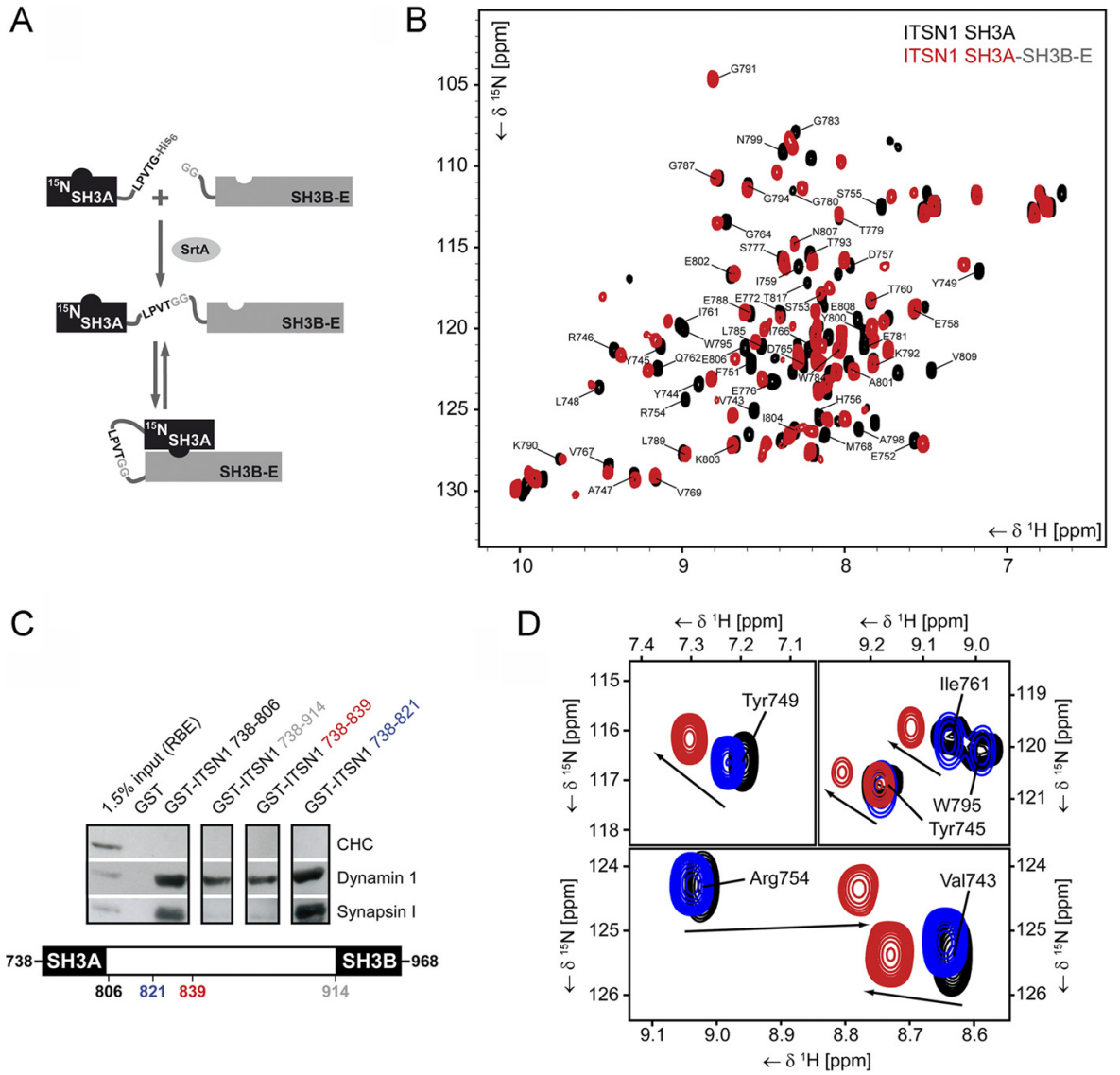

Fig. S6. Molecular analysis of intramolecular complex formation of intersectin 1-SH3A. (*A*) Concept of domain-selective ^{15}N-labeling of huITSN1 SH3A within a five-domain SH3A–SH3E construct applying SrtA from *S. aureus*. (*B*) Overlay of ^{1}H-^{15}N-HSQC spectra recorded from isolated (black) or sortase-ligated (red) SH3A constructs. The backbone assignment is indicated for the individual signals. (*C*) Pulldown experiment with GST–huITSN1–SH3A-linker truncation constructs amino acids 738–806 (black), 738–914 (gray), 738–839 (red), and 738–821 (blue). The samples were analyzed by SDS/PAGE and Western blotting. The construct boundaries are illustrated below. (*D*) Selected peaks from the ^{1}H-^{15}N-HSQC spectra of the SH3A-linker truncation constructs. Color-coding is as in *C*.

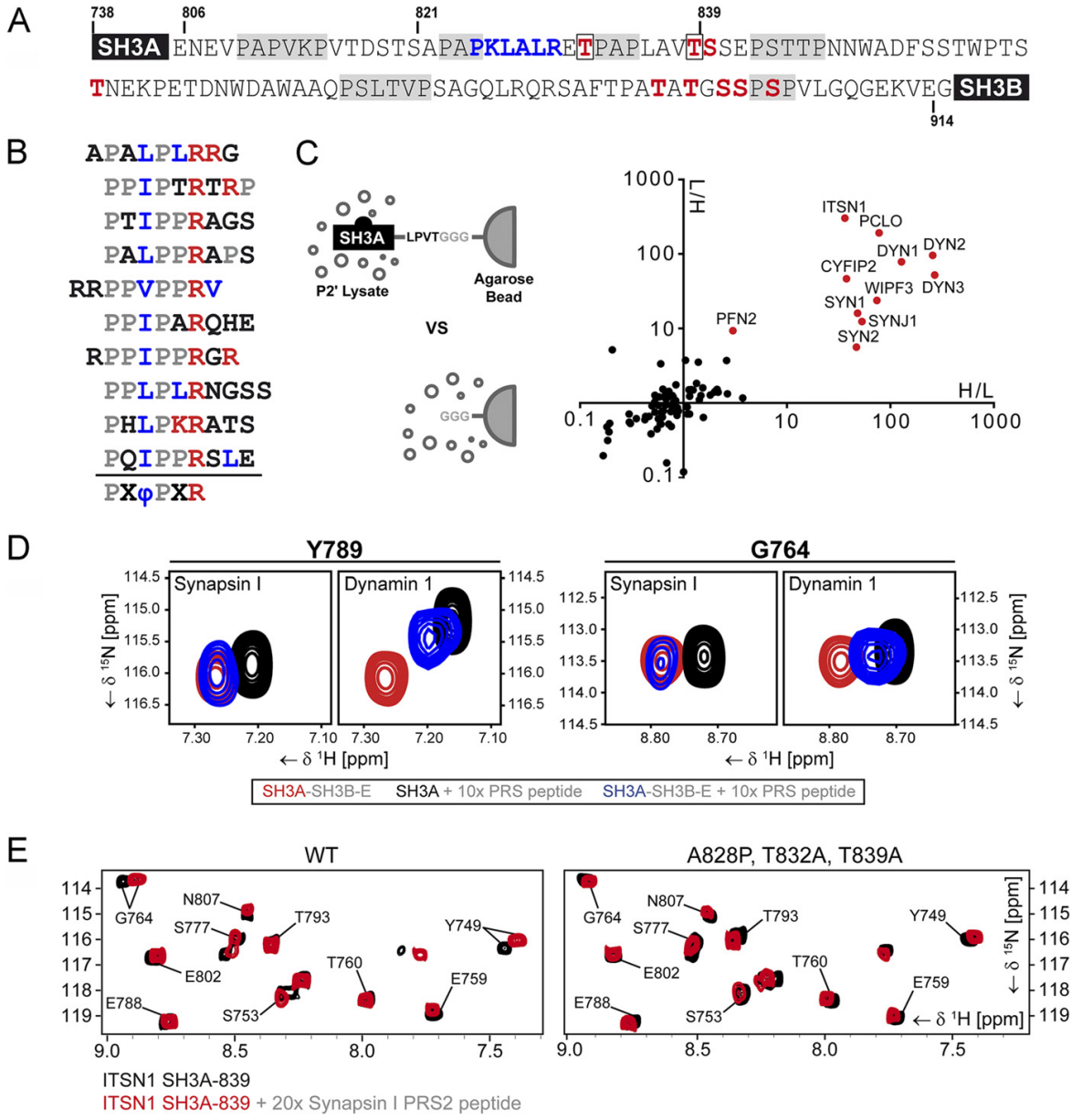

Fig. S7. Proteomic and NMR analysis of protein association with open or locked intersectin 1-SH3A. (*A*) Sequence of the huITSN1 SH3A–SH3B interdomain linker. Proline-rich motifs are highlighted in gray, identified phosphorylated residues listed in the PhosphoSites database (https://www.phosphosite.org/homeAction.action) are shown in red, and potential Cdk5 targets are shown in blue. The two potential phosphosites close to the SH3A intramolecular binding site that were analyzed in more detail are framed. The boundaries of the SH3A-linker truncation constructs are given above. (*B*) Sequence of 10 peptides eluted after three rounds of phage display penning with a ×9 peptide library. Positively charged (red), hydrophobic (blue, φ), and proline (gray) residues are highlighted. The derived binding consensus sequence is given in the bottom line. (*C*) Schematic representation of the pulldown/MS experiment performed to identify intersectin 1-SH3A interaction partners. SH3A compared with empty beads in a pull-down from mouse brain P2′ lysates was used to identify the major binding partners of the domain. Proteins that were enriched by more than a factor of 3 in both experiments are shown in red. (*D*) Selected signals from the overlays of ^{1}H-^{15}N-HSQC spectra of huITSN1 SH3A ligated to SH3B–E (red) with spectra recorded after the addition of a 10-fold molar excess of a synapsin 1- or dynamin 1-derived PRP to the ligated (blue) or isolated (black) domain. (*E*) Excerpts of ^{1}H-^{15}N-HSQC spectra of the extended, locked huITSN1 SH3A (black) overlaid with spectra recorded after supplementation with a 20-fold excess of synapsin-derived PRP2 peptide (red). While the WT (*Left*) shows a few small shift changes indicative of an partial opening of the locked conformation at this peptide excess, the A828P, T832A, T839A mutant (*Right*) remains nearly unaffected.

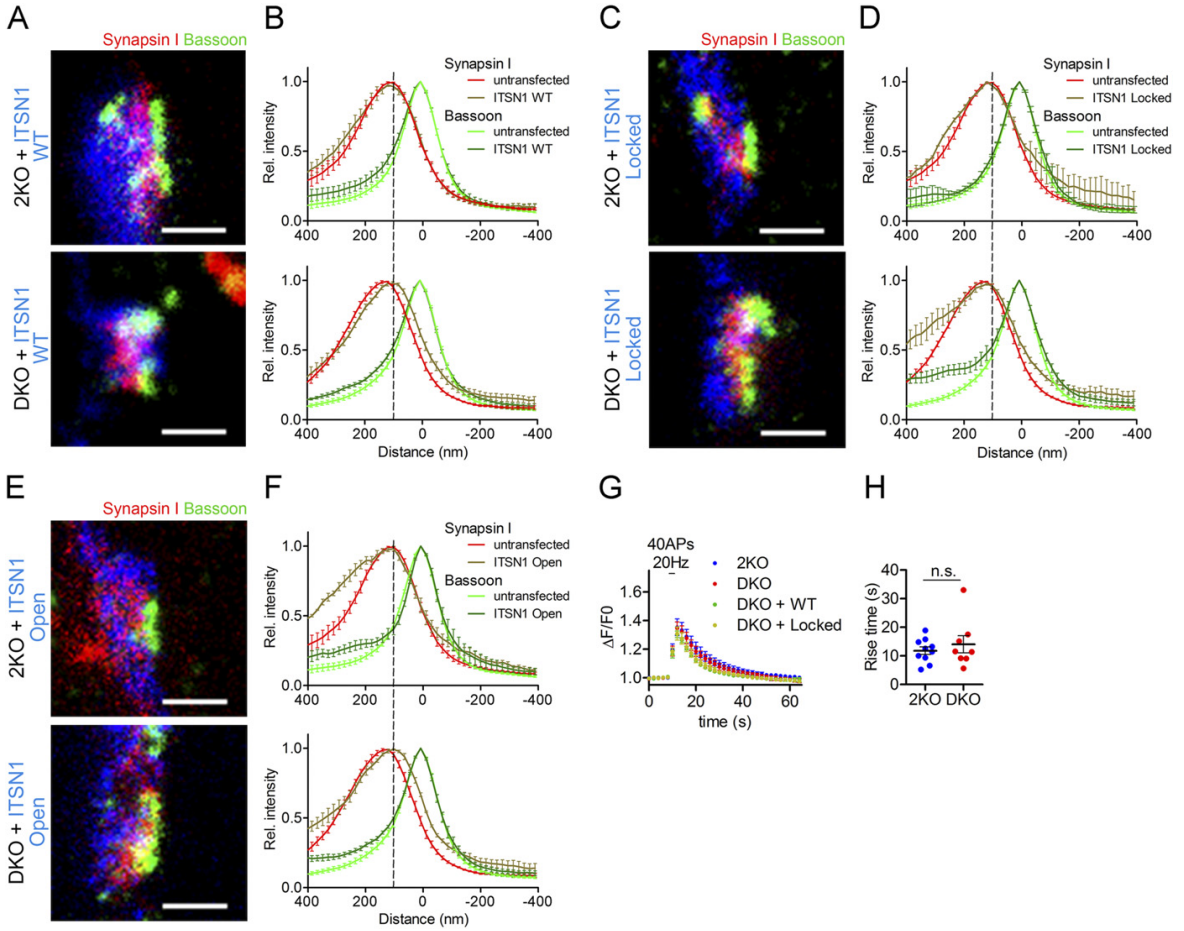

Fig. S8. Functional analysis of intersectin 1–synapsin complex formation. (*A*, *C*, and *E*) Representative sum intensity projected gSTED images displayed as three-channel overlays show the distance between synapsin 1 and the AZ marker bassoon and WT (*A*), locked (*C*), or open (*E*) CFP–intersectin 1. (Scale bars: 500 nm.) (*B*, *D*, and *F*) Line plot profiles from side views of synapses expressing WT (*B*), locked (*D*), or open (*F*) CFP–intersectin 1 and untransfected controls aligned to bassoon. Data are mean intensity values ± SEM. (*G*) Average traces of synaptophysin–pHluorin–expressing hippocampal neurons stimulated with 40 APs at 20 Hz to measure RRP size. Data were normalized to baseline. Data are mean ± SEM of 4–10 independent experiments; two-way RM ANOVA using Bonferroni's multiple comparisons test (control: DKO) did not detect significant differences. (*H*) Exocytic rise times for the 600-AP stimulation shown in Fig. 4*E* do not differ between intersectin 2KO and DKO. Dots represent 8–10 independent experiments; unpaired Student's *t* test; n.s., not significant.

Table S1. Antibodies used in this study

Antigen for primary Ab	Clone	Species	Source	Dilution Western blot/SPOT	Dilution IF	Amount IP
AP-1(γ)		Mouse	BD transduction 610386	1:2,000		
AP180	LP2D11	Mouse	Kind gift of Pietro DeCamilli*	1:25,000		
AP-2(α)		Mouse	BD transduction 610502	1:500		
AP2-(α)	AP6	Mouse	Abcam ab2730		1:100	
AP-2 (μ)		Mouse	BD transduction 611351	1:500		
AP-3 μ)	p47	Mouse	BD transduction 610901	1:250		
β-Actin	AC-15	Mouse	Sigma A5441	1:10,000		
Bassoon		Guinea pig	Synaptic Systems 141004		1:100	
Bassoon	219E1	Mouse	Synaptic Systems 141021		1:250	
Clathrin heavy chain	TD-1	Mouse	Purchased from Hybridoma, purified in house	1:10		
Clathrin light chain	C157.1	Mouse	Kind gift of Reinhard Jahn†	1:50		
Dynamin 1	Dyn DG-1	Rabbit	Kind gift of Pietro DeCamilli*	1:1,000		
Endophilin 1		Rabbit	Synaptic Systems 159002	1:1,000	1:200	
GFP	3E6	Mouse	Invitrogen		1:500	
GluR2		Mouse	Millipore MAB397	1:500		
GST		Rabbit	Santa Cruz	1:1,000		
HA-tag	HA.11	Mouse	Babco (Covance)	1:1,000	1:1,000	
Homer 1		Rabbit	Synaptic Systems 160003		1:200	
Homer 1		Guinea pig	Synaptic Systems 160004		1:200	
Hsc70	1B5	Mouse	Affinity Bioreagents MA3006	1:3,000		
Intersectin 1 aa 1–440	S750	Rabbit	In-house	1:250–1:1,000	1:200	
Intersectin 2		Rabbit	Kind gift of Alla Rynditch‡ (2)	1:1,000		
Intersectin 2		Rabbit	Sigma HPA 036475	1:250	1:50	
Numb		Goat	Abcam ab4147	1:1,000		
Phospho-dynamin 1 (S774)		Sheep	Abcam ab18090	1:500		
Piccolo		Rabbit	Synaptic Systems 142002		1:100	
Stonin2	2,424.5	Rabbit	In-house	1:500		
Synapsin I	46.1	Mouse	Synaptic Systems 106001	1:1,000	1:500	
Synapsin I	G-246	Rabbit	Kind gift of Pietro DeCamilli*	1:500		
Synapsin I		Rabbit	Synaptic Systems 106103		1:200	
Synapsin 1/2		Guinea pig	Synaptic Systems 106004			15 μL
Synapto-brevin 2	69.1	Mouse	Synaptic Systems104211	1:1,000	1:400	
Synapto-janin 1	"Ottavio"	Rabbit	Kind gift of Ottavio Cremona§ and Pietro De Camilli*	1:1,000		
Synapto-physin 1	7.2	Mouse	Synaptic Systems 101011	1:5,000		
Synapto-tagmin 1	41.1	Mouse	Synaptic Systems 105011	1:250		

IM, immunofluorescence; IP, immunoprecipitated.
*Howard Hughes Medical Institute, Yale University, New Haven, CT.
†Department of Neurobiology, Max-Planck-Institute for Biophysical Chemistry, Göttingen, Germany.
‡Institute of Molecular Biology and Genetics, National Academy of Sciences, Kiev, Ukraine.
§Facoltà di Medicina e Chirurgia, Universita Vita Salute-San Raffaele, Milan, Italy.

Table S2. Secondary antibodies

Secondary Ab raised in	IgG species recognized	Fluorophore/conjugate	Dilution	Source	Application
Goat	Mouse	AlexaFluor488	1:200	Invitrogen	IF/STED
Goat	Rabbit	AlexaFluor568	1:200	Invitrogen	IF
Goat	Guinea pig	AlexaFluor568	1:200	Invitrogen	STED
Goat	Rabbit	AlexaFluor594	1:200	Invitrogen	STED
Donkey	Guinea pig	AlexaFluor488	1:200	Jackson ImmunoResearch	STED
Goat	Mouse	Atto647N	1:200	Active Motif	STED
Goat	Rabbit	Atto647N	1:200	Active Motif	STED
Goat	Mouse	HRP	1:10,000	Jackson ImmunoResearch	WB
Goat	Rabbit	HRP	1:10,000	Jackson ImmunoResearch	WB

Table S3. Protein identification by mass spectrometry

Protein name	Gene	Isotopic ratio 1	Isotopic ratio 2
SH3A vs. control (Fig. S7*C*)			
Dynamin-3	*DYN3*	271.1171082	50.9771987
Dynamin-2	*DYN2*	259.1397287	93.79297865
Dynamin-1	*DYN1*	129.4751634	76.74629026
Protein piccolo	*PCLO*	78.59268789	187.8393051
WAS/WASL-interacting protein family member 3	*WIPF3*	74.93566773	23.25370974
Synaptojanin-1	*SYNJ1*	53.64867308	12.12088310
Synapsin-1	*SYN1*	48.72054965	15.66413319
Synapsin-2	*SYN2*	47.49273955	5.483170467
Cytoplasmic FMR1-interacting protein 2	*CYFP2*	38.04723336	45.54831705
Intersectin-1	*ITSN1*	36.69178097	296.2359754
Profilin-2	*PROF2*	3.036474435	9.138617445
Myelin basic protein	*MBP*	2.637699799	3.624683315
SH3A vs. SH3A locked (Fig. 4*A*)			
Synapsin-1	*SYN1*	14.0697148	3.23771843
Synapsin-2	*SYN2*	12.35294118	2.29255962
Cytoplasmic FMR1-interacting protein 2	*CYFP2*	2.413668134	3.14320255
Profilin-2	*PROF2*	2.326927876	1.715792944
WAS/WASL-interacting protein family member 3	*WIPF3*	2.292035398	1.408946038
Dynamin-2	*DYN2*	2.008184364	2.177821739
Synaptojanin-1	*SYNJ1*	1.926446281	0.998791076
Dynamin-1	*DYN1*	1.868537074	1.767666777
Myelin basic protein	*MBP*	1.823586935	1.020112100
Dynamin-3	*DYN3*	1.61790734	2.228816353

5 Discussion

5.1 Functions of intersectin in the synaptic vesicle cycle

The scaffold protein intersectin is known to interact with proteins of diverse pathways and to function as a scaffold by providing an interaction platform for these proteins. In the mammalian synapse intersectin has been described as early factor in CME as well as in actin remodeling (Hunter et al., 2013). In the present thesis I showed so far unknown functions of the scaffold protein intersectin in the mammalian synapse. First of all we demonstrated a function of intersectin in later stages of CME by facilitating the recruitment of endophilin to CCPs. Secondly, we observed an association of intersectin with the postfusion SNARE complex and described intersectin's contribution to release site clearance of these complexes. Finally, we identified a regulatory function of intersectin during SV clustering by association with synapsin. All these findings broadened our understanding of the diverse functions a single protein can execute depending on its interaction partners.

5.1.1 Intersectin's function in late-stage CME

Within the first project we focused on intersectin's well established function in clathrin-mediated endocytosis. We found a so far unknown interaction between intersectin 1 and endophilin A1 that facilitates the recruitment of synaptojanin and uncoating of CCVs. These findings solve the question of how endophilin is recruited to CCPs as endophilin itself does not interact with clathrin or AP-2.

The described association depends on intersectin 1's SH3B domain recognizing a non-canonical site within the SH3 domain of endophilin A1. This unusual interaction enables endophilin A1 to interact in parallel with dynamin and synaptojanin via proline rich peptide recognition of its SH3 domain (Sundborger et al., 2011, Verstreken et al., 2003). Additionally, such non-canonical interactions increase also intersectin's potential to serve as an interaction platform although specificity has to be ensured. Intersectin is described as one of the early acting endocytic proteins together with FCHo and Eps15, and its localization to the edge of CCPs has recently been shown (Sochacki et al., 2017). Its contribution to early stage CME was shown in many different systems, like *drosophila* (Koh et al., 2004, Marie et al., 2004), *C. elegans* (Rose et al., 2007) and

mammalian cells (Sengar et al., 1999). Nevertheless, intersectin does not dissociate from the membrane during maturation of the CCP, but stays and associates with AP-2 and dynamin also at late stage constricted necks. Its function in recruitment of endophilin could be an explanation for that. Endophilin has furthermore been implicated in other clathrin independent modes of endocytosis like ultrafast endocytosis or fast endophilin-mediated endocytosis (FEME) (Watanabe et al., 2018, Boucrot et al., 2015). If intersectin-mediated recruitment of endophilin or another function of intersectin is also important in these endocytosis modes has to be determined. A contribution of intersectin is however likely, as dynamin, one of intersectin's high affinity interaction partners (Okamoto et al., 1999), is necessary for ultrafast endocytosis as well as for FEME (Watanabe et al., 2013, Boucrot et al., 2015). Moreover, it was reported that activity of Cdc42 upstream of endophilin is critical for FEME, a function conceivably implemented by intersectin (Boucrot et al., 2015).

Endophilin A1,2,3 TKO hippocampal neurons show a decrease in endocytic kinetics measured using pHluorin-tagged synaptobrevin as well as an accumulation of CCVs (Milosevic et al., 2011), phenotypes also observed in mice depleted of synaptojanin (Cremona et al., 1999). In contrast, depletion of intersectin 1 does not impair endocytosis in cultured neurons or change basal synaptic transmission measured in acute slices (Jakob et al., 2017). This discrepancy together with the less severe accumulation of CCVs in intersectin 1 KO mice might be explained by the increased expression of intersectin 2, which we detected in intersectin 1 KO mice that could compensate for intersectin 1 loss. In line with this, we observed binding of intersectin 2 to endophilin, and unpublished data from intersectin 1/2 DKO neurons show an impairment in endocytosis in pHluorin assays.

The described association of endophilin and intersectin facilitates recruitment of the phosphatase synaptojanin. Interestingly, intersectin 1 itself is able to directly interact with synaptojanin (Okamoto et al., 1999). This interaction is possibly regulated by intersectin's association with AP-2 as AP-2 binding to intersectin blocks synaptojanin association (Pechstein et al., 2010a). Therefore we suggest the following model. Intersectin 1 associates with early endocytic proteins like FCHo and Eps15 and binds subsequently to AP-2. Binding to AP-2 prevents premature synaptojanin binding to intersectin (Pechstein et al., 2010a). Endophilin recognizes late-stage constricted CCP necks via its BAR domain and additionally binds to intersectin. The endophilin – intersectin complex is at this stage able to efficiently recruit synaptojanin. If endophilin and AP-2 also compete for intersectin 1 binding is still an open question.

5.1.2 Intersectin removes SNARE complexes from release sites

Another function of intersectin that was described in project II is the clearance of release sites from postfusion SNARE complexes. Based on biochemical observations, we found an interaction of intersectin with the assembled SNARE complex. Further pHluorin based results led us to a model in which intersectin associates with assembled postfusion SNARE complexes and removes these complexes from release sites to enable subsequent docking and fusion events.

Several other proteins have been suggested to be involved in release site clearance. For example, inhibition of endocytic proteins, like dynamin or AP-2 was shown to impair replenishment of release-ready vesicles, likely due to the accumulation of not removed exocytosed material from release sites (Hosoi et al., 2009). Intersectin represents the perfect candidate to couple exocytosed material (i.e. SNARE complexes) and proteins of the endocytic machinery, with which it interacts. Using pHluorin-tagged probes we detected a reduction in the exocytosis rate in intersectin 1 KO neurons upon sustained stimulation. This effect is in accordance with the impaired replenishment of fast releasing vesicles in the calyx of Held synapse of intersectin 1 KOs (Sakaba et al., 2013) that we also detected after injection of SH3 domains. Another protein that was described in release site clearance is the SV protein secretory carrier membrane protein 5 (SCAMP5) that also interacts with AP-2. Depletion of SCAMP5 in hippocampal neurons led to exocytic depression upon sustained stimulation as well as to a frequency-dependent depression (Park et al., 2018). These phenotypes are similar to the ones we observed in intersectin 1 KO hippocampal neurons. A direct cargo that is removed from release sites by SCAMP5 has not been proposed but it appears possible that intersectin and SCAMP5 cooperate in the same process (conceivably via a direct interaction) or that the SV protein SCAMP5 is involved in recruitment of intersectin to sites of vesicle fusion. Interestingly, intersectin, via its EH-domains interacts with N-terminal NPF repeats in SCAMP1 that itself is involved in CME (Fernández-Chacón et al., 2000). The observed reduction in exocytic rates upon sustained stimulation using pHluorin imaging could also conceivably be explained by a function of intersectin in SV priming. But impaired SV priming as seen for example after depletion of Munc13 results in a general reduction in exocytosis (Varoqueaux et al., 2002) which we did not detect using a single stimulation in pHluorin imaging. There is so far also no other data supporting this idea.

We observed a direct binding of intersectin to the assembled SNARE complex, and by overexpression of an intersectin-binding deficient mutant of synaptobrevin 2 we were able to phenocopy the exocytic depression seen in intersectin 1 KO neurons. While we

argue that intersectin 1 specifically clears SNARE complexes from release sites, others described a release site clearance mechanism for synaptobrevin 2 molecules. One possibility to remove synaptobrevin 2 molecules from the neuronal surface is by recognition through its endocytic adaptor protein AP180/CALM and thereby link synaptobrevin 2 molecules to CME (Koo et al., 2015). Similar to binding of AP180/CALM the SV protein synaptophysin is as well only able to interact with synaptobrevin 2 alone but not with the assembled SNARE complex (Koo et al., 2011, Edelmann et al., 1995). Synaptophysin associates with synaptobrevin 2 to prevent cis-SNARE complex formation at the membrane (Rajappa et al., 2016). The described function of synaptophysin is in accordance with our data as we showed that binding of intersectin to the SNARE proteins is as efficient in synaptophysin KO brains as it is in WT controls and therefore independent of synaptophysin. Furthermore, depletion of synaptophysin results in short term synaptic depression in hippocampal neurons comparable to the phenotypes seen in intersectin 1 and SCAMP5 KO neurons, respectively (Kwon and Chapman, 2011, Rajappa et al., 2016). The function of synaptophysin in preventing cis-SNARE complex formation is consistent with our hypothesis of the release site blocking ability of assembled SNARE complexes. Moreover, inhibition of the disassembling protein NSF using peptides results in reduced neurotransmitter release (Kuner et al., 2008, Schweizer et al., 1998), likely due to accumulation of assembled SNARE complexes. Along this line, SNARE complex disassembly by NSF needs at least 100 ms (Choi et al., 2018). The short-term depression effects seen in the calyx of Held synapse appeared already after less than 100 ms (Hosoi et al., 2009, Sakaba et al., 2013). These results clearly give evidence for the necessity of SNARE complex removal from release sites prior to disassembly.

The differences we detected between primary cultures of hippocampal neurons and the calyx of Held synapse are likely based on their different properties regarding the stimulation frequency, release probability or the number of SVs in the different pools. The increased number of release-ready vesicles (2000 vesicles in the RRP) in combination with a high release probability in the calyx of Held can explain the expanded need for efficient release site clearance and thereby the stronger phenotypes seen in the calyx (Rizzoli and Betz, 2005). Moreover, the calyx of Held synapse shows two components of release, a fast and a slow releasing vesicle pool. The fast releasing vesicles exhibit a higher release probability, arguing for their docking at release sites in close proximity to calcium channels while the slow releasing vesicles are docked further away from calcium channels (Sakaba and Neher, 2001). In accordance to that, we detected a phenotype upon intersectin SH3 domain injection only for the fast-releasing pool as only for this

pool release site clearance is crucial. Compared to hippocampal neurons with only 5-20 vesicles in the RRP and a consequential reduced demand for release site clearance the observed rather small effects on exocytic depression upon sustained stimulation are plausible.
With the data known so far the following model can be proposed. After SV fusion cis-SNARE complexes are removed from release sites by association with intersectin 1. Depending on stimulation strength these complexes are possibly directly endocytosed or αSNAP and NSF disassemble cis-SNARE complexes in areas adjacent to release sites. Uncomplexed synaptobrevin 2 molecules are bound by synaptophysin to inhibit reformation of SNARE complexes at the membrane until synaptobrevin 2 is recognized by its sorting adaptor AP180. This model is also in accordance with our observation of an unperturbed synaptobrevin 2 endocytosis in intersectin 1 KO neurons. There are around 70 synaptobrevin 2 molecules on one SV (Takamori et al., 2006) but only a few of them (2-10) are involved in SNARE complex formation (Manca et al., 2019, Sinha et al., 2011, Domanska et al., 2009). Only those are a target for intersectin 1 binding, clearance from release sites and possibly sorting for endocytosis. The majority of synaptobrevin 2 molecules is recognized by AP180/CALM for proper sorting onto SVs, a mechanism that is not impaired upon loss of intersectin 1 but might even be enhanced as we detected increased AP180 protein levels in intersectin 1 KO brains.

A question that remains is if intersectin is able to sort SNARE complexes specifically to a particular mode of endocytosis (i.e. CME or CIE) or if intersectin is only involved in removal of the complexes independent of subsequent endocytic processes. So far intersectin is well studied during CME but as the necessity for removal of SNARE complexes is highest under sustained high-frequency stimulations a coupling to faster endocytic modes is likely. Moreover, mathematical modeling has shown that the lateral diffusion constant of syntaxin dramatically decreases as soon as syntaxin is in a complex with SNAP25 or an exocytic complex (Ribrault et al., 2011). Slower lateral diffusion of the assembled SNARE complex might be another explanation for the need of active removal from release sites.
Instead of the removal of exocytosed material the reformation of functional release sites could as well be rate-limiting for sustained activity. Exocytic proteins, like RIM, Muncs, complexin and others associate with the trans-SNARE complex prior to fusion to build up the highly efficient release machinery which enables fast and synchronous SV fusion at release sites. It is likely that these proteins are also still associated with the SNARE complex after fusion. Therefore it is conceivable that the term release site clearance constitutes the reformation of functional release sites including the necessary release

machinery proteins (e.g. Muncs). Our data is in accordance with such a model but further experiments are necessary to proof the exact mechanism.
Either way this mechanism additionally provides a tool to adapt presynaptic short-term plasticity (Regehr, 2012). If the interaction between intersectin and the SNARE complex is regulated depending on the status of the synapse, release site clearance can be switched on and off and thereby control SV fusion during sustained stimulations. Of course such a mechanism is reliant on postsynaptic feedback signaling. If there is a connection between intersectin and transsynaptic proteins like the postsynaptic protein neuroligin that is known to regulate presynaptic release is so far not known (Futai et al., 2007).

5.1.3 Intersectin regulates refilling of the recycling SV pool

In project III we investigated the possible function of intersectin in regulating SV clustering. Our biochemical data showed an autoregulated mechanisms within intersectin 1 that controls association with synapsin I in an activity dependent manner. Super-resolution microscopy, electrophysiological recordings as well as pHluorin imaging led us to a model in which intersectin 1 binds free synapsin I molecules and prevents premature reclustering of SVs which enables proper replenishment of the recycling SV pool.

The ability of synapsins to interact with SVs depends on its phosphorylation status. In line with the activity dependent phosphorylation changes of synapsin, the intersectin 1 – synapsin interaction we describe here is as well regulated by phosphorylation and thereby depends on neuronal activity. The interaction we found in rodent brains is based on the SH3A domain of intersectin recognizing a proline rich sequence within synapsin I's D domain. We identified the linker between the SH3A and B domains to fold back onto the SH3A domain depending on phosphorylation of two threonine residues within the linker. Phosphorylation opens the binding between the linker region and the SH3A domain and allows synapsin I binding. The kinase phosphorylating intersectin could not be identified so far, but as this interaction depends on neuronal activity kinases like Cdk5 are potential candidates (Cheung et al., 2006).
A phospho-dependent interaction between synapsin and intersectin has been described before in *drosophila*, albeit in this system the interaction depends on the Dap160 SH3B domain (Winther et al., 2015). Rescue of Dap160 loss using a synapsin binding deficient mutant of Dap160 results in perturbed reclustering of SVs. Stimulating *drosophila* larvae NMJs led to an increased dispersion of synapsin into the axon, a phenotype we

did not detect in intersectin 1/2 DKO hippocampal neurons. However, the reclustering of synapsin and SVs following activity could be mediated by other mechanisms in higher organisms. Moreover, the interaction between synapsin and Dap160 occurs via the Dap160 SH3B domain and is thus probably differently regulated than the intersectin SH3A – synapsin I interaction we detected. The slight differences in the described phenotypes could also be explained by the presence of other proteins within the SV cluster in vertebrates, like amphiphysin (Onofri et al., 2000). Interestingly, the association between amphiphysin and synapsin I decreased synapsin I's ability to bind SVs and actin. We expect a similar pattern for the intersectin 1 – synapsin I interaction, although we did not test it directly. Moreover, besides amphiphysin also endophilin was described to localize to the SV cluster under resting conditions (Sundborger et al., 2011). The localization of endocytic proteins within the SV cluster proposes an additional function of these proteins in SV clustering by forming a sophisticated interaction network in conjunction with synapsin I homo- or heterodimers (Shupliakov et al., 2011). In line with that, a recent study proposed that the formation of a liquid phase for the separation of SVs is accomplished by synapsin and its low-affinity interaction partners carrying SH3 domains (Milovanovic et al., 2018). Notably, this study showed, that high concentrations of intersectin SH3 domains lowered liquid phase separation according to our model in which intersectin restrains synapsin from SV clustering. Furthermore, many endocytic proteins undergo cycling dependent on the activity status of the synapse similar to the dispersion of synapsin I. For example, intersectin and dynamin localize to the SV cluster during rest but relocate to periactive sites during stimulation (Evergren et al., 2007, Sundborger et al., 2011). We made use of superresolution STED microscopy to visualize synapsin I in intersectin 1/2 DKO synapses and detected an increased distance of synapsin I to the active zone, a phenotype we did not see for other intersectin binding partners like endophilin. This data shows that endocytic proteins within the SV cluster (i.e. endophilin) are not regulated by intersectin and that a change in synapsin I localization alone results in a drastic effect on the replenishment rate of vesicles to the recycling pool. Accordingly, the importance of endocytic proteins within the vesicle cluster for clustering is probably minor or depends itself on synapsin I. In line with this, it was suggested that the SV reserve pool serves as a molecular sink for endocytic proteins in which they are stored during resting conditions (Denker et al., 2011).

The still open question is how intersectin prevents synapsin I from prematurely reclustering of SVs. One possibility could be that intersectin's association with synapsin I prevents synapsin's interaction with phosphatases like protein phosphatase 2A that acts at domain D in close proximity to the intersectin binding site (Jovanovic et al., 2001).

Phosphorylation at domain D, similar to domain A, is a main regulator of synapsin I's binding affinity towards SVs and actin (Cesca et al., 2010).

5.2 Regulation of intersectin's diverse functions

It seems that with evolution intersectins implement more versatile functions than just in endocytosis, as we see its contribution to exo-/ endocytic coupling and SV clustering. The question arises why the phenotypes we and others have described in intersectin single or double KO rodents are not more severe. While depletion of the *drosophila* intersectin homologue Dap160 is lethal (Marie et al., 2004), intersectin 1 KO mice are vital, reproduce in Mendelian ratios and show only mild or even no behavioral abnormalities depending on the mice strain used (Sengar et al., 2013, Jakob et al., 2017). Due to the expression of two intersectin genes in mammals loss of intersectin 1 can be compensated by intersectin 2. Accordingly, we detected an increased expression of intersectin 2 in intersectin 1 KO neurons. For many of intersectin 1's interaction partners we could additionally confirm that they as well associate with intersectin 2. To avoid compensation by intersectin 2 in the synapsin study, we made use of intersectin 1/2 DKO mice. Intersectin 1/2 DKO mice show a more severe phenotype in terms of survival rates but also in behavior compared to intersectin 1 single KO mice. Notably, in electrophysiological recordings from acute slices of intersectin 1/2 DKO mice, we observed an impaired replenishment of vesicles from the reserve pool, a phenotype we could not detect in intersectin 1 single KO slices likely due to compensation by intersectin 2. However, intersectin's function in SV clustering could potentially be compensated by endophilin or amphiphysin as both proteins were detected as well in the SV cluster (Shupliakov et al., 2011, Evergren et al., 2004). Even though the phenotypes in intersectin 1/2 DKO mice are more pronounced, we made us of intersectin 1 single KO mice to investigate intersectin's function in release site clearance to avoid possible confusion with the detected synapsin I phenotype in intersectin 1/2 DKOs.

However, intersectin is a scaffold protein and its predominant function is to supply an interaction platform to increase the local concentration of its binding partners. This platform will facilitate diverse processes, but its depletion will never exclude functionality of its binding partners. Especially in higher organisms the loss of a single scaffold protein can well be compensated. Mice depleted of the presynaptic scaffold proteins bassoon or piccolo for example are viable even though survival rates are mildly reduced (Mukherjee et al., 2010, Altrock et al., 2003).

The question remains how intersectin achieves specificity for its several binding partners and how the interactions are temporally and spatially regulated.
The allosteric inhibition of a certain binding site by another protein or autoregulatory mechanisms are modes to temporally regulate a protein dependent on the activity status of the synapse. For example, the interaction between intersectin and AP-2 competes with binding to synaptojanin (Pechstein et al., 2010a). It is likely that there are several competing interactors of intersectin because many of them share common binding domains (see Figure 1.4). So far, for the interactions described in this thesis, such competition for binding domains has not been found. However, we described an autoinhibitory mechanism for the interaction between intersectin's SH3A domain and synapsin I, that depends on neuronal activity triggering the phosphorylation of the SH3A C-terminal linker. Interestingly, intersectin's endocytic binding partner dynamin can open the autoinhibited conformation of intersectin independent of phosphorylation. This example reveals how intersectin can selectively fulfill a function in SV clustering only upon neuronal activity while its contribution to endocytosis, by binding to dynamin and perhaps also endophilin, is constitutively active. An autoregulatory mechanism within intersectin has been described already for the linker region between the SH3 domains and the DH domain which regulates intersectin's GEF activtiy (Kintscher et al., 2010). There are also several other proteins known to regulate their functions via autoregulatory mechanisms, for example the Parkinson's disease associated protein parkin (Chaugule et al., 2011) or the BAR-domain protein SNX9 that is involved in CME (Lo et al., 2017). If also other domains of intersectin and their respective binding properties are regulated by autoinhibition is not known, but domains like the SNARE complex binding SH3B domain could likely be regulated in such a manner.
Besides temporal control another mechanism is the spatial regulation that enables interaction with other proteins only at certain locations in the cell. The PH and C2 domains of intersectin could conceivably recruit intersectin to the cell membrane in an activity and calcium dependent manner (Cho, 2001). So far no data exists, but as these domains are only present in the neuronal isoform, a contribution to intersectin's diverse neuronal functions is likely. Nevertheless, superresolution microscopy as well as our own observations suggest a rather broad distribution of intersectin within the presynapse arguing for a greater importance of availability of interaction partners at a certain location (Wilhelm et al., 2014).
However, regulation of intersectin might be dispensable for some of its interaction partners. Several studies suggest that the association between intersectin and endophilin is involved in different steps of the SV cycle. We described the importance of their

association for recruitment of synaptojanin and CCV uncoating. Other studies showed the abundance of endophilin within the SV cluster and proposed that BAR- and SH3-domain containing proteins are involved in SV clustering in cooperation with synapsin I (Shupliakov et al., 2011). Additionally, recent studies demonstrated that an interaction between endophilin, intersectin and VGLUT leads to the formation of a strengthened SV cluster that shows reduced release probability (Zhang et al., 2018, Weston et al., 2011). Moreover, an exocytic role for intersectin and endophilin has recently been proposed to be involved in fusion of large dense core vesicles in neuroendocrine cells (Milosevic et al., 2019). It is conceivable that an intersectin – endophilin complex is involved in all the different steps of the SV cycle and therefore never dissociates. Although this concept needs to be proven, it is very likely that intersectin fulfills its functions as a part of a bigger network, for example in conjunction with endophilin and dynamin.

Nonetheless, a tight regulation of intersectin's expression and activity levels is crucial for its function as depletion as well as overexpression of intersectin affects endocytosis (Sengar et al., 1999, Yu et al., 2008). This effect can be explained by the regular function of a scaffold protein. The upregulated expression of a scaffold protein sequesters binding partners into different complexes, which can result in the same effect as loss of the respective scaffold protein (Levchenko et al., 2000, Good et al., 2011). This could explain potential pathological consequences of increased intersectin 1 expression in DS as well as in AD patients (Blalock et al., 2004). An accumulation of large early endosomal structures in patient cells implicates an impairment in endocytosis which might be caused by intersectin 1 overexpression (Pucharcós et al., 1999, Hunter et al., 2011). Notably, the expression of many intersectin interaction partners is altered in DS and AD patients, for example SNAP25 and dynamin expression is decreased, while synaptojanin expression is increased (Keating et al., 2006). These observations suggest possible contribution of intersectin 1 in early AD and DS pathology. Furthermore, mutations within synapsin are associated with neurological pathologies, like epilepsy (Garcia et al., 2004), and could possibly also affect intersectin binding and therefore its role in synapsin regulation. Understanding the different interaction modes of intersectin could help to uncover the molecular basis of such disorders.

5.3 Conclusion and future directions

In the present study, we describe the versatile functions of the scaffold protein intersectin in the synaptic vesicle cycle that all depend on its ability to interact with diverse proteins. The numerous processes intersectin facilitates in the presynapse are summarized in figure 5.1.

First, we identified intersectin's contribution to late-stage CME by an interaction with endophilin A1. This association facilitates recruitment of synaptojanin to CCPs, subsequent uncoating of CCVs and thereby reformation of SVs. Additionally, we observed an association between synapsin I and intersectin in an activity dependent manner. This interaction enables proper replenishment of release-ready vesicles from the reserve pool, which is especially important during sustained neurotransmission. Finally, we describe an association of intersectin with the postfusion SNARE complex that is crucial to remove these complexes from release sites and enable subsequent fusion events.

The results obtained in the different projects show that intersectin in all its diverse functions in the SV cycle is crucial to maintain synaptic functionality during sustained activity. Intersectin's function as a facilitator in these different pathways also suggests that active regulation of its binding capabilities could represent a mechanism to control

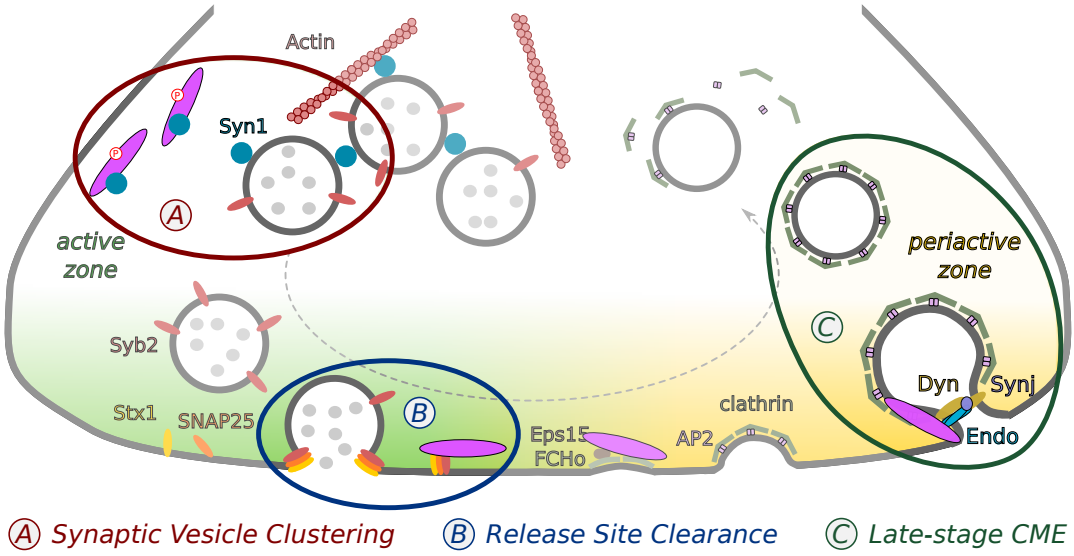

Fig. 5.1: Intersectin's versatile functions in the presynapse. Intersectin (magenta) was initially described as an early-stage endocytic protein by interacting with Eps15 and FCHo. In the present study, we described the autoregulated interaction between intersectin and synapsin I and its implication in regulation of the reserve SV pool (A). Moreover, we demonstrated that intersectin mediates release site clearance of postfusion SNARE complexes to sustain fast neurotransmission (B). Finally, we showed intersectin's function additionally in late-stage CME by associating with endophilin, an interaction that facilitates synaptojanin recruitment (C).

the speed and efficiency of the synaptic vesicle cycle and could thereby serve as a hub to adopt plasticity. Understanding the precise regulation modes of intersectin's versatile interactions will help to reveal how the synapse maintains proper functionality especially under sustained activity. However, the identification of the exact neuron types and circuits in the brain that rely most on intersectin's function would be of great interest to further understand its importance and implications in diseases, learning and memory.

Abbreviations

AD	Alzheimer's disease
AP	action potential
AP-2	adaptor protein 2
BAR	Bin-amphiphysin-Rvs
C2	protein kinase C conserved 2
CaMK	Ca^{2+}/calmodulin-dependent protein kinase
CAZ	cytomatrix of the active zone
CC	coiled coil
Cdk	cyclin-dependent kinase
CCP	clathrin-coated pit
CCV	clathrin-coated vesicle
CIE	clathrin-independent endocytosis
CME	clathrin-mediated endocytosis
Dap160	dynamin-associated protein 160 kDa
DH	Dbl homology
DKO	double knock-out
DS	Down syndrome
EH	Eps15 homology
EPSP	excitatory postsynaptic potential
FEME	fast endophilin-mediated endocytosis
GEF	guanosine triphosphate exchange factor
ITSN	intersectin
KO	knock-out
NMJ	neuromuscular junction
NSF	N-ethylmaleimide-sensitive factor
N-WASP	neuronal Wiskott-Aldrich syndrome protein
PH	Pleckstrin homology
PI3KC2β	phosphatidylinositol 3-kinase class II beta
PI(4,5)P_2	phosphatidylinositol 4,5-bisphosphate
PKA	protein kinase A
PSD	postsynaptic density
RIM	rab3-interacting molecule
RBP	RIM binding protein
RRP	readily-releasable pool
SCAMP	secretory carrier membrane protein
SH3	Src homology 3
SNX	sorting nexin
SNAP	soluble NSF attachment protein
SNARE	soluble NSF attachment protein receptor
Sos	Son of Sevenless

Syb	synaptobrevin
Syn	synapsin
Syp	synaptophysin
Syt	synaptotagmin
STED	stimulated emission depletion
Stx	syntaxin
SV	synaptic vesicle
TMD	transmembrane domain
TKO	triple knock-out
TTX	tetrodotoxin
VAMP	vesicle-associated membrane protein
V-ATPase	vacuolar H^+-adenosine triphosphatase
VGLUT	vesicular glutamate transporter
VGCC	voltage-gated calcium channel
WT	wild-type

List of Figures

Bibliography

Ackermann, F.; Waites, C. L., and Garner, C. C. Presynaptic active zones in invertebrates and vertebrates. *EMBO reports*, 16(8):923–938, 2015.

Acuna, C.; Liu, X.; Gonzalez, A., and Südhof, T. C. RIM-BPs Mediate Tight Coupling of Action Potentials to Ca2+-Triggered Neurotransmitter Release. *Neuron*, 87(6):1234–1247, 2015.

Altrock, W. D.; tom Dieck, S.; Sokolov, M.; Meyer, A. C.; Sigler, A.; Brakebusch, C.; Fässler, R.; Richter, K.; Boeckers, T. M.; Potschka, H.; Brandt, C.; Löscher, W.; Grimberg, D.; Dresbach, T.; Hempelmann, A.; Hassan, H.; Balschun, D.; Frey, J. U.; Brandstätter, J. H.; Garner, C. C.; Rosenmund, C., and Gundelfinger, E. D. Functional Inactivation of a Fraction of Excitatory Synapses in Mice Deficient for the Active Zone Protein Bassoon. *Neuron*, 37(5):787–800, 2003.

Aoyagi, K.; Sugaya, T.; Umeda, M.; Yamamoto, S.; Terakawa, S., and Takahashi, M. The Activation of Exocytotic Sites by the Formation of Phosphatidylinositol 4,5-Bisphosphate Microdomains at Syntaxin Clusters. *Journal of Biological Chemistry*, 280(17):17346–17352, 2005.

Augustin, I.; Rosenmund, C.; Südhof, T. C., and Brose, N. Munc13-1 is essential for fusion competence of glutamatergic synaptic vesicles. *Nature*, 400(6743):457–461, 1999.

Azevedo, F. A. C.; Carvalho, L. R. B.; Grinberg, L. T.; Farfel, J. M.; Ferretti, R. E. L.; Leite, R. E. P.; Filho, W. J.; Lent, R., and Herculano-Houzel, S. Equal numbers of neuronal and nonneuronal cells make the human brain an isometrically scaled-up primate brain. *Journal of Comparative Neurology*, 513(5):532–541, 2009.

Baumert, M.; Maycox, P. R.; Navone, F.; Camilli, P. De, and Jahn, R. Synaptobrevin: an integral membrane protein of 18,000 daltons present in small synaptic vesicles of rat brain. *The EMBO Journal*, 8(2):379–384, 1989.

Bellocchio, E. E.; Reimer, R. J.; Fremeau, R. T., and Edwards, R. H. Uptake of Glutamate into Synaptic Vesicles by an Inorganic Phosphate Transporter. *Science*, 289(5481):957–960, 2000.

Blalock, E. M.; Geddes, J. W.; Chen, K. C.; Porter, N. M.; Markesbery, W. R., and Landfield, P. W. Incipient Alzheimer's disease: Microarray correlation analyses reveal major transcriptional and tumor suppressor responses. *Proceedings of the National Academy of Sciences*, 101(7):2173–2178, 2004.

Boucrot, E.; Ferreira, A. P. A.; Almeida-Souza, L.; Debard, S.; Vallis, Y.; Howard, G.; Bertot, L.; Sauvonnet, N., and McMahon, H. T. Endophilin marks and controls a clathrin-independent endocytic pathway. *Nature*, 517(7535):460–465, 2015.

Bykhovskaia, M. Synapsin regulation of vesicle organization and functional pools. *Seminars in Cell & Developmental Biology*, 22(4):387–392, 2011.

Böhme, M. A.; Beis, C.; Reddy-Alla, S.; Reynolds, E.; Mampell, M. M.; Grasskamp, A. T.; Lützkendorf, J.; Bergeron, D. D.; Driller, J. H.; Babikir, H.; Göttfert, F.; Robinson, I. M.; O'Kane, C. J.; Hell, S. W.; Wahl, M. C.; Stelzl, U.; Loll, B.; Walter, A. M., and Sigrist, S. J. Active zone scaffolds differentially accumulate Unc13 isoforms to tune Ca^{2+}\$ channel–vesicle coupling. *Nature Neuroscience*, 19(10):1311–1320, 2016.

Cazares, V. A.; Njus, M. M.; Manly, A.; Saldate, J. J.; Subramani, A.; Ben-Simon, Y.; Sutton, M. A.; Ashery, U., and Stuenkel, E. L. Dynamic Partitioning of Synaptic Vesicle Pools by the SNARE-Binding Protein Tomosyn. *Journal of Neuroscience*, 36(44):11208–11222, 2016.

Cesca, F.; Baldelli, P.; Valtorta, F., and Benfenati, F. The synapsins: Key actors of synapse function and plasticity. *Progress in Neurobiology*, 91(4):313–348, 2010.

Chaugule, V. K.; Burchell, L.; Barber, K. R.; Sidhu, A.; Leslie, S. J.; Shaw, G. S., and Walden, H. Autoregulation of Parkin activity through its ubiquitin-like domain. *The EMBO Journal*, 30(14): 2853–2867, 2011.

Cheung, Z. H.; Fu, A. K. Y., and Ip, N. Y. Synaptic Roles of Cdk5: Implications in Higher Cognitive Functions and Neurodegenerative Diseases. *Neuron*, 50(1):13–18, 2006.

Chiang, Chung-Wei; Chang, Che-Wei, and Jackson, Meyer B. The Transmembrane Domain of Synaptobrevin Influences Neurotransmitter Flux through Synaptic Fusion Pores. *Journal of Neuroscience*, 38(32):7179–7191, 2018.

Cho, W. Membrane Targeting by C1 and C2 Domains. *Journal of Biological Chemistry*, 276(35): 32407–32410, 2001.

Choi, Ucheor B; Zhao, Minglei; White, K Ian; Pfuetzner, Richard A; Esquivies, Luis; Zhou, Qiangjun, and Brunger, Axel T. NSF-mediated disassembly of on- and off-pathway SNARE complexes and inhibition by complexin. *eLife*, 7:e36497, 2018.

Cousin, Michael A and Robinson, Phillip J. The dephosphins: dephosphorylation by calcineurin triggers synaptic vesicle endocytosis. *Trends in Neurosciences*, 24(11):659–665, 2001.

Cremona, O.; Di Paolo, G.; Wenk, M. R.; Lüthi, A.; Kim, W. T.; Takei, K.; Daniell, L.; Nemoto, Y.; Shears, S. B.; Flavell, R. A.; McCormick, D. A., and De Camilli, P. Essential Role of Phosphoinositide Metabolism in Synaptic Vesicle Recycling. *Cell*, 99(2):179–188, 1999.

Das, M.; Scappini, E.; Martin, N. P.; Wong, K. A.; Dunn, S.; Chen, Y.-J.; Miller, S. L. H.; Domin, J., and O'Bryan, J. P. Regulation of Neuron Survival through an Intersectin-Phosphoinositide 3-Kinase C2β-AKT Pathway. *Molecular and Cellular Biology*, 27(22):7906–7917, 2007.

Dean, C. and Dresbach, T. Neuroligins and neurexins: linking cell adhesion, synapse formation and cognitive function. *Trends in Neurosciences*, 29(1):21–29, 2006.

Deitcher, D. L.; Ueda, A.; Stewart, B. A.; Burgess, R. W.; Kidokoro, Y., and Schwarz, T. L. Distinct Requirements for Evoked and Spontaneous Release of Neurotransmitter Are Revealed by Mutations in theDrosophila Gene neuronal-synaptobrevin. *Journal of Neuroscience*, 18(6):2028–2039, 1998.

Deng, L.; Kaeser, P. S.; Xu, W., and Südhof, T. C. RIM Proteins Activate Vesicle Priming by Reversing Autoinhibitory Homodimerization of Munc13. *Neuron*, 69(2):317–331, 2011.

Denker, A.; Kröhnert, K.; Bückers, J.; Neher, E., and Rizzoli, S. O. The reserve pool of synaptic vesicles acts as a buffer for proteins involved in synaptic vesicle recycling. *Proceedings of the National Academy of Sciences*, 108(41):17183–17188, 2011.

Dergai, O.; Novokhatska, O.; Dergai, M.; Skrypkina, I.; Tsyba, L.; Moreau, J., and Rynditch, A. Intersectin 1 forms complexes with SGIP1 and Reps1 in clathrin-coated pits. *Biochemical and Biophysical Research Communications*, 402(2):408–413, 2010.

Deák, F.; Schoch, S.; Liu, X.; Südhof, T. C., and Kavalali, E. T. Synaptobrevin is essential for fast synaptic-vesicle endocytosis. *Nature Cell Biology*, 6(11):1102–1108, 2004.

Di Paolo, G. and De Camilli, P. Phosphoinositides in cell regulation and membrane dynamics. *Nature*, 443(7112):651–657, 2006.

Diril, M. K.; Wienisch, M.; Jung, N.; Klingauf, J., and Haucke, V. Stonin 2 Is an AP-2-Dependent Endocytic Sorting Adaptor for Synaptotagmin Internalization and Recycling. *Developmental Cell*, 10(2):233–244, 2006.

Domanska, M. K.; Kiessling, V.; Stein, A.; Fasshauer, D., and Tamm, L. K. Single vesicle millisecond fusion kinetics reveals number of SNARE complexes optimal for fast SNARE-mediated membrane fusion. *Journal of Biological Chemistry*, 284(46):32158–32166, 2009.

Edelmann, L.; Hanson, P. I.; Chapman, E. R., and Jahn, R. Synaptobrevin binding to synaptophysin: a potential mechanism for controlling the exocytotic fusion machine. *The EMBO Journal*, 14(2): 224–231, 1995.

Edwards, R. H. The Neurotransmitter Cycle and Quantal Size. *Neuron*, 55(6):835–858, 2007.

Eggermann, E.; Bucurenciu, I.; Goswami, S. P., and Jonas, P. Nanodomain coupling between Ca^{2+} channels and sensors of exocytosis at fast mammalian synapses. *Nature Reviews Neuroscience*, 13 (1):7–21, 2012.

Evergren, E.; Marcucci, M.; Tomilin, N.; Löw, P.; Slepnev, V.; Andersson, F.; Gad, H.; Brodin, L.; De Camilli, P., and Shupliakov, O. Amphiphysin is a Component of Clathrin Coats Formed During Synaptic Vesicle Recycling at the Lamprey Giant Synapse. *Traffic*, 5(7):514–528, 2004.

Evergren, E.; Gad, H.; Walther, K.; Sundborger, A.; Tomilin, N., and Shupliakov, O. Intersectin Is a Negative Regulator of Dynamin Recruitment to the Synaptic Endocytic Zone in the Central Synapse. *Journal of Neuroscience*, 27(2):379–390, 2007.

Farisello, P.; Boido, D.; Nieus, T.; Medrihan, L.; Cesca, F.; Valtorta, F.; Baldelli, P., and Benfenati, F. Synaptic and Extrasynaptic Origin of the Excitation/Inhibition Imbalance in the Hippocampus of Synapsin I/II/III Knockout Mice. *Cerebral Cortex*, 23(3):581–593, 2013.

Farsi, Z.; Gowrisankaran, S.; Krunic, M.; Rammner, B.; Woehler, A.; Lafer, E. M.; Mim, C.; Jahn, R., and Milosevic, I. Clathrin coat controls synaptic vesicle acidification by blocking vacuolar ATPase activity. *eLife*, 7:e32569, 2018.

Fernandez-Alfonso, T. and Ryan, T. A. A heterogeneous "resting" pool of synaptic vesicles that is dynamically interchanged across boutons in mammalian CNS synapses. *Brain Cell Biology*, 36(1): 87–100, 2008.

Fernández-Chacón, R.; Achiriloaie, M.; Janz, R.; Albanesi, J. P., and Südhof, T. C. SCAMP1 function in endocytosis. *The Journal of Biological Chemistry*, 275(17):12752–12756, 2000.

Futai, K.; Kim, M. J.; Hashikawa, T.; Scheiffele, P.; Sheng, M., and Hayashi, Y. Retrograde modulation of presynaptic release probability through signaling mediated by PSD-95–neuroligin. *Nature Neuroscience*, 10(2):186–195, 2007.

Garcia, C. C.; Blair, H. J.; Seager, M.; Coulthard, A.; Tennant, S.; Buddles, M.; Curtis, A., and Goodship, J. A. Identification of a mutation in synapsin I, a synaptic vesicle protein, in a family with epilepsy. *Journal of Medical Genetics*, 41(3):183–186, 2004.

Gerber, S. H.; Rah, J.-C.; Min, S.-W.; Liu, X.; Wit, H. de; Dulubova, I.; Meyer, A. C.; Rizo, J.; Arancillo, M.; Hammer, R. E.; Verhage, M.; Rosenmund, C., and Südhof, T. C. Conformational Switch of Syntaxin-1 Controls Synaptic Vesicle Fusion. *Science*, 321(5895):1507–1510, 2008.

Gerth, F.; Jäpel, M.; Pechstein, A.; Kochlamazashvili, G.; Lehmann, M.; Puchkov, D.; Onofri, F.; Benfenati, F.; Nikonenko, A. G.; Fredrich, K.; Shupliakov, O.; Maritzen, T.; Freund, C., and Haucke, V. Intersectin associates with synapsin and regulates its nanoscale localization and function. *Proceedings of the National Academy of Sciences*, 114(45):12057–12062, 2017.

Gerth, F.; Jäpel, M.; Sticht, J.; Kuropka, B.; Schmitt, X.J.; Driller, J. H.; Loll, B.; Wahl, M. C.; Pagel, K.; Haucke, V., and Freund, C. Exon inclusion modulates conformational plasticity and autoinhibition of the intersectin 1 SH3a domain. *Structure*, accepted, 2019.

Good, M. C.; Zalatan, J. G., and Lim, W. A. Scaffold Proteins: Hubs for Controlling the Flow of Cellular Information. *Science*, 332(6030):680–686, 2011.

Gordon, S. L.; Leube, R. E., and Cousin, M. A. Synaptophysin Is Required for Synaptobrevin Retrieval during Synaptic Vesicle Endocytosis. *Journal of Neuroscience*, 31(39):14032–14036, 2011.

Granseth, B.; Odermatt, B.; Royle, S. J., and Lagnado, L. Clathrin-Mediated Endocytosis Is the Dominant Mechanism of Vesicle Retrieval at Hippocampal Synapses. *Neuron*, 51(6):773–786, 2006.

Gray, E. G. Electron microscopy of presynaptic organelles of the spinal cord. *Journal of Anatomy*, 97 (1):101–106, 1963.

Greaves, J.; Prescott, G. R.; Fukata, Y.; Fukata, M.; Salaun, C., and Chamberlain, L. H. The Hydrophobic Cysteine-rich Domain of SNAP25 Couples with Downstream Residues to Mediate Membrane Interactions and Recognition by DHHC Palmitoyl Transferases. *Molecular Biology of the Cell*, 20(6):1845–1854, 2009.

Guipponi, M.; Scott, H. S.; Chen, H.; Schebesta, A.; Rossier, C., and Antonarakis, S. E. Two Isoforms of a Human Intersectin (ITSN) Protein Are Produced by Brain-Specific Alternative Splicing in a Stop Codon. *Genomics*, 53(3):369–376, 1998.

Henne, W. M.; Boucrot, E.; Meinecke, M.; Evergren, E.; Vallis, Y.; Mittal, R., and McMahon, H. T. FCHo Proteins Are Nucleators of Clathrin-Mediated Endocytosis. *Science*, 328(5983):1281–1284, 2010.

Herrero-Garcia, E. and O'Bryan, J. P. Intersectin scaffold proteins and their role in cell signaling and endocytosis. *Biochimica et Biophysica Acta - Molecular Cell Research*, 1864(1):23–30, 2017.

Heuser, J. E. and Reese, T. S. Evidence for Recycling of Synaptic Vesicle Membrane During Transmitter Release at the Frog Neuromuscular Junction. *The Journal of Cell Biology*, 57(2):315–344, 1973.

Hilfiker, S.; Pieribone, V. A.; Czernik, A. J.; Kao, H.-T.; Augustine, G. J., and Greengard, P. Synapsins as regulators of neurotransmitter release. *Philosophical Transactions of the Royal Society of London B: Biological Sciences*, 354(1381):269–279, 1999.

Hosoi, N.; Holt, M., and Sakaba, T. Calcium Dependence of Exo- and Endocytotic Coupling at a Glutamatergic Synapse. *Neuron*, 63(2):216–229, 2009.

Hua, Y.; Woehler, A.; Kahms, M.; Haucke, V.; Neher, E., and Klingauf, J. Blocking Endocytosis Enhances Short-Term Synaptic Depression under Conditions of Normal Availability of Vesicles. *Neuron*, 80(2):343–349, 2013.

Hunter, M. P.; Nelson, M.; Kurzer, M.; Wang, X.; Kryscio, R. J.; Head, E.; Pinna, G., and O'Bryan, J. P. Intersectin 1 contributes to phenotypes in vivo: implications for Down Syndrome. *Neuroreport*, 22(15):767–772, 2011.

Hunter, M. P.; Russo, A., and O'Bryan, J. P. Emerging Roles for Intersectin (ITSN) in Regulating Signaling and Disease Pathways. *International Journal of Molecular Sciences*, 14(4):7829–7852, 2013.

Hussain, N. K.; Yamabhai, M.; Ramjaun, A. R.; Guy, A. M.; Baranes, D.; O'Bryan, J. P.; Der, C. J.; Kay, B. K., and McPherson, P. S. Splice Variants of Intersectin Are Components of the Endocytic Machinery in Neurons and Nonneuronal Cells. *Journal of Biological Chemistry*, 274(22):15671–15677, 1999.

Hussain, N. K.; Jenna, S.; Glogauer, M.; Quinn, C. C.; Wasiak, S.; Guipponi, M.; Antonarakis, S. E.; Kay, B. K.; Stossel, T. P.; Lamarche-Vane, N., and McPherson, P. S. Endocytic protein intersectin-l regulates actin assembly via Cdc42 and N-WASP. *Nature Cell Biology*, 3(10):927–932, 2001.

Imig, C.; Min, S.-W.; Krinner, S.; Arancillo, M.; Rosenmund, C.; Südhof, T. C.; Rhee, J. S.; Brose, N., and Cooper, B. H. The Morphological and Molecular Nature of Synaptic Vesicle Priming at Presynaptic Active Zones. *Neuron*, 84(2):416–431, 2014.

Jahn, R. and Scheller, R. H. SNAREs – engines for membrane fusion. *Nature Reviews Molecular Cell Biology*, 7(9):631–643, 2006.

Jakob, B.; Kochlamazashvili, G.; Jäpel, M.; Gauhar, A.; Bock, H. H.; Maritzen, T., and Haucke, V. Intersectin 1 is a component of the Reelin pathway to regulate neuronal migration and synaptic plasticity in the hippocampus. *Proceedings of the National Academy of Sciences*, 114(21):5533–5538, 2017.

Jenna, S.; Hussain, N. K.; Danek, E. I.; Triki, I.; Wasiak, S.; McPherson, P. S., and Lamarche-Vane, N. The Activity of the GTPase-activating Protein CdGAP Is Regulated by the Endocytic Protein Intersectin. *Journal of Biological Chemistry*, 277(8):6366–6373, 2002.

Jovanovic, J. N.; Sihra, T. S.; Nairn, A. C.; Hemmings, H. C.; Greengard, P., and Czernik, A. J. Opposing Changes in Phosphorylation of Specific Sites in Synapsin I During Ca2+-Dependent Glutamate Release in Isolated Nerve Terminals. *Journal of Neuroscience*, 21(20):7944–7953, 2001.

Kaksonen, M.; Toret, C. P., and Drubin, D. G. Harnessing actin dynamics for clathrin-mediated endocytosis. *Nature Reviews Molecular Cell Biology*, 7(6):404–414, 2006.

Kao, H.-T.; Porton, B.; Hilfiker, S.; Stefani, G.; Pieribone, V. A.; DeSalle, R., and Greengard, P. Molecular evolution of the synapsin gene family. *Journal of Experimental Zoology*, 285(4):360–377, 1999.

Katz, B. and Miledi, R. The timing of calcium action during neuromuscular transmission. *The Journal of Physiology*, 189(3):535–544, 1967.

Kawasaki, F.; Hazen, M., and Ordway, R. W. Fast synaptic fatigue in shibire mutants reveals a rapid requirement for dynamin in synaptic vesicle membrane trafficking. *Nature Neuroscience*, 3(9): 859–860, 2000.

Keating, D. J.; Chen, C., and Pritchard, M. A. Alzheimer's disease and endocytic dysfunction: Clues from the Down syndrome-related proteins, DSCR1 and ITSN1. *Ageing Research Reviews*, 5(4): 388–401, 2006.

Kiernan, M. C.; Isbister, G. K.; Lin, C. S.-Y.; Burke, D., and Bostock, H. Acute tetrodotoxin-induced neurotoxicity after ingestion of puffer fish. *Annals of Neurology*, 57(3):339–348, 2005.

Kim, S. H. and Ryan, T. A. CDK5 Serves as a Major Control Point in Neurotransmitter Release. *Neuron*, 67(5):797–809, 2010.

Kintscher, C.; Wuertenberger, S.; Eylenstein, R.; Uhlendorf, T., and Groemping, Y. Autoinhibition of GEF activity in intersectin 1 is mediated by the short SH3-DH domain linker. *Protein Science*, 19 (11):2164–2174, 2010.

Kiyonaka, S.; Wakamori, M.; Miki, T.; Uriu, Y.; Nonaka, M.; Bito, H.; Beedle, A. M.; Mori, E.; Hara, Y.; Waard, M. De; Kanagawa, M.; Itakura, M.; Takahashi, M.; Campbell, K. P., and Mori, Y. RIM1 confers sustained activity and neurotransmitter vesicle anchoring to presynaptic Ca2+ channels. *Nature Neuroscience*, 10(6):691–701, 2007.

Klein, I. K.; Predescu, D. N.; Sharma, T.; Knezevic, I.; Malik, A. B., and Predescu, S. Intersectin-2l Regulates Caveola Endocytosis Secondary to Cdc42-mediated Actin Polymerization. *Journal of Biological Chemistry*, 284(38):25953–25961, 2009.

Koh, T.-W.; Verstreken, P., and Bellen, H. J. Dap160/Intersectin Acts as a Stabilizing Scaffold Required for Synaptic Development and Vesicle Endocytosis. *Neuron*, 43(2):193–205, 2004.

Kononenko, N. L.; Puchkov, D.; Classen, G. A.; Walter, A. M.; Pechstein, A.; Sawade, L.; Kaempf, N.; Trimbuch, T.; Lorenz, D.; Rosenmund, C.; Maritzen, T., and Haucke, V. Clathrin/AP-2 Mediate Synaptic Vesicle Reformation from Endosome-like Vacuoles but Are Not Essential for Membrane Retrieval at Central Synapses. *Neuron*, 82(5):981–988, 2014.

Koo, S. J.; Markovic, S.; Puchkov, D.; Mahrenholz, C. C.; Beceren-Braun, F.; Maritzen, T.; Dernedde, J.; Volkmer, R.; Oschkinat, H., and Haucke, V. SNARE motif-mediated sorting of synaptobrevin by the endocytic adaptors clathrin assembly lymphoid myeloid leukemia (CALM) and AP180 at synapses. *Proceedings of the National Academy of Sciences*, 108(33):13540–13545, 2011.

Koo, S. J.; Kochlamazashvili, G.; Rost, B.; Puchkov, D.; Gimber, N.; Lehmann, M.; Tadeus, G.; Schmoranzer, J.; Rosenmund, C.; Haucke, V., and Maritzen, T. Vesicular Synaptobrevin/VAMP2 Levels Guarded by AP180 Control Efficient Neurotransmission. *Neuron*, 88(2):330–344, 2015.

Kuner, T.; Li, Y.; Gee, K. R.; Bonewald, L. F., and Augustine, G. J. Photolysis of a caged peptide reveals rapid action of N-ethylmaleimide sensitive factor before neurotransmitter release. *Proceedings of the National Academy of Sciences*, 105(1):347–352, 2008.

Kwon, S. E. and Chapman, E. R. Synaptophysin Regulates the Kinetics of Synaptic Vesicle Endocytosis in Central Neurons. *Neuron*, 70(5):847–854, 2011.

Lehmann, M.; Gottschalk, B.; Puchkov, D.; Schmieder, P.; Schwagerus, S.; Hackenberger, C. P. R.; Haucke, V., and Schmoranzer, J. Multicolor Caged dSTORM Resolves the Ultrastructure of Synaptic Vesicles in the Brain. *Angewandte Chemie International Edition*, 54(45):13230–13235, 2015.

Levchenko, A.; Bruck, J., and Sternberg, P. W. Scaffold proteins may biphasically affect the levels of mitogen-activated protein kinase signaling and reduce its threshold properties. *Proceedings of the National Academy of Sciences*, 97(11):5818–5823, 2000.

Li, X.; Radhakrishnan, A.; Grushin, K.; Kasula, R.; Chaudhuri, A.; Gomathinayagam, S.; Krishnakumar, S. S.; Liu, J., and Rothman, J. E. Symmetrical organization of proteins under docked synaptic vesicles. *FEBS Letters*, 593(2):144–153, 2019.

Li, Y.; Wang, S.; Li, T.; Zhu, L., and Ma, C. Tomosyn guides SNARE complex formation in coordination with Munc18 and Munc13. *FEBS Letters*, 592(7):1161–1172, 2018.

Lo, W.-T.; Vujičić Žagar, A.; Gerth, F.; Lehmann, M.; Puchkov, D.; Krylova, O.; Freund, C.; Scapozza, L.; Vadas, O., and Haucke, V. A Coincidence Detection Mechanism Controls PX-BAR Domain-Mediated Endocytic Membrane Remodeling via an Allosteric Structural Switch. *Developmental Cell*, 43(4):522–529, 2017.

Ma, C.; Li, W.; Xu, Y., and Rizo, J. Munc13 mediates the transition from the closed syntaxin–Munc18 complex to the SNARE complex. *Nature Structural & Molecular Biology*, 18(5):542–549, 2011.

Ma, Y. J.; Okamoto, M.; Gu, F.; Obata, K.; Matsuyama, T.; Desaki, J.; Tanaka, J., and Sakanaka, M. Neuronal distribution of EHSH1/intersectin: Molecular linker between clathrin-mediated endocytosis and signaling pathways. *Journal of Neuroscience Research*, 71(4):468–477, 2003.

Malacombe, M.; Ceridono, M.; Calco, V.; Chasserot-Golaz, S.; McPherson, P. S.; Bader, M.-F., and Gasman, S. Intersectin-1l nucleotide exchange factor regulates secretory granule exocytosis by activating Cdc42. *The EMBO Journal*, 25(15):3494–3503, 2006.

Manca, F.; Pincet, F.; Truskinovsky, L.; Rothman, J. E.; Foret, L., and Caruel, M. SNARE machinery is optimized for ultrafast fusion. *Proceedings of the National Academy of Sciences*, 116(7):2435–2442, 2019.

Marie, B.; Sweeney, S. T.; Poskanzer, K. E.; Roos, J.; Kelly, R. B., and Davis, G. W. Dap160/Intersectin Scaffolds the Periactive Zone to Achieve High-Fidelity Endocytosis and Normal Synaptic Growth. *Neuron*, 43(2):207–219, 2004.

Maritzen, T. and Haucke, V. Coupling of exocytosis and endocytosis at the presynaptic active zone. *Neuroscience Research*, 127:45–52, 2018.

Martin, N. P.; Mohney, R. P.; Dunn, S.; Das, M.; Scappini, E., and O'Bryan, J. P. Intersectin Regulates Epidermal Growth Factor Receptor Endocytosis, Ubiquitylation, and Signaling. *Molecular Pharmacology*, 70(5):1643–1653, 2006.

Martin, T. F. J. PI(4,5)P2-binding effector proteins for vesicle exocytosis. *Biochimica et Biophysica Acta - Molecular and Cell Biology of Lipids*, 1851(6):785–793, 2015.

Maschi, D. and Klyachko, V. A. Spatiotemporal Regulation of Synaptic Vesicle Fusion Sites in Central Synapses. *Neuron*, 94(1):65–73, 2017.

McMahon, H. T. and Boucrot, E. Molecular mechanism and physiological functions of clathrin-mediated endocytosis. *Nature Reviews Molecular Cell Biology*, 12(8):517–533, 2011.

Milosevic, I.; Giovedi, S.; Lou, X.; Raimondi, A.; Collesi, C.; Shen, H.; Paradise, S.; O'Toole, E.; Ferguson, S.; Cremona, O., and De Camilli, P. Recruitment of Endophilin to Clathrin-Coated Pit Necks Is Required for Efficient Vesicle Uncoating after Fission. *Neuron*, 72(4):587–601, 2011.

Milosevic, I.; Gowrisankaran, S.; Steubler, V.; Houy, S.; del Castillo, J. G. P.; Gelker, M.; Kroll, J.; Pinheiro, P. S.; Halbsgut, N.; Raimundo, N., and Soerensen, J. B. Endophilin-A controls recruitment, priming and fusion of neurosecretory vesicles. *bioRxiv*, 2019.

Milovanovic, D.; Wu, Y.; Bian, X., and De Camilli, P. A liquid phase of synapsin and lipid vesicles. *Science*, 361(6402):604–607, 2018.

Momboisse, F.; Ory, S.; Ceridono, M.; Calco, V.; Vitale, N.; Bader, M.-F., and Gasman, S. The Rho Guanine Nucleotide Exchange Factors Intersectin 1l and β-Pix Control Calcium-Regulated Exocytosis in Neuroendocrine PC12 Cells. *Cellular and Molecular Neurobiology*, 30(8):1327–1333, 2010.

Mukherjee, K.; Yang, X.; Gerber, S. H.; Kwon, H.-B.; Ho, A.; Castillo, P. E.; Liu, X., and Südhof, T. C. Piccolo and bassoon maintain synaptic vesicle clustering without directly participating in vesicle exocytosis. *Proceedings of the National Academy of Sciences*, 107(14):6504–6509, 2010.

Neher, E. What is Rate-Limiting during Sustained Synaptic Activity: Vesicle Supply or the Availability of Release Sites. *Frontiers in Synaptic Neuroscience*, 2, 2010.

Nicholson-Fish, J. C.; Kokotos, A. C.; Gillingwater, T. H.; Smillie, K. J., and Cousin, M. A. VAMP4 Is an Essential Cargo Molecule for Activity-Dependent Bulk Endocytosis. *Neuron*, 88(5):973–984, 2015.

Nishimura, T.; Yamaguchi, T.; Tokunaga, A.; Hara, A.; Hamaguchi, T.; Kato, K.; Iwamatsu, A.; Okano, H., and Kaibuchi, K. Role of Numb in Dendritic Spine Development with a Cdc42 GEF Intersectin and EphB2. *Molecular Biology of the Cell*, 17(3):1273–1285, 2006.

Okamoto, M.; Schoch, S., and Südhof, T. C. EHSH1/Intersectin, a Protein That Contains EH and SH3 Domains and Binds to Dynamin and SNAP-25. *Journal of Biological Chemistry*, 274(26):18446–18454, 1999.

Onofri, F.; Giovedı, S.; Kao, H.-T.; Valtorta, F.; Borbone, L. B.; De Camilli, P.; Greengard, P., and Benfenati, F. Specificity of the Binding of Synapsin I to Src Homology 3 Domains. *Journal of Biological Chemistry*, 275(38):29857–29867, 2000.

Park, D.; Lee, U.; Cho, E.; Zhao, H.; Kim, J. A.; Lee, B. J.; Regan, P.; Ho, W.-K.; Cho, K., and Chang, S. Impairment of Release Site Clearance within the Active Zone by Reduced SCAMP5 Expression Causes Short-Term Depression of Synaptic Release. *Cell Reports*, 22(12):3339–3350, 2018.

Park, Y.; Seo, J. B.; Fraind, A.; Pérez-Lara, A.; Yavuz, H.; Han, K.; Jung, S.-R.; Kattan, I.; Walla, P. J.; Choi, M. Y.; Cafiso, D. S.; Koh, D.-S., and Jahn, R. Synaptotagmin-1 binds to PIP2-containing membrane but not to SNAREs at physiological ionic strength. *Nature Structural & Molecular Biology*, 22(10):815–823, 2015.

Pechstein, A.; Bacetic, J.; Vahedi-Faridi, A.; Gromova, K.; Sundborger, A.; Tomlin, N.; Krainer, G.; Vorontsova, O.; Schäfer, J. G.; Owe, S. G.; Cousin, M. A.; Saenger, W.; Shupliakov, O., and Haucke, V. Regulation of synaptic vesicle recycling by complex formation between intersectin 1 and the clathrin adaptor complex AP2. *Proceedings of the National Academy of Sciences*, 107(9):4206–4211, 2010a.

Pechstein, A.; Shupliakov, O., and Haucke, V. Intersectin 1: a versatile actor in the synaptic vesicle cycle. *Biochemical Society Transactions*, 38(1):181–186, 2010b.

Pechstein, A.; Gerth, F.; Milosevic, I.; Jäpel, M.; Eichhorn-Grünig, M.; Vorontsova, O.; Bacetic, J.; Maritzen, T.; Shupliakov, O.; Freund, C., and Haucke, V. Vesicle uncoating regulated by SH3-SH3 domain-mediated complex formation between endophilin and intersectin at synapses. *EMBO reports*, 16(2):232–239, 2015.

Peter, B. J.; Kent, H. M.; Mills, I. G.; Vallis, Y.; Butler, P. J. G.; Evans, P. R., and McMahon, H. T. BAR Domains as Sensors of Membrane Curvature: The Amphiphysin BAR Structure. *Science*, 303 (5657):495–499, 2004.

Pucharcós, C.; Fuentes, J.-J.; Casas, C.; de la Luna, S.; Alcántara, S.; Arbonés, M. L.; Soriano, E.; Estivill, X., and Pritchard, M. Alu-splice cloning of human Intersectin (ITSN), a putative multivalent binding protein expressed in proliferating and differentiating neurons and overexpressed in Down syndrome. *European Journal of Human Genetics*, 7(6):704–712, 1999.

Rajappa, R.; Gauthier-Kemper, A.; Böning, D.; Hüve, J., and Klingauf, J. Synaptophysin 1 Clears Synaptobrevin 2 from the Presynaptic Active Zone to Prevent Short-Term Depression. *Cell Reports*, 14(6):1369–1381, 2016.

Regehr, W. G. Short-Term Presynaptic Plasticity. *Cold Spring Harbor Perspectives in Biology*, 4(7): a005702, 2012.

Ribrault, C.; Reingruber, J.; Petković, M.; Galli, T.; Ziv, N. E.; Holcman, D., and Triller, A. Syntaxin1a Lateral Diffusion Reveals Transient and Local SNARE Interactions. *Journal of Neuroscience*, 31(48): 17590–17602, 2011.

Ringstad, N.; Nemoto, Y., and De Camilli, P. The SH3p4/Sh3p8/SH3p13 protein family: Binding partners for synaptojanin and dynamin via a Grb2-like Src homology 3 domain. *Proceedings of the National Academy of Sciences*, 94(16):8569–8574, 1997.

Ringstad, N.; Gad, H.; Löw, P.; Di Paolo, G.; Brodin, L.; Shupliakov, O., and De Camilli, P. Endophilin/SH3p4 Is Required for the Transition from Early to Late Stages in Clathrin-Mediated Synaptic Vesicle Endocytosis. *Neuron*, 24(1):143–154, 1999.

Rizo, J. and Xu, J. The Synaptic Vesicle Release Machinery. *Annual Review of Biophysics*, 44(1): 339–367, 2015.

Rizzoli, S. O. and Betz, W. J. Synaptic vesicle pools. *Nature Reviews Neuroscience*, 6(1):57–69, 2005.

Roos, J. and Kelly, R. B. Dap160, a Neural-specific Eps15 Homology and Multiple SH3 Domain-containing Protein That Interacts with DrosophilaDynamin. *Journal of Biological Chemistry*, 273 (30):19108–19119, 1998.

Rose, S.; Malabarba, M. G.; Krag, C.; Schultz, A.; Tsushima, H.; Di Fiore, P. P.; Salcini, A. E., and Schmid, S. Caenorhabditis elegans Intersectin: A Synaptic Protein Regulating Neurotransmission. *Molecular Biology of the Cell*, 18(12):5091–5099, 2007.

Ryu, J.-K.; Jahn, R., and Yoon, T.-Y. Progresses in understanding N-ethylmaleimide sensitive factor (NSF) mediated disassembly of SNARE complexes. *Biopolymers*, 105(8):518–531, 2016.

Sakaba, T. and Neher, E. Calmodulin Mediates Rapid Recruitment of Fast-Releasing Synaptic Vesicles at a Calyx-Type Synapse. *Neuron*, 32(6):1119–1131, 2001.

Sakaba, T.; Kononenko, N. L.; Bacetic, J.; Pechstein, A.; Schmoranzer, J.; Yao, L.; Barth, H.; Shupliakov, O.; Kobler, O.; Aktories, K., and Haucke, V. Fast neurotransmitter release regulated by the endocytic scaffold intersectin. *Proceedings of the National Academy of Sciences*, 110(20):8266–8271, 2013.

Saksela, K. and Permi, P. SH3 domain ligand binding: What's the consensus and where's the specificity? *FEBS Letters*, 586(17):2609–2614, 2012.

Salcini, A. E.; Confalonieri, S.; Doria, M.; Santolini, E.; Tassi, E.; Minenkova, O.; Cesareni, G.; Pelicci, P. G., and Di Fiore, P. P. Binding specificity and in vivo targets of the EH domain, a novel protein–protein interaction module. *Genes & Development*, 11(17):2239–2249, 1997.

Sankaranarayanan, S. and Ryan, T. A. Real-time measurements of vesicle-SNARE recycling in synapses of the central nervous system. *Nature Cell Biology*, 2(4):197–204, 2000.

Schikorski, T. and Stevens, C. F. Quantitative Ultrastructural Analysis of Hippocampal Excitatory Synapses. *Journal of Neuroscience*, 17(15):5858–5867, 1997.

Schoch, S.; Deák, F.; Königstorfer, A.; Mozhayeva, M.; Sara, Y.; Südhof, T. C., and Kavalali, E. T. SNARE Function Analyzed in Synaptobrevin/VAMP Knockout Mice. *Science*, 294(5544):1117–1122, 2001.

Schoch, S.; Castillo, P. E.; Jo, T.; Mukherjee, K.; Geppert, M.; Wang, Y.; Schmitz, F.; Malenka, R. C., and Südhof, T. C. RIM1α forms a protein scaffold for regulating neurotransmitter release at the active zone. *Nature*, 415(6869):321–326, 2002.

Schuske, K. R.; Richmond, J. E.; Matthies, D. S.; Davis, W. S.; Runz, S.; Rube, D. A.; van der Bliek, A. M., and Jorgensen, E. M. Endophilin Is Required for Synaptic Vesicle Endocytosis by Localizing Synaptojanin. *Neuron*, 40(4):749–762, 2003.

Schweizer, F. E.; Dresbach, T.; DeBello, W. M.; O'Connor, V.; Augustine, G. J., and Betz, H. Regulation of Neurotransmitter Release Kinetics by NSF. *Science*, 279(5354):1203–1206, 1998.

Sengar, A. S.; Wang, W.; Bishay, J.; Cohen, S., and Egan, S. E. The EH and SH3 domain Ese proteins regulate endocytosis by linking to dynamin and Eps15. *The EMBO Journal*, 18(5):1159–1171, 1999.

Sengar, A. S.; Ellegood, J.; Yiu, A. P.; Wang, H.; Wang, W.; Juneja, S. C.; Lerch, J. P.; Josselyn, S. A.; Henkelman, R. M.; Salter, M. W., and Egan, S. E. Vertebrate Intersectin1 Is Repurposed to Facilitate Cortical Midline Connectivity and Higher Order Cognition. *Journal of Neuroscience*, 33 (9):4055–4065, 2013.

Sharma, S. and Lindau, M. Molecular mechanism of fusion pore formation driven by the neuronal SNARE complex. *Proceedings of the National Academy of Sciences*, 115(50):12751–12756, 2018.

Shupliakov, O.; Löw, P.; Grabs, D.; Gad, H.; Chen, H.; David, C.; Takei, K.; De Camilli, P., and Brodin, L. Synaptic Vesicle Endocytosis Impaired by Disruption of Dynamin-SH3 Domain Interactions. *Science*, 276(5310):259–263, 1997.

Shupliakov, O.; Haucke, V., and Pechstein, A. How synapsin I may cluster synaptic vesicles. *Seminars in Cell & Developmental Biology*, 22(4):393–399, 2011.

Sinha, R.; Ahmed, S.; Jahn, R., and Klingauf, J. Two synaptobrevin molecules are sufficient for vesicle fusion in central nervous system synapses. *Proceedings of the National Academy of Sciences*, 108(34): 14318–14323, 2011.

Sochacki, K. A.; Dickey, A. M.; Strub, M.-P., and Taraska, J. W. Endocytic proteins are partitioned at the edge of the clathrin lattice in mammalian cells. *Nature Cell Biology*, 19(4):352–361, 2017.

Soykan, T.; Maritzen, T., and Haucke, V. Modes and mechanisms of synaptic vesicle recycling. *Current Opinion in Neurobiology*, 39:17–23, 2016.

Soykan, T.; Kaempf, N.; Sakaba, T.; Vollweiter, D.; Goerdeler, F.; Puchkov, D.; Kononenko, N. L., and Haucke, V. Synaptic Vesicle Endocytosis Occurs on Multiple Timescales and Is Mediated by Formin-Dependent Actin Assembly. *Neuron*, 93(4):854–866, 2017.

Staras, K.; Branco, T.; Burden, J. J.; Pozo, K.; Darcy, K.; Marra, V.; Ratnayaka, A., and Goda, Y. A Vesicle Superpool Spans Multiple Presynaptic Terminals in Hippocampal Neurons. *Neuron*, 66(1): 37–44, 2010.

Sundborger, A.; Soderblom, C.; Vorontsova, O.; Evergren, E.; Hinshaw, J. E., and Shupliakov, O. An endophilin–dynamin complex promotes budding of clathrin-coated vesicles during synaptic vesicle recycling. *Journal of Cell Science*, 124(1):133–143, 2011.

Söllner, T.; Bennett, M. K.; Whiteheart, S. W.; Scheller, R. H., and Rothman, J. E. A protein assembly-disassembly pathway in vitro that may correspond to sequential steps of synaptic vesicle docking, activation, and fusion. *Cell*, 75(3):409–418, 1993.

Südhof, Thomas C. The Synaptic Vesicle Cycle. *Annual Review of Neuroscience*, 27(1):509–547, 2004.

Südhof, T. C. The Presynaptic Active Zone. *Neuron*, 75(1):11–25, 2012.

Takamori, S.; Holt, M.; Stenius, K.; Lemke, E. A.; Grønborg, M.; Riedel, D.; Urlaub, H.; Schenck, S.; Brügger, B.; Ringler, P.; Müller, S. A.; Rammner, B.; Gräter, F.; Hub, J. S.; De Groot, B. L.; Mieskes, G.; Moriyama, Y.; Klingauf, J.; Grubmüller, H.; Heuser, J.; Wieland, F., and Jahn, R. Molecular Anatomy of a Trafficking Organelle. *Cell*, 127(4):831–846, 2006.

Tan, T. C.; Valova, V. A.; Malladi, C. S.; Graham, M. E.; Berven, L. A.; Jupp, O. J.; Hansra, G.; McClure, S. J.; Sarcevic, B.; Boadle, R. A.; Larsen, M. R.; Cousin, M. A., and Robinson, P. J. Cdk5 is essential for synaptic vesicle endocytosis. *Nature Cell Biology*, 5(8):701–710, 2003.

Tang, A.-H.; Chen, H.; Li, T. P.; Metzbower, S. R.; MacGillavry, H. D., and Blanpied, T. A. A trans-synaptic nanocolumn aligns neurotransmitter release to receptors. *Nature*, 536:210–214, 2016.

Tong, X.-K.; Hussain, N. K.; de Heuvel, E.; Kurakin, A.; Abi-Jaoude, E.; Quinn, C. C.; Olson, M. F.; Marais, R.; Baranes, D.; Kay, B. K., and McPherson, P. S. The endocytic protein intersectin is a major binding partner for the Ras exchange factor mSos1 in rat brain. *The EMBO Journal*, 19(6): 1263–1271, 2000.

Trimbuch, T. and Rosenmund, C. Should I stop or should I go? The role of complexin in neurotransmitter release. *Nature Reviews Neuroscience*, 17(2):118–125, 2016.

Tsyba, L.; Gryaznova, T.; Dergai, O.; Dergai, M.; Skrypkina, I.; Kropyvko, S.; Boldyryev, O.; Nikolaienko, O.; Novokhatska, O., and Rynditch, A. Alternative splicing affecting the SH3a domain controls the binding properties of intersectin 1 in neurons. *Biochemical and Biophysical Research Communications*, 372(4):929–934, 2008.

Tucker, W. C. and Chapman, E. R. Role of synaptotagmin in Ca2+-triggered exocytosis. *Biochemical Journal*, 366(1):1–13, 2002.

van den Bogaart, G.; Holt, M. G.; Bunt, G.; Riedel, D.; Wouters, F. S., and Jahn, R. One SNARE complex is sufficient for membrane fusion. *Nature Structural & Molecular Biology*, 17(3):358–364, 2010.

Varoqueaux, F.; Sigler, A.; Rhee, J.-S.; Brose, N.; Enk, C.; Reim, K., and Rosenmund, C. Total arrest of spontaneous and evoked synaptic transmission but normal synaptogenesis in the absence of Munc13-mediated vesicle priming. *Proceedings of the National Academy of Sciences*, 99(13):9037–9042, 2002.

Verhage, M.; Maia, A. S.; Plomp, J. J.; Brussaard, A. B.; Heeroma, J. H.; Vermeer, H.; Toonen, R. F.; Hammer, R. E.; van den Berg, T. K.; Missler, M.; Geuze, H. J., and Südhof, T. C. Synaptic Assembly of the Brain in the Absence of Neurotransmitter Secretion. *Science*, 287(5454):864–869, 2000.

Verstegen, A. M. J.; Tagliatti, E.; Lignani, G.; Marte, A.; Stolero, T.; Atias, M.; Corradi, A.; Valtorta, F.; Gitler, D.; Onofri, F.; Fassio, A., and Benfenati, F. Phosphorylation of Synapsin I by Cyclin-Dependent Kinase-5 Sets the Ratio between the Resting and Recycling Pools of Synaptic Vesicles at Hippocampal Synapses. *Journal of Neuroscience*, 34(21):7266–7280, 2014.

Verstreken, P.; Koh, T.-W.; Schulze, K. L.; Zhai, R. G.; Hiesinger, P. R.; Zhou, Y.; Mehta, S. Q.; Cao, Y.; Roos, J., and Bellen, H. J. Synaptojanin Is Recruited by Endophilin to Promote Synaptic Vesicle Uncoating. *Neuron*, 40(4):733–748, 2003.

Vinatier, J.; Herzog, E.; Plamont, M.-A.; Wojcik, S. M.; Schmidt, A.; Brose, N.; Daviet, L.; El Mestikawy, S., and Giros, B. Interaction between the vesicular glutamate transporter type 1 and endophilin A1, a protein essential for endocytosis. *Journal of Neurochemistry*, 97(4):1111–1125, 2006.

Voglmaier, S. M.; Kam, K.; Yang, H.; Fortin, D. L.; Hua, Z.; Nicoll, R. A., and Edwards, R. H. Distinct Endocytic Pathways Control the Rate and Extent of Synaptic Vesicle Protein Recycling. *Neuron*, 51 (1):71–84, 2006.

Wadel, K.; Neher, E., and Sakaba, T. The Coupling between Synaptic Vesicles and Ca2+ Channels Determines Fast Neurotransmitter Release. *Neuron*, 53(4):563–575, 2007.

Walter, A. M.; Müller, R.; Tawfik, B.; Wierda, K. D. B.; Pinheiro, P. S.; Nadler, A.; McCarthy, A. W.; Ziomkiewicz, I.; Kruse, M.; Reither, G.; Rettig, J.; Lehmann, M.; Haucke, V.; Hille, B.; Schultz, C., and Sørensen, J. B. Phosphatidylinositol 4,5-bisphosphate optical uncaging potentiates exocytosis. *eLife*, 6:e30203, 2017.

Wang, S. S. H.; Held, R. G.; Wong, M. Y.; Liu, C.; Karakhanyan, A., and Kaeser, P. S. Fusion Competent Synaptic Vesicles Persist upon Active Zone Disruption and Loss of Vesicle Docking. *Neuron*, 91(4):777–791, 2016.

Wang, X.; Hu, B.; Zieba, A.; Neumann, N. G.; Kasper-Sonnenberg, M.; Honsbein, A.; Hultqvist, G.; Conze, T.; Witt, W.; Limbach, C.; Geitmann, M.; Danielson, H.; Kolarow, R.; Niemann, G.; Lessmann, V., and Kilimann, M. W. A Protein Interaction Node at the Neurotransmitter Release Site: Domains of Aczonin/Piccolo, Bassoon, CAST, and Rim Converge on the N-Terminal Domain of Munc13-1. *Journal of Neuroscience*, 29(40):12584–12596, 2009.

Wang, Y.; Okamoto, M.; Schmitz, F.; Hofmann, K., and Südhof, T. C. Rim is a putative Rab3 effector in regulating synaptic-vesicle fusion. *Nature*, 388(6642):593–598, 1997.

Watanabe, S.; Liu, Q.; Davis, M. W.; Hollopeter, G.; Thomas, N.; Jorgensen, N. B., and Jorgensen, E. M. Ultrafast endocytosis at Caenorhabditis elegans neuromuscular junctions. *eLife*, 2:e00723, 2013.

Watanabe, S.; Mamer, L. E.; Raychaudhuri, S.; Luvsanjav, D.; Eisen, J.; Trimbuch, T.; Söhl-Kielczynski, B.; Fenske, P.; Milosevic, I.; Rosenmund, C., and Jorgensen, E. M. Synaptojanin and Endophilin Mediate Neck Formation during Ultrafast Endocytosis. *Neuron*, 98(6):1184–1197, 2018.

Weston, M. C.; Nehring, R. B.; Wojcik, S. M., and Rosenmund, C. Interplay between VGLUT Isoforms and Endophilin A1 Regulates Neurotransmitter Release and Short-Term Plasticity. *Neuron*, 69(6): 1147–1159, 2011.

Wilhelm, B. G.; Mandad, S.; Truckenbrodt, S.; Kröhnert, K.; Schäfer, C.; Rammner, B.; Koo, S. J.; Claßen, G. A.; Krauss, M.; Haucke, V.; Urlaub, H., and Rizzoli, S. O. Composition of isolated synaptic boutons reveals the amounts of vesicle trafficking proteins. *Science*, 344(6187):1023–1028, 2014.

Winther, Å. M. E.; Vorontsova, O.; Rees, K. A.; Näreoja, T.; Sopova, E.; Jiao, W., and Shupliakov, O. An Endocytic Scaffolding Protein together with Synapsin Regulates Synaptic Vesicle Clustering in the *Drosophila* Neuromuscular Junction. *Journal of Neuroscience*, 35(44):14756–14770, 2015.

Wong, K. A.; Wilson, J.; Russo, A.; Wang, L.; Okur, M. N.; Wang, X.; Martin, N. P.; Scappini, E.; Carnegie, G. K., and O'Bryan, J. P. Intersectin (ITSN) Family of Scaffolds Function as Molecular Hubs in Protein Interaction Networks. *PLOS ONE*, 7(4):e36023, 2012.

Wu, X.-S.; McNeil, B. D.; Xu, J.; Fan, J.; Xue, L.; Melicoff, E.; Adachi, R.; Bai, L., and Wu, L.-G. Ca2+and calmodulin initiate all forms of endocytosis during depolarization at a nerve terminal. *Nature Neuroscience*, 12(8):1003–1010, 2009.

Wu, X.-S.; Zhang, Z.; Zhao, W.-D.; Wang, D.; Luo, F., and Wu, L.-G. Calcineurin Is Universally Involved in Vesicle Endocytosis at Neuronal and Nonneuronal Secretory Cells. *Cell Reports*, 7(4): 982–988, 2014.

Yamabhai, M.; Hoffman, N. G.; Hardison, N. L.; McPherson, P. S.; Castagnoli, L.; Cesareni, G., and Kay, B. K. Intersectin, a Novel Adaptor Protein with Two Eps15 Homology and Five Src Homology 3 Domains. *Journal of Biological Chemistry*, 273(47):31401–31407, 1998.

Yu, Y.; Chu, P.-Y.; Bowser, D. N.; Keating, D. J.; Dubach, D.; Harper, I.; Tkalcevic, J.; Finkelstein, D. I., and Pritchard, M. A. Mice deficient for the chromosome 21 ortholog Itsn1 exhibit vesicle-trafficking abnormalities. *Human Molecular Genetics*, 17(21):3281–3290, 2008.

Zhai, R. G. and Bellen, H. J. The Architecture of the Active Zone in the Presynaptic Nerve Terminal. *Physiology*, 19(5):262–270, 2004.

Zhang, X. M.; Francois, U.; Silm, K.; Angelo, M. F.; Busch, M. V. F.; Maged, M.; Martin, C.; Cordelières, F. P.; Deshors, M.; Pons, S.; Maskos, U.; Bemelmans, A. P.; Wojcik, S. M.; Mestikawy, S. E.; Humeau, Y., and Herzog, E. Mammalian vesicular glutamate transporter VGLUT1 reduces synaptic vesicle superpool size and spontaneous release frequency. *bioRxiv*, 2018.

For reasons of data protection, the curriculum vitae is not included in the online version.

For reasons of data protection, the curriculum vitae is not included in the online version.

For reasons of data protection, the curriculum vitae is not included in the online version.